



HELLENIC REPUBLIC

**National and Kapodistrian
University of Athens**

EST. 1837

School of Health Sciences

School of Medicine and Department of Pharmacy

Interdisciplinary Postgraduate Studies Program in

Nanomedicine

Academic year 2018-2019

*“Nanoparticles in combination with Radiotherapy and/or
Hyperthermia in the treatment of Head & Neck Cancer*

A critical appraisal”

MSc Student: Krompas Konstantinos MD

Supervisor: Assoc. Prof. Kouloulas Vasileios MD, MSc, PhD

Selection Board: Prof. Efstathopoulos Efstathios MSc, PhD

Assist. Prof. Platoni Kalliopi MSc, PhD

August 2019

Contents

1. Introduction.....	2
2. Head & Neck Cancer Therapy.....	3
3. Radiotherapy	3
3.1 Introduction	3
3.2 Radiation Physics	4
3.2.1 Interaction of radiation and matter	4
3.2.1.1 Photoelectric Effect	5
3.2.1.2 Compton Scattering.....	5
3.2.1.3 Pair Production	6
3.2.1.4 Charged Particle Interactions	6
3.3 Generation of Therapeutic Radiation	7
3.3.1 Linear Accelerators (linacs)	7
3.3.2 Radiation Treatment Goals	8
3.4 Biological effects of Radiotherapy	9
3.4.1 Tissue Types H,F	11
3.4.2 Radiation Sensitivity	12
3.4.3 Radiosensitization	13
3.5 Radiation Treatment Planning & Delivery	14
3.5.1 Three-dimensional Conformal Radiotherapy (3-DCRT).....	15
3.5.2 Intensity Modulated Radiotherapy (IMRT)	16
3.6 Particle Therapy	16
3.6.1 Protons	17
3.6.2 Neutrons.....	17
3.6.3 Heavy Ions	18
3.7 Acute and Late Normal Tissue Reactions.....	18
3.8 Nanotechnology in Radiotherapy	18
3.8.1 Nanoparticle Radio-Enhancement Principles.....	20
3.9 Nanoparticles' Properties	21
3.9.1 Nanoparticle Size.....	22
3.9.2 Nanoparticle Shape	22
3.9.3 Nanoparticle Surface	22
3.9.4 Nanoparticle Charge.....	22
3.9.5 Passive and Active Targeting.....	23
3.10 Nano-Radio-Enhancers (NREs).....	24
3.10.1 Gold Nanoparticles (AuNPs).....	24
3.10.1.1 Targeted AuNPs as radiosensitizer agents.....	25
3.10.1.2 AuNPs enhancing X-ray induced apoptosis in HNSCC	26
3.10.1.3 Cancer cells' radiosensitization by folate conjugated Au@Fe ₂ O ₃ nanocomplex.....	27

3.10.1.4	Inhibition of the EGFR with nanoparticles enhances radiosensitivity in SCCVII cells	30
3.10.1.5	Personalized targeted AuNPs impact on radiosensitivity & imaging of adenoid cystic.....	33
3.10.2	Nanoparticles alternatives to AuNPs	37
3.10.3	Particle therapy and nanomedicine	38
3.10.3.1	Proton radiotherapy combined with nanoparticles	39
3.10.3.2	Carbon ions radiotherapy combined with nanoparticles	40
3.10.3.3	Proton therapy enhanced by metal-containing nanoparticles.....	41
3.11	Challenges & Contradictions of Metal-NP applications as Nano-Radio-Enhancers.....	43
4.	Hyperthermia	47
4.1	Hyperthermia Techniques	48
4.1.1	Radiofrequency (RF)	48
4.1.2	Ultrasound.....	49
4.1.3	Microwave.....	49
4.1.4	Near-Infrared Photothermal Therapy (PTT)	50
4.2	Biological effects of Hyperthermia	50
4.3	Local Hyperthermia application in Head and Neck Cancer.....	52
4.4	Nanotechnology-based Hyperthermia in Head and Neck Cancer	53
4.5	Types of nanoparticle-enhanced Hyperthermia	54
4.5.1	Nano-Photo-Thermal Therapy (NPTT).....	54
4.5.1.1	EGFRmAb–AuNPs enhanced photothermal therapy induces apoptosis in hypopharyngeal.....	55
4.5.1.2	Platelet-facilitated Photothermal Therapy.....	57
4.5.2	Nano-Magnetic Hyperthermia (NMH).....	59
4.5.2.1	Polyphosphate Magnetic Nanoparticles enhanced Hyperthermia for Oral Cancer	61
4.5.3	Nano-Radio-Frequency Ablation (NaRFA)	63
4.5.4	Nano-Ultrasound Hyperthermia (NUH)	64
4.6	Combination of Nanoparticle Enhanced Hyperthermia and Radiotherapy.....	66
4.6.1	Nano-Photo-thermal therapy and radiotherapy enhanced by folate conjugated gold nanorods (AuNRs) on KB nasopharyngeal carcinoma cells	66
4.6.2	Treatment of HNSCC with nano-Quadrapeutics.....	70
4.6.3	Single NP-agent for radio- and radio-photothermal therapy in anaplastic thyroid cancer	73
5.	Discussion	75
5.1	Future Perspectives	77
6.	Conclusion	78
	References.....	80

Abstract

Despite the progress that has been made in cancer therapy methods, head and neck cancer still remains a major cause of morbidity and mortality. Radiation therapy has evolved greatly the last decade, but there are many factors that limit its efficacy, such as the radioresistance of cancer cells and the adverse effects that are produced from healthy tissue damage.

The application of nanotechnology in cancer treatment shows great potential in improving the therapeutic outcomes of radiation therapy, by enhancing its efficiency and counteracts the radioresistance of cancer cells. Furthermore it limits the dose absorbed by healthy tissue, resulting in the reduction of the adverse effects. In addition, the implementation of nanoparticles in various hyperthermia methods may restore this treatment modality as an adjuvant therapy for head and neck cancer.

The combination of radiotherapy and hyperthermia enhanced by nanoparticle-agents, may lead to a revolution in head and neck cancer therapy, resulting in a dramatic improvement of the survival rates and the quality of life of these patients.

1. Introduction

Nanobiotechnology is a multidisciplinary scientific field, which refers to the use of nanoparticles in diagnosis and treatment of diseases. The application of nanoparticles provides the potential of improving the current methods as well as developing novel diagnostic and therapeutic methods. In particular, nanotechnology can increase the sensitivity and specificity of imaging modalities and also improve the selectivity and efficiency of the therapeutic modalities.

The current treatment methods for head and neck cancer have major limitations. Several important structures of head and neck region limit significantly, the surgical resection. Residual disease, left behind near vital structures, may lead to recurrence of cancer. Furthermore, toxicity of radiotherapy limits the dose given to a full course treatment. Nanotechnology introduces new tools in modern clinical practice, providing the potential of molecular imaging as well as novel therapeutic devices, such as photothermal probes and radiation enhancers.

The current bibliographic research refers to the use of radiotherapy and hyperthermia for the treatment of head and neck cancer, combined with the implementation of nanoparticles (NPs), in order to achieve the enhancement of the efficiency and reduction of the adverse effects of these treatment methods. The aim of this study is the investigation of the advantages that result from the application of NPs in radiotherapy and hyperthermia techniques, in head and neck cancer therapy, as well as the analysis of the key mechanisms of the nano-enhancement, in these therapeutic modalities.

The first unit refers to the basics of radiation therapy in head and neck cancer and the application of NPs as nano-radio-enhancers in various in-vitro and in-vivo studies, of the last five to eight years. The therapeutic outcomes of nano-radio-enhancement are presented, showing the benefits that result from the application of NPs in radiotherapy. In the second unit, the application of hyperthermia treatment modalities in combination with NPs is presented, by analyzing the results from in-vitro and in-vivo studies, showing the potential of this method, resulting from the capability of nanoparticles to effectively improve the outcomes, by enhancing the thermal effects in tumor cells.

Lastly, the results that are produced by the combination of nano-enhanced radiotherapy and hyperthermia are being analyzed.

2. Head & Neck Cancer Therapy

Head and neck cancer remains the sixth leading cause of cancer related morbidity and mortality, despite the research and the expanding knowledge, concerning the etiologic factors and tumor biology. Multidisciplinary approach is required for effective management. To this day, the major treatment modalities are still surgery, radiotherapy and chemotherapy. Exploration of novel methods and strategies are more than necessary, in order to achieve considerable improvement in the treatment outcomes and quality of life, in these patients.

Radiotherapy (RT) has evolved greatly, the past 10 years, with the application of conformal and intensity modulated techniques. The major goal of RT is the achievement of locoregional control of head and neck cancer, with minimum damage to the critical organs of the region.¹ However, there are major limitations to achieve this goal, because of the complexity of the regional anatomy, and also the extent of primary tumor and neck lymphadenopathy, especially in the case of locally advanced disease.¹ Tumor relapse is often, with current treatment modalities. As such, a personalized approach, involving novel treatment methods, is required.

3. Radiotherapy

3.1 Introduction

One of the widely applied treatment methods in cancer patients is radiotherapy (RT). Like surgery, radiotherapy is a locoregional treatment method. The objective is to achieve tumor control, while preserving functionality of normal tissues. It is often used with surgery and chemotherapy to improve therapeutic outcomes.² Radiotherapy can be defined as the use of radiation (electromagnetic or particulate radiation) for the purpose of destroying microscopic regions of tumor extension. In order to understand the therapeutic use of ionizing radiation, a basic comprehension of both the physics of

radiation therapy delivery and the biological effects of the interaction of radiation with matter is required.³

3.2 Radiation Physics

There are two general categories of radiation, electromagnetic and particulate. Despite many years of research, the main therapeutic modality in radiotherapy still constitutes of photon-beams (electromagnetic radiation), because of many unresolved technical issues related to the use of particulate radiation.^{2,3}

3.2.1 Interaction of radiation with matter

The therapeutic effects of radiation are caused by the interaction of ionizing radiation with matter. These effects can be produced when packets of energy are deposited in a volume of tissue, producing ionization. Ionization is the process by which an atom acquires a negative or positive charge by gaining or losing electrons. Ionization can result from the loss of one or more electrons after collisions with subatomic particles.³

Photons can interact with (in order of increasing energy):

- the atom as a whole
- tightly bound inner shell electrons
- loosely bound outer shell electrons
- the extranuclear space surrounding the nucleus
- the nucleus itself

Interactions of electromagnetic radiation with matter, with clinical importance in radiotherapy, have three major forms. These are Compton effect, photoelectric effect and pair production. In modern-day megavoltage RT, Compton effect is of the greatest

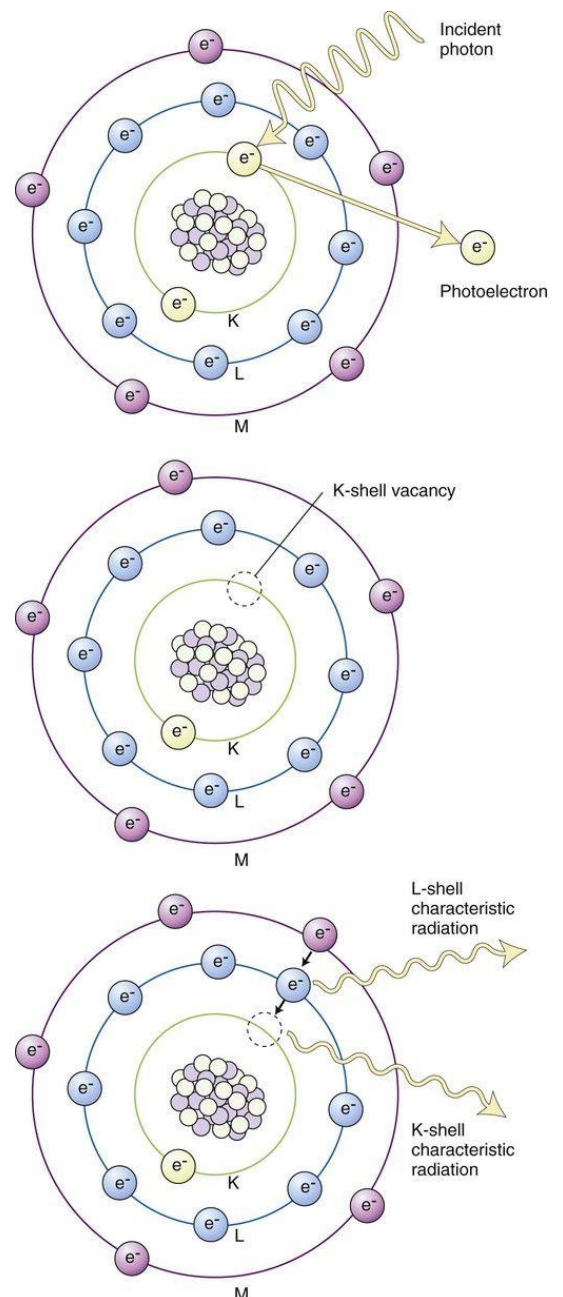


Figure 1: Photoelectric Effect⁴

importance. Photoelectric effect is important in diagnostic radiology and has only historical importance in present day RT.²

3.2.1.1 Photoelectric Effect

Photoelectric effect (figure 1) can occur when photons have sufficient energy to produce ionization of an atomic electron. Photon energy is entirely absorbed. Some is lost in breaking the electron binding energy. The rest is carried away as kinetic energy of the ejected electron. When the electron (photoelectron) is ejected from the inner-shell orbital, an electron of the upper shell fills the vacant place, which leads to the emission of characteristic X-rays or Auger electrons. The probability of a photoelectric interaction scales with the cube of the atomic number (Z) and the inverse cube of the photon energy (E), making the photoelectric effect very sensitive to material type and much more prevalent for lower photon energies. Photoelectric effect is the dominant interaction in tissue, below 30 keV.³

3.2.1.2 Compton Scattering

When photon energy is significantly higher than the binding energy of an electron, the photon can scatter from the electron without being absorbed. This interaction leads to a photon with reduced energy and new direction and a recoil electron with some fraction of the initial photon energy. The energy of the scattered electron varies with the scattering direction. A scattered electron in the direction of the incident photon has most of the initial photon energy, whereas electrons scattered at greater angles have successively less energy. Compton scattering is only weakly dependent on Z and is the dominant photon interaction in tissue between 30 keV and 30 MeV.³

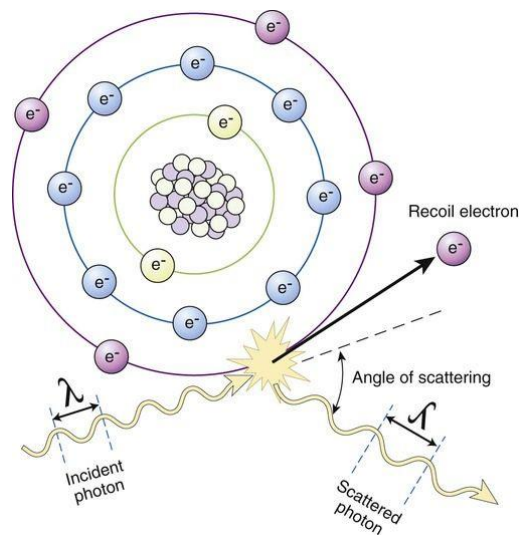


Figure 2: Compton Scattering⁴

3.2.1.3 Pair Production

Above 1.022 MeV, photons can interact in the presence of a strong nuclear field. The photon will disappear and spontaneously become an electron-positron pair. The electron and positron will divide the initial photon energy between them to create

their mass and kinetic energy.³ When these particles interact with the surrounding materials, they will lose their energy. Upon losing all their energy, the electrons will be absorbed into an atom. The positron, on the other hand, will annihilate by interacting with a local electron, creating two 511 keV photons (this annihilation is what positron emission tomography scanning detects). Pair production is the dominant atomic interaction in tissue for photons above 30 MeV and therefore has only a minor effect in radiation therapy, because of the significantly lower energies.³

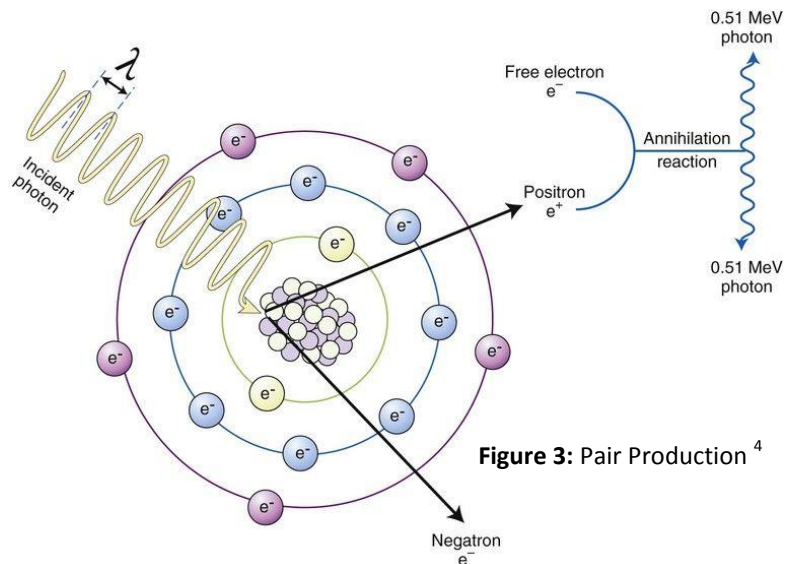


Figure 3: Pair Production ⁴

3.2.1.4 Charged Particle Interactions

Charged particles lose and transfer energy to a medium through collision and radiation. Collision leads to energy transfer resulting in ionization, excitation, and molecular damage. Energy is absorbed in the medium at or very near the site of the interaction. Collision energy loss accounts for more than 95% of energy loss in tissue for therapeutic-energy electrons and is the major source of absorbed dose along the path of the electrons. Radiative energy loss occurs when particles are accelerated in the electric field of a nucleus and emit a fraction of their energy as a photon. This process, called bremsstrahlung, is relatively unimportant in tissue but is fundamental to the production of therapeutic photons in a linac.³

Most electromagnetic interactions result from interplay between photons and electrons, because many photon interactions result in atomic ionization and release of an energetic electron, with some of the electron energy converted back into photons through the bremsstrahlung process. Thus the effects of therapeutic beams passing through tissue can

be described as a photon-electron shower, with the highly penetrating photons carrying energy deeper into tissue until a scattering event occurs, and the resulting scattered electrons depositing most of the resulting energy locally through collisional interactions.³

3.3 Generation of Therapeutic Radiation

Therapeutic radiation must be generated in such way that it can be directed at the site of interest. The main systems used for generation of therapeutic radiation are linear accelerators (linacs).

3.3.1 Linear Accelerators (linacs)

In radiation oncology, external beam radiation therapy is the most common modality. The majority of therapeutic electromagnetic radiation is generated in a linear accelerator (linac). A linac is a device that accelerates charged particles (electrons), to velocities near the speed of light, using oscillating electric fields to propel the electrons through a series of accelerating cavities. Electrons are accelerated to energies typically between 4 and 18 MeV. High-energy electrons are focused and steered by electric and magnetic fields focus, to strike a thin metal target that stops the electron beam. The electron energy is converted, with some fraction, to a spray of photons through the bremsstrahlung process. The bremsstrahlung photons (X-rays), have approximately the same motion direction as the electrons and an energy spectrum, ranging between a few 10's of keV and the maximum energy of the initial electrons. Then the photon beam passes through a series of filters and beam-shaping elements that flatten and define the edges of the beam. Intensity of the photon beam (number of photons per unit area) determines the dose. The beam intensity decreases as it passes through tissue, by two major effects. It decreases with increasing distance from the source and second, as photons are attenuated from the beam via absorption and scattering effects. Intensity decrease varies, depended on photon energy. Although intensity decreases immediately upon entering a material, the energy released through photon interactions is spread over a few centimeters, as the electrons scattered by the photons gradually lose their energy. Dose distribution is characterized by a region of rapid increase near the surface, a leveling off at a depth of 1 to 3 cm, and gradual dose falloff as depth increases. The plot of dose

versus depth is called a percent depth dose curve. Because higher energy photons are more penetrating, higher energy beams will attenuate more slowly, leading to a more gradual decrease in dose with depth.³

Linacs producing photon beams, can produce electron beams as well, by removing the photon-generating target and replacing it with a thinner electron scattering foil, which allows the transmission of the initial electron beam, but not without scattering the initially narrow beam into a broader distribution.³

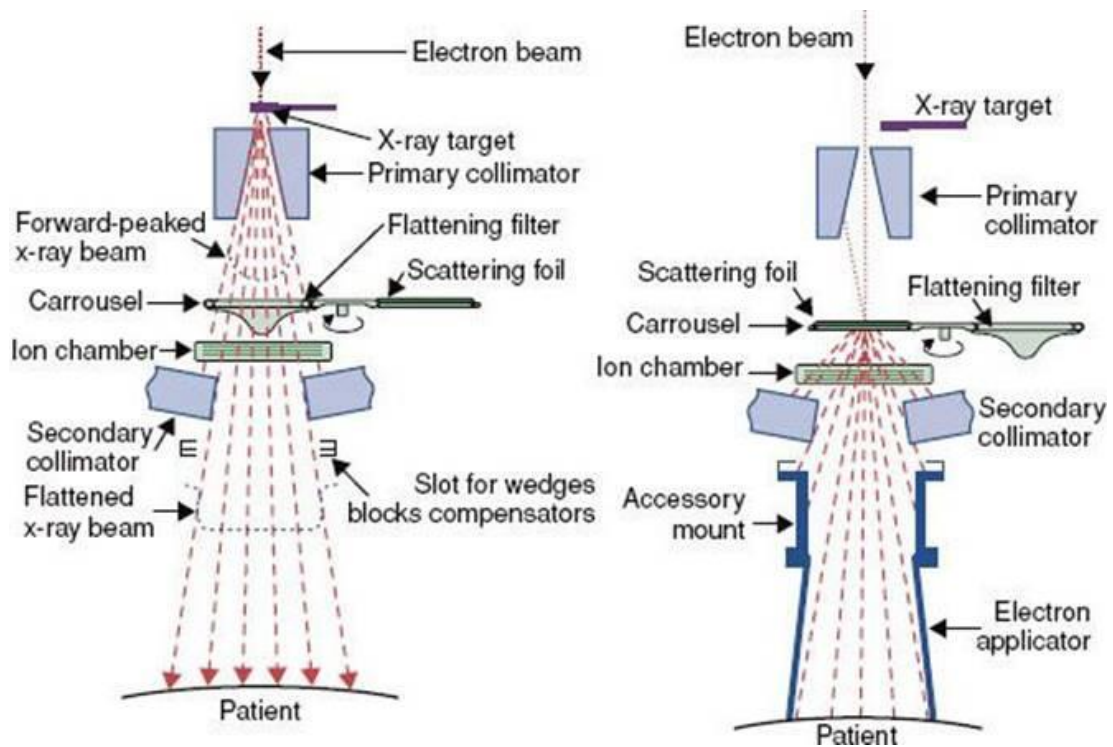


Figure 4: Linear Accelerator (Linac)⁵

3.3.2 Radiation Treatment Goals

Ionizing radiation, with its cytotoxic properties, contributes to tumor control but measures should be taken to limit the exposure of healthy tissue. Linacs are mounted on rotating gantries so that beams can pass through the site of interest from a variety of directions. The target is placed at or near the center of rotation, thus, making possible the delivery of high dose to the tumor region and lower dose to surrounding healthy tissue. In brachytherapy, proper dose to the target is achieved by designing and delivering a three-dimensional (3D) distribution of radioactive seeds within the tumor region. A high-dose region is created, that decreases rapidly beyond the tumor site.³

Requirements for both treatment modalities are:

- 3D understanding of tumor location within the patient anatomy
- Treatment plan customization for an individual patient
- Reliable and reproducible positioning of the patient relative to the radiation sources, in order to achieve precise radiation delivery, according to the plan.³

3.4 Biological effects of Radiotherapy

Ionizing radiation, passing through the medium, deposits energy in a random and discrete manner. Energy transfer is achieved through energetic packets called quanta, resulting in ionization of atoms. The molecules or atoms of the medium are potential targets. Additional damage can also occur by secondary particles, which are set in motion by the original ionization event (from the incident photon or particle) and this leads to a chain reaction that continues until all the energy is consumed.³

The biological results of radiotherapy are determined not only by the amount of energy deposited to the biomolecules. The pattern of that energy deposition plays an important role in determining the biological effectiveness of RT. This pattern is defined by the density of the discrete ionization events that occur along the track of the particle or

photon. The term linear energy transfer (LET) indicates the average amount of energy that is being deposited per unit path-length. Most of RT is performed using photons or electrons. However, radiation therapy that uses high LET particles, like neutrons or even higher LET heavy ions (such as carbon ions), achieve tumor control with lower total doses than RT that uses x-rays, γ -rays, or electrons.³ The biological importance of a particular molecule ionization depends on its role in cell's function and survival and how many copies of this molecule are present in the cell. The most important cellular macromolecule is DNA, which is present as a single, double-stranded copy.³

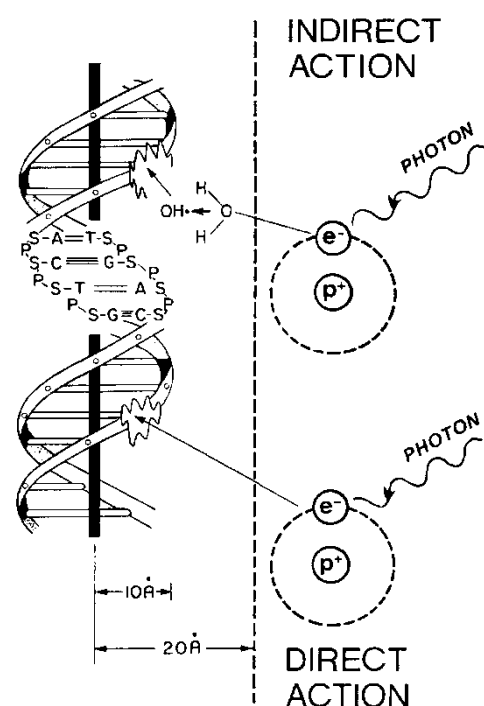
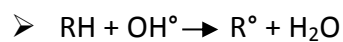


Figure 5: Mechanisms of Radiation Damage⁶

DNA may be hit directly from radiation, causing ionization of the atoms in the DNA molecule. However the most abundant molecule in the cellular microenvironment is water and as such, water has much higher probability for ionization. Water molecule ionization leads to radiolysis and the formation of free radicals (hydroxyl radicals), which are unstable and extremely reactive.³ Their range is as less as 100 Angstrom (Å). If a molecule of an organic material (RH), like DNA, is sited inside this range, it will react with them, which will lead to the production of free radicals of organic origin (R°).



This will result in transformation and damage of the organic structure of DNA indirectly (approximately 70% of total DNA damage).^{3,6}

The success of radiotherapy in tumor control depends on radio-sensitivity of tumor cells, as well as the tolerance of the surrounding normal tissue. Therapeutic index (TI) is defined as the ratio of NTT/TLD, where NTT is the surrounding normal tissue tolerance, while TLD is the tumor lethal dose, which is the dose of radiation that produces, in vivo, the complete and permanent regression of tumor. In case of highly radiosensitive tumor, NTT is much greater than TLD and TI is high. For radioresistant tumors, TLD is much higher than NTT and TI is very low.²

Delivery of therapeutic radiation in small dose fractions is based on the 4R's of radiobiology, namely: repair, repopulation, redistribution and reoxygenation. Repair is considered as the most important factor for fractionation. Fractionation enables normal tissue recovery (from sub-lethal damage) between fractions and therefore reduces the toxicity of RT. Repopulation occurs when the interval is more than six hours, which results in increase of surviving fraction. Repopulation is desirable in normal tissues but quite undesirable for tumor cells as it can lead to tumor recurrence.^{3,2}

Redistribution of proliferating cell populations from radioresistant to radiosensitive phase throughout the cell cycle increases cell kill in fractionated treatment.² Increase of tumor mass increases the need for blood-flow/oxygenation, which causes neo-angiogenesis. However these new vessels are abnormal and, as such, fail to provide enough blood/oxygen. Cells sited in distance more than 100-180µm from a vessel are hypoxic (because of low PO₂), which results in hypoxia, necrosis and radio-tolerance. Due to the fact that molecular oxygen in the radiated region produces many free radicals, when cells

get reoxygenated, which occurs during a fractionated course of treatment, they become more radiosensitive.^{3,2}

Macromolecules like DNA that have been ionized, undergo a series of chemical transmutations to get rid of unpaired electrons, which can produce further breakage of chemical bonds (which may lead to breakage of both DNA strands).³ This residual DNA damage, which constitutes a chromosome aberration, usually leads to cell death when it attempts to go through mitosis.^{3,2}

3.4.1 Tissue Types H,F

There are three cell types:

- Stem cells replicate to produce daughter cells, which either maintain the stem cell population or differentiate into other types.
- Functional cells are differentiated and incapable of further division.
- Maturing partially differentiated cells exist between the two states. They may still divide but with limited capability (do not possess telomerase).

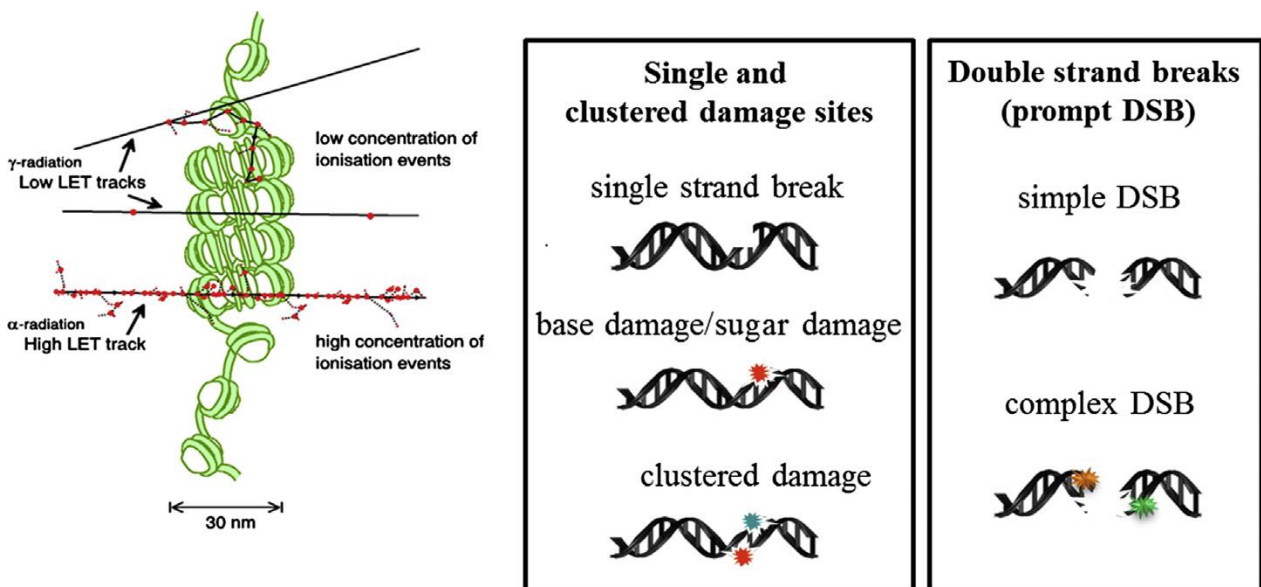


Figure 6: Types of Radiation-induced DNA damage⁷

- Hierarchical tissues (H-type) have all three cell types, with stem cells constantly produce maturing cells which differentiate and become functional cells. Hierarchical tissues include most epithelial cells and bone marrow.

- Flexible tissues (F-type) with cells that rarely divide but may be induced to by damage. Cells are functional but retain the ability to re-enter the cell cycle if required. Flexible tissues include liver, thyroid and dermis.

H-type tissues respond rapidly to radiation damage (acute effect: <6 months) as the stem cell population is killed and life-time of functional cells is similar with the reaction time to irradiation. F-type tissues may not display damage for some time (late effect: >6 months), especially if the dose is small, as not all cells enter the cell cycle immediately.^{3,2,8}

3.4.2 Radiation Sensitivity

To achieve tumor control, all clonogenic cells (tumor stem cells) must be killed. The most important factor is the radioresistance of cancer cells which can be estimated by measuring of cell killing efficiency per unit radiation dose. By plotting the amount of growth delay (in days) as a function of radiation dose, a dose response curve can be generated. The degree of tumor shrinkage assumed to be a reflection of the fraction of clonogenic tumor cells killed. Intrinsic and extrinsic to the cell, factors can alter its radiosensitivity.^{3,8}

Radiotherapy induced tumor control depends on clinical factors like stage and size of the tumor, as well as treatment factors like radiation dose, fractionation and total duration of radiotherapy. Biologic intrinsic radioresistance is determined by a complex network of molecular mechanisms in tumor cell (e.g. oncogenes, tumor suppressor genes).³ There is a cell-cycle specific response to radiotherapy, where the most radioresistant is the late S-phase.⁹

Apoptosis, a genetically encoded cell death program, is characterized by specific morphologic and biochemical changes. Apoptosis may be disrupted in tumor cells, which can result in a biologically aggressive tumor cell phenotype. Apoptosis can also counterbalance progression of tumorigenesis triggered by oncogenes.⁹ Tumor suppressor protein p53, which activation is triggered from radiation induced DNA damage, controls the expression of proteins, with an important role in cell cycle control and factors related to cell death execution.^{2,9}

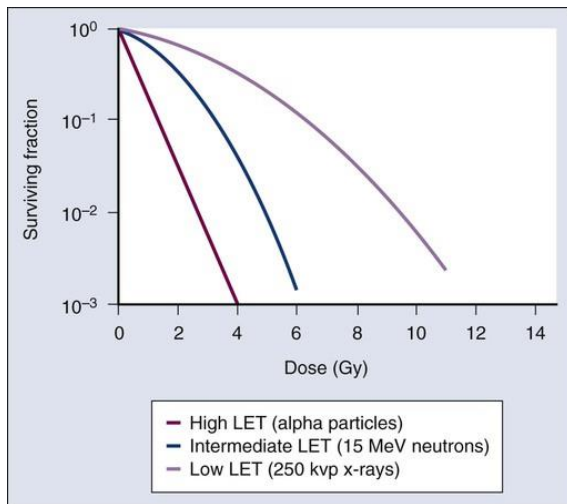


Figure 7: Dose response curves for radiations of differing linear energy transfer (LET). The relative biological effectiveness (RBE) of neutrons or alpha particles relative to that of x-rays is defined as the ratio of doses (x-rays/neutrons) to yield the same biological effect.³

3.4.3 Radiosensitization

A physical factor of great importance is the radiation type used for therapy. High LET radiation is more biologically effective than low LET type. Relative biological effectiveness (RBE) is defined as the ratio of doses of a known type of low LET radiation to that of higher LET radiation. Chemical modifiers are also important with molecular oxygen as the more potent.³ Oxygen is an extremely electron-affinic molecule that participates in the chemical reactions that lead to the production of free radicals after the absorption of energy from ionizing radiation, thus enhancing the radiation damage to DNA and other cellular macromolecules. This is called oxygen effect.³ Radiosensitivity increases as the oxygen tension increases from anoxia to 10 Torr, but then plateaus, with no further significant increase as the oxygen tension increases through the range found in healthy tissue. Because the underlying chemical reactions are essentially complete within a few milliseconds after irradiation, oxygen must only be present during irradiation to produce full radiosensitization.^{3,9}

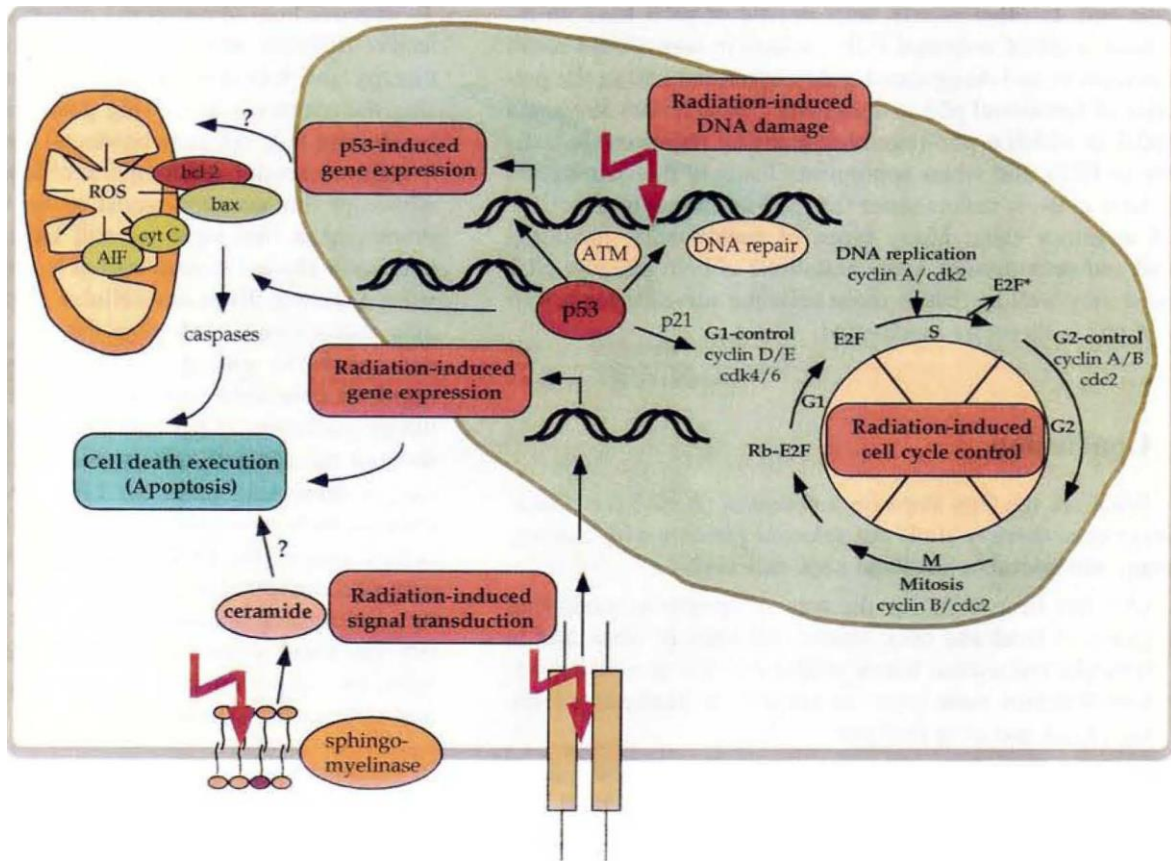


Figure 8: Selected intracellular targets for ionizing radiation ⁹

3.5 Radiation Treatment Planning & Delivery

External beam fractionated radiotherapy is the most common technique used. Beams are delivered through multiple angles. In order to achieve maximum dose delivery to the tumor while minimizing normal tissue exposure to radiation, each of the beams must be shaped and altered in intensity.³ Traditional equipments were cobalt units since they were reliable and easy to maintain. However they have been partly replaced by linear accelerators, which can produce low (6MV) or high (10 to 15MV) energy X-rays, as well as electron beams of various energies.²

Prior to radiation delivery, simulation and treatment planning must be completed. Simulation determines proper selection and orientation of beams to properly overlap the area of interest.³ Dose calculation requires patient's dimensions and determination or creation of identifiable reference points are needed for correct beam targeting. Recent techniques use CT scan of a patient (Virtual Simulation). After the CT scan, with the patient still positioned on the scanning table, the physician uses the superior soft tissue

contrast of the CT scan to select a location as isocenter, within the target area.³ A laser system moves to indicate the position of the physician-selected isocenter on the patient surface, allowing the external markers or tattoos to be placed for future alignment with the linear accelerator vault laser systems.^{3,2}

Treatment planning uses CT scan and images from other modalities (MRI, PET) which are transferred to the treatment planning system. Identification of target volumes and normal structures and selection and modification of beams are necessary in order to achieve specified dosimetric goals.³ The target volume is determined by combining:

- Gross tumor volume (GTV): all detectable disease,
- Clinical tumor volume (CTV): expansion of GTV, including possible microscopic disease, adjacent tissue and draining lymph nodes,
- Planning target volume (PTV): a further expansion of CTV to account anatomic motion and position variations of daily setup.³

The next step is selection and arrangement of radiation beams, as well as total dose and fractionation of the treatment. Limiting normal tissue exposure can be achieved by the use of customized block but also, on latest systems, by using automated beam-shaping (multileaf collimator).^{3,2}

3.5.1 Three-dimensional Conformal Radiotherapy (3-DCRT)

3-DCRT is a useful technique for tumors, which are in close vicinity to important structures. The radiation field conforms to the shape of the target volume. The volume to be treated is marked in every CT slice. A 3-D image of the target volume is generated by the computer and critical structures can be highlighted. The best beam arrangement is defined and the optimum dose distribution is calculated. Critical structures can be shielded by beam shaping, with the use of customized lead blocks or multileaf collimators, which are computer-controlled motorized movable lead leaves within the treatment machine and can block part of the radiation field. A typical duration of treatment session is approximately 15-30 minutes.²

3.5.2 Intensity Modulated Radiotherapy (IMRT)

Achieving an homogeneous radiation dose distribution across a tumor area can be difficult, because of a variety of reasons, such as the presence of a sensitive normal structure in the vicinity of the target or irregular patient surfaces.³ Intensity modulated radiation therapy (IMRT) is an advanced form of 3-DCRT. It uses sophisticated systems (hardware and software) to vary the shape and intensity of radiation delivered to different parts of the site of interest.² The difference with 3-DCRT is the varying intensity of multiple radiation beams, in IMRT, which improves the overall homogeneity of the dose to the tumor area and decreases the dose to normal tissue. This is made practical by the use of multileaf collimators. Computer algorithms (optimizers) calculate intensity distributions and beam orientations to meet the requirements of dose goals and toxicity limits.³

In every treatment day, the patient must have the exact position as in the simulation. Rough alignment can be achieved by aligning the tattoos from the simulation, with lasers in the accelerator vault. More precise alignment can be accomplished by image-guided radiation therapy (IGRT) techniques. Improvement of patient alignment also includes the use of in-room CT scanners or linac-mounted cone-beam CT scans.³

3.6 Particle Therapy

Photon beams is the most commonly used form of radiotherapy. However, particle beams also have useful properties. Light charged particles, such as electrons, lose energy gradually, depositing dose approximately evenly, until all energy is expended. Electron beams are limited to depths of 5 to 6 cm. Also, electrons can scatter at large angles, causing the electron beam to spread as it passes through tissue. Beams consisting of heavier particles (protons, neutrons, heavy ions) can overcome these limitations.³

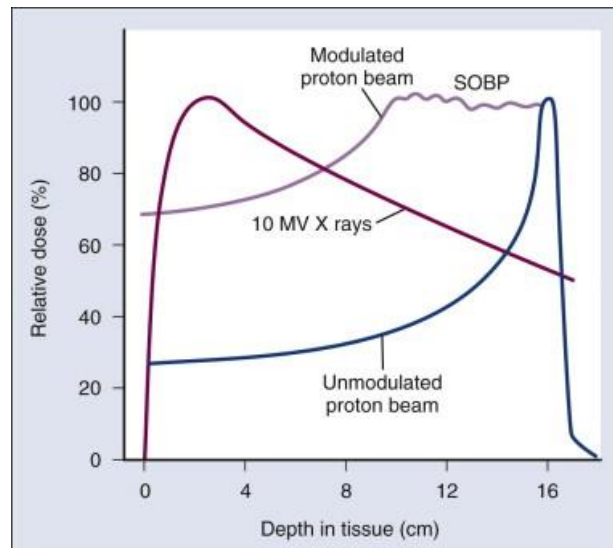
Radiotherapy that uses heavier particle beams has many advantages:

1. Scattering occurs at smaller angles, allowing less blurring at the edges of dose distribution and more precise dose delivery.
2. It has higher LET, resulting in greater biological effectiveness.
3. Particle beams (such as proton beams) have a sharp distal end of dose distribution, avoiding irradiation of normal tissues deeper than the tumor region.³

3.6.1 Protons

Proton beam therapy is the most common type. Proton beams are produced by accelerating ionized hydrogen. Devices like cyclotron or synchrotron are used for the production of these beams, with energies in excess of 100 MeV. Protons lose energy at an increasing rate as the beam loses energy with depth. This effect culminates in a region of rapid dose deposition near the depth of maximum penetration, called the Bragg peak. Because of the fact that the depth of Bragg peak increases with beam energy, it is possible to achieve highest dose delivery to tumor region, with lower doses upstream and negligible dose downstream of the target area, by appropriate selection of beam's energy.³

Figure 21: Depth-dose comparison between x-rays, unmodulated, and modulated proton beams. (From Verhey LJ, Petti PL. Principles of radiation physics. In: Hoppe RT, Phillips TS, Roach M, editors. Leibel and Phillips textbook of radiation oncology. 3rd ed. Philadelphia: Saunders; 2010).³



3.6.2 Neutrons

Neutrons are heavy particles, not charged, produced by specialized equipment. Neutrons interact with matter through different mechanisms than photons and protons. They can cause low-energy protons and heavier ions to be ejected during collisions. Ejected particles cause biological damage relative to their LET. Neutrons do not have a dose distribution advantage over x-rays. However, because of their higher RBE, they are more potent biologically and have the potential to destroy effectively, tumors that are relatively radioresistant. Although that many studies have been conducted, it has been difficult to find an advantage to the use of neutrons over conventional radiotherapy methods.³

3.6.3 Heavy Ions

Researchers have had a long-standing interest in using heavy ions, such as accelerated carbon ions, for therapeutic applications and that interest still continues. These particles have the potential to combine the biological advantages of neutrons and the dose distribution advantage of protons. However the high cost of the necessary equipment has limited their development.³

3.7 Acute and Late Normal Tissue Reactions

The acute complications from normal tissue exposure to radiation are observed within three months, while late effects can occur even months and years after RT. The tissues that divide rapidly (e.g, mucous membranes) respond acutely to radiation and are responsible for much of the acute morbidity of the treatment.² Late side effects are caused by microvasculature damage or stem cell depletion. Side effects are related to site, dose, volume and time of treatment. When radiotherapy is combined with other forms of treatment (surgery, chemotherapy), probability of radiation-related morbidity can increase, as well as its severity.²

3.8 Nanotechnology in Radiotherapy

Despite the significant progress that has been made in clinical oncology, the level of knowledge and understanding in aetiopathology of head and neck cancer as well as long-term survival rates for those patients, still remain low.¹⁰ An important reason for the failure, in many cases, of current therapeutic modalities and tumor relapse is the development of resistance to these treatment methods. The reasons of radiotherapy failure include the limitations of radiation dose, because of the possibility of injury to the surrounding normal tissue. Another reason is that some tumor cells are farther away from the site of radiation and might receive a lower intensity of the radiation beam. Furthermore, the cells can develop resistance to the radiation.¹¹ In addition, another important factor for radioresistance is the hypoxic tumor core. In recent years, the research in the field of nanotechnology and its applications in medicine are *impressively promising*. The use of nanoparticles, consisting of high Z (atomic number) elements, as radiosensitizers, has attracted great interest in radiation oncology. Irradiation of

nanoparticles leads to the production of photoelectrons and Auger electrons, which can contribute to the dose enhancement and subsequent radiobiological enhancement.¹² Specifically, the electrons, from the initial ionizing events, can induce inner shell ionization of the nanoparticle's atoms. When ionized by X-ray or Gamma(γ)-ray energy, mid- to high-Z elements can produce a cascade of low-energy Auger electrons, in the subsequent relaxation of the excited core, that can locally enhance the effective radiation dose and damage cells through direct or indirect action (Kobayashi et al., 2010).^{13,12} The radiation dose enhancement, that dense inorganic nanoparticles can provide, depends on the composition and size of the particles, uptake into cells, and the energy of the applied radiation.¹³

Last years' studies, have shown that gold nanoparticles (AuNPs) may improve radiosensitivity and radiotherapy efficacy. Gold is a biologically safe material, with flexibility in terms of nanoparticle size, shape, and functional groups. AuNPs have a wide range of applications in medicine in general and in cancer therapy in particular. Recent studies have suggested the use of gold nanoparticles as drug carriers, photothermal agents, imaging contrast agents, and radiosensitizers. Furthermore, AuNPs, with their unique surface properties, can be conjugated to various peptides, antibodies, and other biomolecules for surface functionalization.¹⁴

Heavy elements have significantly higher photoelectric cross-sections than soft tissue for sub-MeV energies, approximated for "X-ray energies".¹⁵ High atomic number of gold (Z=79) makes AuNPs ideal radiosensitizing agents, because of great absorption of photons (when irradiated) and release of secondary energy in the form of photoelectrons, Auger electrons, and X-rays into the surrounding tissue. If accumulation of AuNPs in cancer cells is achieved, the probability of DNA damage can increase significantly. Accumulation of gold nanoparticles in cancer cells can be managed through active targeting (functionalization of NPs with targeting ligands) or passive targeting (EPR effect), leading to enhancement of the radiation effect on the tumor. Several studies have shown that increased absorption of radiation may have important clinical implications in terms of tumor shrinkage and prolonged survival of cancer patients.¹⁴

3.8.1 Nanoparticle Radio-Enhancement Principles

The use of high-Z NPs offers the potential of amplification of radiation induced effects selectively in the tumor site, enhancing therapeutic efficacy. This “nano-radio-enhancement” is possible due to the atomic excitation of nanoparticles by incident radiation and the enhanced electron release, compared to water molecules.¹⁶

Excitation of high-Z nanoparticles, caused by irradiation (photons, electrons or fast ions), is followed by de-excitation via redistribution/rearrangement of electronic states, resulting in fluorescent photon emission (predominantly K-shell transitions) and Auger electron emission (predominant for inner shells, other than the K orbital). These secondary particles can ionise surrounding biomolecules and neighbouring nanoparticles, resulting in the enhancement of the radiation-induced damage to target cells.¹⁶

The most important interaction of incident photons with high-Z atoms is the photoelectric absorption. Because of the fact that photoelectric cross-section strongly depends on Z, high-Z nanoparticles have the potential to transfer energy to the medium, when irradiated (through photoabsorption and subsequent electronic emission), much more effectively than water.¹⁶

Photoelectron ejection from any shell, results in an electronic perturbation around the nanoparticle. Multiple photoelectrons emitted from many atoms in a high-Z NP, can produce an enhancement in dose. Furthermore, an additional enhancement effect (nanoscale enhancement) is produced by the following atomic de-excitation process that amplifies the electronic perturbation in the immediate vicinity of NP. For high-Z atomic targets, K-shell de-excitation occurs mainly via fluorescence emission. De-excitation of high-Z atoms via Auger electron emission occurs mostly from inner shells higher than the K-shell. Fluorescent photons travel further than Auger electrons and delocalise the local perturbation away from a nanoparticle. For smaller nanoparticles, the chain of escaping multiple low-energy Auger electrons may result in a highly reactive nanoparticle with highly charged atomic states. The nanoparticle atoms, excited by intra-atomic Auger decay, can de-excite via inter-atomic/-molecular electronic decay, involving neighbouring water and other biomolecules.¹⁷ Both inter-atomic Coulomb decay,^{18,19,20} driven by energy transfer, and electron-transfer mediated decay, driven by charge transfer,²¹ are ultra-fast

relaxation processes that may ionize surrounding molecules and produce slow electrons, thereby amplifying radiation damage beyond that predicted by Auger decay alone.¹⁶

3.9 Nanoparticles' Properties

High-Z elements have the potential to interact effectively with ionizing radiation, but these properties are not enough to manufacture an efficient radio-enhancer. High-Z elements assembled as a high electron density material, are required to achieve the absorption/deposition of a high-energy dose, when irradiated.²² Beyond the selection of composition and structure of nanoparticles, well-controlled physico-chemical characteristics of NPs (size, shape, surface properties) can be independently optimized to determine their bioavailability and interactions with cells.²³

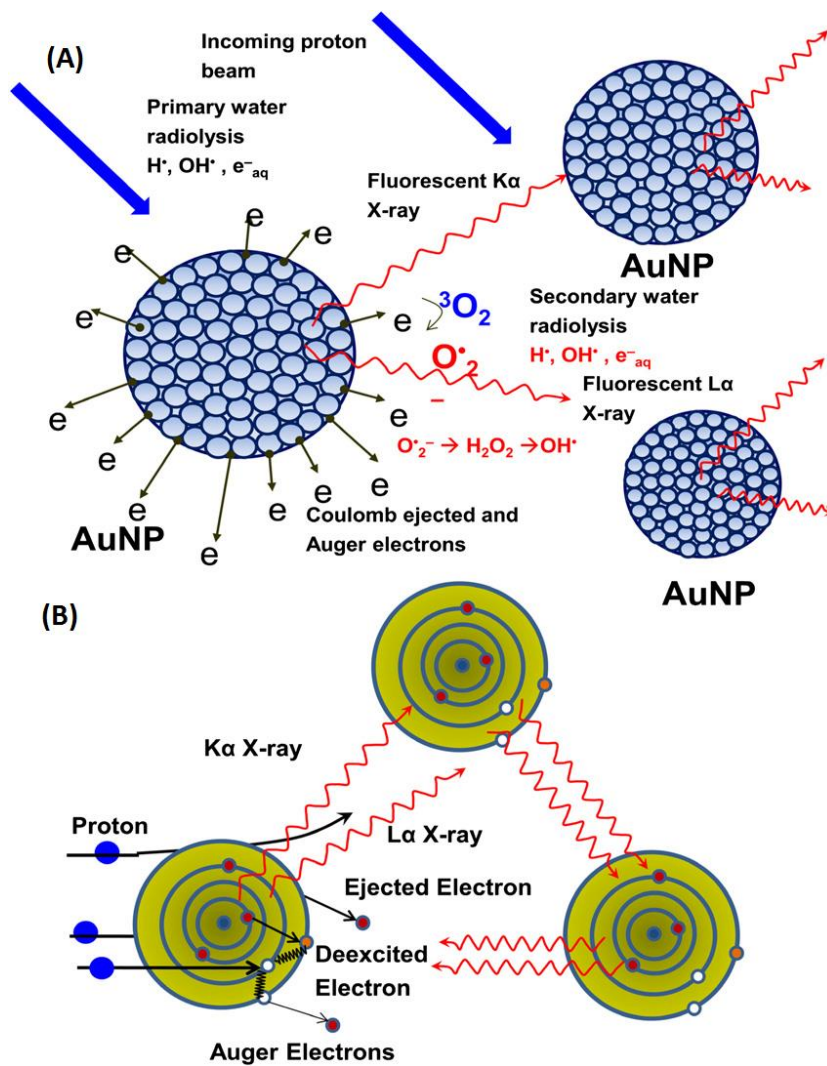


Figure 9: Enhanced ROS generation from proton-irradiated AuNPs. Incident protons have Coulomb collisions with tumoral NPs to ionize atomic electrons, followed by generation of x-ray and Auger electrons from the subsequent de-excitation process, collectively termed PIRT. This PIRT loses energy by ROS generation through secondary water radiolysis in an aqueous environment, contributing to the therapeutic enhancement of PIRT (A). Fluorescent x-rays or electrons emitted from one atom may excite nearby atoms and thereby release more secondary particles (B).²⁴

3.9.1 Nanoparticle Size

Size is a fundamental property for NPs transportation, accumulation and retention at the target site. Inorganic nanoparticles larger than 10 nm, tend to preferentially accumulate in liver and spleen (RES). Nanoparticles' size limit for renal and lung barriers are reported around 5.5 nm and 34 nm respectively. Passive targeting is associated with the enhanced permeability and retention (EPR) effect, where tumor transvascular pore barrier is reported to be 100–200 nm. The particle size is also important characteristic for efficient trafficking at the cellular and subcellular level. Metal-based nanoparticles with size around 50 nm have been reported to maximize cellular uptake. Aggregation of nanoparticles in biological media is also an important factor, participating to nanoparticles' cell uptake.²³

3.9.2 Nanoparticle Shape

Shape of NPs influences blood exposure by modulating interactions with the MPS. Effective nanoparticles accumulation within tumor vasculature has been reported using thin disc-like porous silicon particles. Also spherical shaped nanoparticles have been found more effective than rod-shape for a high gold nanoparticles cancer cell uptake.^{23,25}

3.9.3 Nanoparticle Surface

The surface of nanoparticles is an important property determining the interactions with biological systems. Stealth properties may be useful to increase circulation time, using neutral hydrophilic polymers (such as PEGylation). However, negatively or positively charged nanoparticles may contribute to rapid and strong non-specific interactions with cells' membrane.²³

3.9.4 Nanoparticle Charge

Charge of macromolecules²⁶ and nanomaterials^{27,28} alters systemic circulation times and intratumoral processes.²⁹ The presence of surface charge can alter the opsonization profile of the material, its recognition by cells in the organs of the MPS and its overall

plasma circulation profile.^{27,28,30-36} Negative surface charges can either affect or have no impact on the blood clearance of NPs, but positive charges generally have a negative effect on the plasma exposure to the nanomaterial. Positive charges possibly favor interactions of the NPs with the tumor blood vessels and eliminate their predisposition to diffuse deeper in the tumor, while preventing their redistribution in the systemic circulation. Also, charged colloids interact with the tumor longer than their neutral counterparts.^{25,30-42}

3.9.5 Passive and Active Targeting

Distribution of molecules to the tumor is determined by three major factors:

- a) extravasation of colloids from blood vessels
- b) further diffusion through extravascular tissue
- c) interaction with intracellular and/or extracellular targets within tumor micro-environment²⁵

Extravasation of colloids is influenced by their concentration in the blood, the relative permeability of the vascular wall to macromolecules and NPs as well as the nature of the extravascular environment. After extravasation to the tumor, their surrounding environment is composed of interstitial fluid, cancer and stromal cells and the extracellular matrix (ECM). Tumor's disorganized vasculature and congested extravascular environment are both the cause of the EPR effect and the principal source of uneven tumor accumulation and retention of nanomaterials. The third parameter represents the interactions of the colloids with the tumor whether through adsorption phenomena, cellular uptake or degradation and metabolism, which can affect the equilibrium of accumulation inside the tumor. They depend on the nature of the material, its affinity for components of the tissue and tumor composition.²⁵

Active targeting depends on the recognition of the ligand by its target substrate. Targeting ligands include antibodies, proteins, peptides, nucleic acids, sugars, and small molecules.^{25,43} Target molecules can be proteins, sugars or lipids present in diseased organs or on the surface of cells.^{44,45} Interactions of functionalized nanoparticle systems with their target are enhanced by the multivalent nature of the NP architecture. Multiple copies of the ligand increase the avidity of the NP for its target.^{25,46}

Actively-targeted NPs must be in the vicinity of their target in order to recognize and interact with it. However, systemic clearance of NPs affects the amounts available in the bloodstream supplying the tumor. Since tumor blood flow is low relative to the flow in MPS (Mononuclear Phagocyte System) organs,²⁸ increase in the NPs' affinity for the tumor targeted sites cannot always compensate for the clearance processes. Therefore, proper design of actively-targeted NPs is required for achieving the necessary prolonged circulation times. Similarly, because molecular targets are mostly situated in the extravascular space of the tumor, NPs rely on the EPR effect to reach their targets.^{47,48} As such, active targeting strategies cannot radically alter the biodistribution profiles of nanomaterials.⁴⁹⁻⁵¹

3.10 Nano-Radio-Enhancers (NREs)

3.10.1 Gold Nanoparticles (AuNPs)

Gold nanoparticles and their use in cancer diagnosis, imaging and especially treatment have attracted an increasing interest, due to the biocompatible properties of AuNPs and the ability for economical synthesis with different sizes and shapes. AuNPs have also the potential of active targeting, through functionalization of nanoparticle's surface with various ligands, as well as passive targeting through EPR effect (Enhanced permeability and retention effect).^{14,16,52,53}

Gold nanoparticles are ideal as radiosensitizing agents, due to the high atomic number of gold ($Z = 79$). Their greater absorption of photons (during irradiation) and the ensuing release of secondary energy (photoelectrons, auger electrons, and X-rays) into surrounding tissue, contributes significantly to dose enhancement. Accumulation of AuNPs in cancer cells increases the probability of creating DNA strand breaks, which is the primary mechanism of radiation-induced cytotoxicity. However, there is unclarity regarding the mechanism underlying cell death. The main suggested mechanism that leads to radiation-induced cell death, includes increased apoptosis, increased generation of intracellular reactive oxygen species or direct DNA damage causing DNA double strand breaks.¹⁴

3.10.1.1 Targeted AuNPs as radiosensitizer agents

A significant problem with the use of ultra-small, non-targeted nanoparticles, is rapid excretion by the kidneys. The amount of Au needed in early studies was above 2 g Au/kg body weight, which was very large amount of for human use, as it may cause toxicity. Moreover it's very costly. Also, irradiation in the experiments was performed immediately after particle administration. Longer circulation times of nanoparticles and delivery in multiple doses, are desirable for clinical applications. These goals can be achieved by optimization of the size, surface chemistry, and functionalization of the Au nanoparticles, which can prolong circulation times and accumulation in specific tumors.¹⁵

The fact that tumors have an increased metabolic rate, relative to normal tissue, results in a high demand for glucose. In many studies, thioglucose-conjugated Au nanoparticles were used, in order to increase uptake of NPs by cancer cells. When glucose-coated AuNPs accumulated into cells, increase of radiosensitivity was observed.¹⁵

Cancer cells are characterized by a lower pH than normal cells due to hypoxia and consequent anaerobic metabolism within tumors. The use of pH-sensitive pHLIP peptide, in 2013 study by Yao et al., to target AuNPs to mice bearing HeLa tumors, led to radiotherapy enhancement. This study demonstrated that pHLIP can mediate targeted delivery of nanoparticles to tumors. pHLIP technology can improve the delivery of gold nanoparticles to primary tumors (and possibly metastatic lesions) by providing specificity of targeting, enhancing local concentrations, and improving retention in the tumor mass for an extended period (several days).^{15,54}

In a 2015 study, Popovtzer et al. determined the radiosensitizing effect of cetuximab coated AuNPs, on Head and Neck Squamous Cell Carcinoma, in vivo and investigated the biological mechanisms as well as the toxicity of nanoparticles used. After subcutaneous injection of A431 cells (2×10^6) into the back flank area of 36 nude mice aged 10–11 weeks, tumor volume was measured until it reached diameter of 8–10 mm. Mice were then divided into 6 groups, which underwent treatment

Groups*	Type of treatment
Group 1	Control (no treatment)
Group 2	Radiation
Group 3	CTX
Group 4	Radiation + CTX
Group 5	Radiation + IgG-GNP
Group 6	Radiation + CTX-GNP

Figure 10: 6 mice in each group¹⁴

with radiation, cetuximab (CTX) or GNP, alone and in various combinations.¹⁴

One group was untreated and served as a control. AuNPs were with PEG layer, which was covalently conjugated to a CTX monoclonal antibody and, as a negative control, to an anti-rabbit IgG antibody. The mice were anesthetized, and irradiated, using a Varian linear accelerator. Radiation was administered as a single fraction of 25 Gy. Tumor volumes in the mouse groups were measured 5 weeks after irradiation. The size of the tumor (largest diameter) in the first and last measurements for each group were: group 1: 1.1 to 2.1 cm, group 2: 1.1 to 1.4 cm, group 3: 1.1 to 2 cm, group 4: 1.5 to 1.9 cm, group 5: 1.3 to 1.9 cm, group 6: from 1.3 to 1.3 cm. The difference in tumor volume from the control group was statistically significant for the radiation + CTX-GNP group, marginally significant for the radiation + CTX group, and non-significant for the other groups.¹⁴

The radiation + CTX-GNP group showed higher apoptosis at first week and less at 6 weeks post treatment, compared to the radiation-only group. The radiation + CTX-GNP group displayed a reduced level of proliferation and tissue repair. There was an evaluation of acute and late toxicity, in six mice that were injected with CTX-GNP. All six mice survived the full study period and there was no difference in blood count among the groups. This study showed that the use of targeted AuNPs is a promising novel method, which can improve radiosensitivity and radiation absorption in the tumor and consequently, increase survival in locally advanced HNSCC.¹⁴

3.10.1.2 AuNPs enhancing X-ray induced apoptosis in HNSCC

Electronically active surface of gold is the main reason for its catalytic properties on chemical reactions and promotion of ROS production. Radiosensitization through AuNPs use is based on gold's high absorbance properties, resulting in the deposition of photoelectrons and auger electrons energy in surrounding tissue.⁵⁵

Teraoka et al., in 2018 study, investigated the potential of AuNPs in enhancing X-ray irradiation effects on head and neck cancer cells, in vitro and the underlying mechanisms inducing cytotoxicity. Cell culture consisted of human head and neck carcinoma cell line HSC-3 (tongue carcinoma). AuNPs were diluted at different concentrations and added to culture dishes. Cells were exposed to a fixed X-ray dose (2, 4 or 8 Gy).⁵⁵

The effect of four concentrations of AuNPs without X-ray treatment was assessed in HSC-3 cells, with no significant difference between total cell number of the control cells and the cells treated with AuNPs. X-ray irradiation alone reduced total cell number.⁵⁵

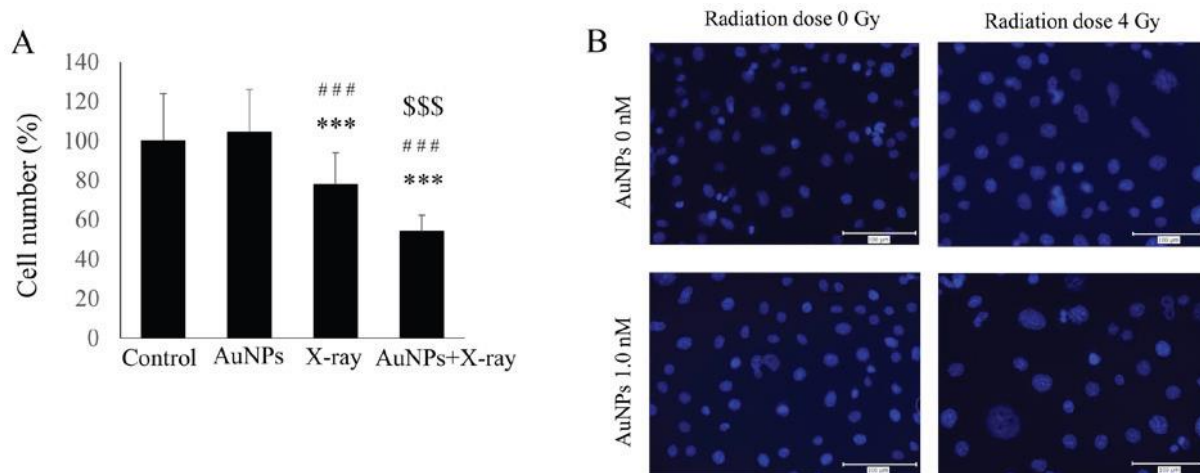


Figure 11: Combined treatment with 4 Gy X-ray irradiation and 1.0 nM AuNPs significantly reduced the total number of cells compared with in the control and 4 Gy X-ray irradiation alone groups. Y-axis values indicate percentage with the control as 100%. (B) DAPI staining of HSC-3 cells treated as controls (top left) with 4 Gy X-ray irradiation (top right); with 1.0 nM AuNPs alone (bottom left); and with 4 Gy irradiation plus 1.0 nM AuNPs (bottom right).⁵⁵

Combination of AuNPs and X-ray irradiation resulted in significant reduce in total cell number and proliferation and apoptosis were evaluated.⁵⁵

AuNPs have different toxicities, depending on concentration, size, shape, and surface chemistry. Combination of 1.0 nM AuNPs and 4 Gy X-ray irradiation resulted in a significant reduction in total cell number compared with irradiation alone. The reduction in the total cell number may be caused mostly from the induction of apoptosis, and not a decrease in cell viability. This is concluded from the observation that combined therapy of X-ray irradiation and AuNPs, increased the percentage of apoptotic HSC-3 cells without affecting the proliferation rate. The study has shown the potential of AuNPs in enhancing the cytotoxic effects of X-ray irradiation against human head and neck cancer cells in vitro.⁵⁵

3.10.1.3 Cancer cells' radiosensitization by folate conjugated Au@Fe₂O₃ nanocomplex

Gold nanoparticles (AuNPs) present synthetic versatility in size and shape and have high ability to conjugate with active targeting ligands. In addition, AuNPs have the potential for

both diagnostic and therapeutic applications. Core shell structures in the form of gold-coated magnetic nanoplateforms (like Au@Fe₂O₃NPs) are very useful due to high stability, greater biocompatibility and good surface reactivity, as well as their capability for active targeting strategy. Folic acid (FA) or folate is frequently used as a targeting molecule for functionalized NPs, as surface of cancer cells is FA receptor rich. Thus, it is a great chance to achieve NPs accumulation in cancer cells, using folate conjugation.⁵⁶

In 2018 study, Mirrahimi et al. described the role of folate conjugated Au@Fe₂O₃ NPs in selective accumulation in cancer cells and their capabilities as radiosensitizers. Two states of KB cancer cell (derived from mouth epidermal carcinoma) were used (because of their high levels of folate receptors), loaded with FA-Au@Fe₂O₃ NPs and free Au@Fe₂O₃ NPs. Morphology and size distribution of the synthesized NPs were analyzed by high-resolution transmission electron microscopy (HR-TEM). Hydrodynamic diameter and surface charge of NPs were measured by dynamic light scattering (DLS). KB cancer cells were incubated with FA-Au@Fe₂O₃ at concentration of 20 μM and exposed to 6MV X-ray at different doses (2 and 4 Gy) and compared with L929 healthy cells in the same conditions. Cell viability and apoptosis rate were also compared.⁵⁶

The dependence of cell death on increasing the dose in the presence of FA-Au@Fe₂O₃ is significant (P value < 0.05). Survival of KB cells treated with FA-Au@Fe₂O₃ and exposed to 2 and 4 Gy X-ray radiation decreased from 33.53 to 15.13%.⁵⁶

The effect of dose enhancement on the reduction of cell survival is not considerable, in the case of L929 cell. It was observed that cell survival was decreased from 67.23 to 66.96, which is not significant (P value > 0.05).⁵⁶

Enhancement of deposited energy was observed, by increasing dose in the presence of NPs. Radiation interactions (photoelectric effect, Compton scattering, pair production) with biomolecules such as DNA, induces ionization or excitation and free radical production, causing cell damage and cell death. The current study indicated that folate conjugated nanoparticle has the potential to be effective and targeted radiosensitizer even at a low concentration of 20 μM.⁵⁶

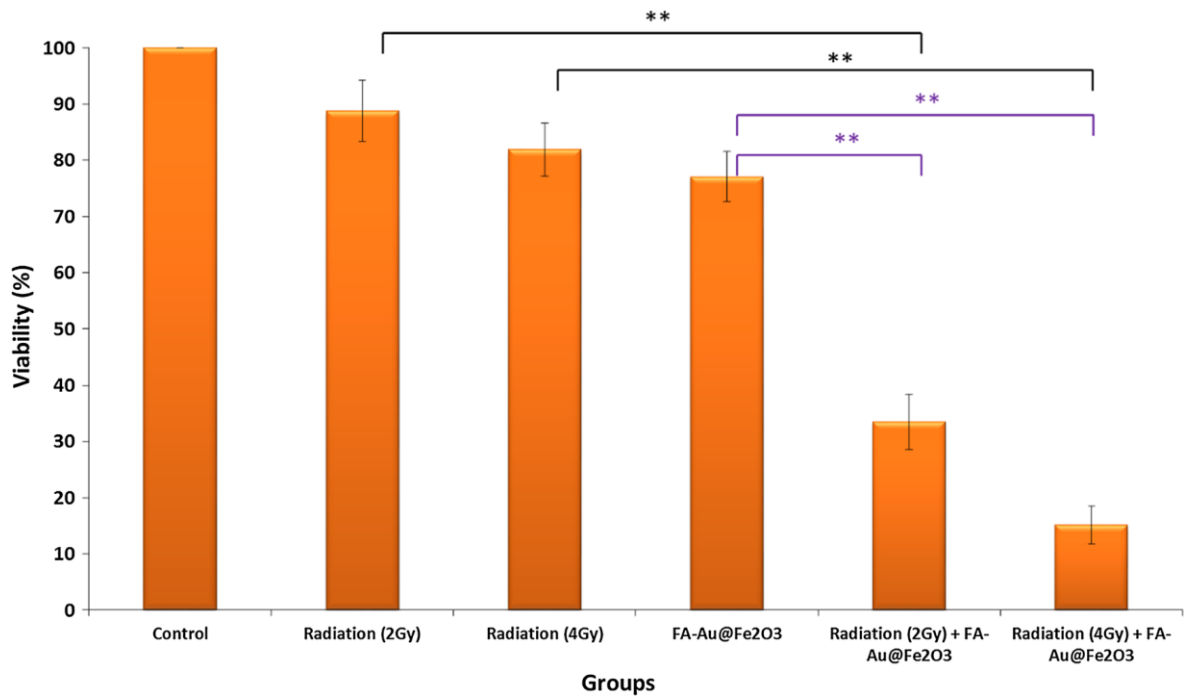


Figure 12: Viability of KB cancer cells received various treatments of nanoparticles and radiation therapy (** stands for $P < 0.001$)⁵⁶

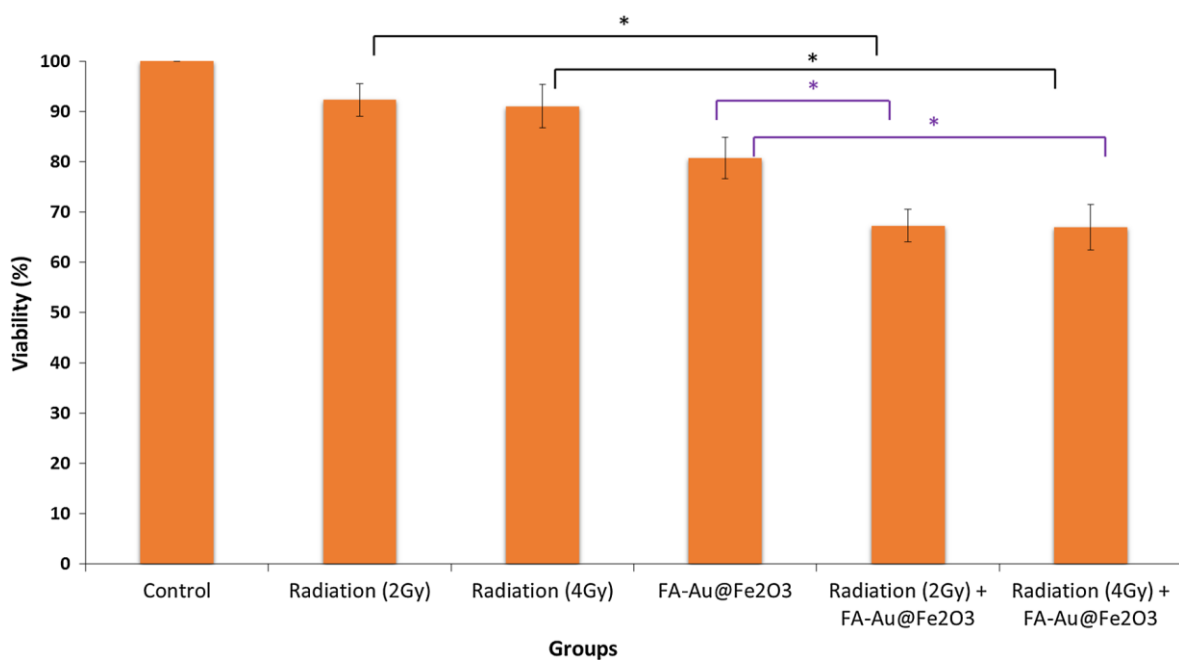


Figure 13: Viability of L929 healthy cells received various treatments of nanoparticles and radiation therapy (* stands for $P < 0.05$)⁵⁶

Targeted radiotherapy aims to achieve more apoptosis and less necrosis. Necrotic cells appear to lose membrane integrity before DNA degradation, with consequent cell swelling, dilation of cytoplasmic vesicles. Apoptotic cells lose membrane integrity after DNA degradation. The most frequent form of irradiation-induced cell death is mitosis-

linked death, usually leading to necrosis. Nanoparticles can change the mechanism of radiotherapy-induced cell death, from necrosis to apoptosis.⁵⁶

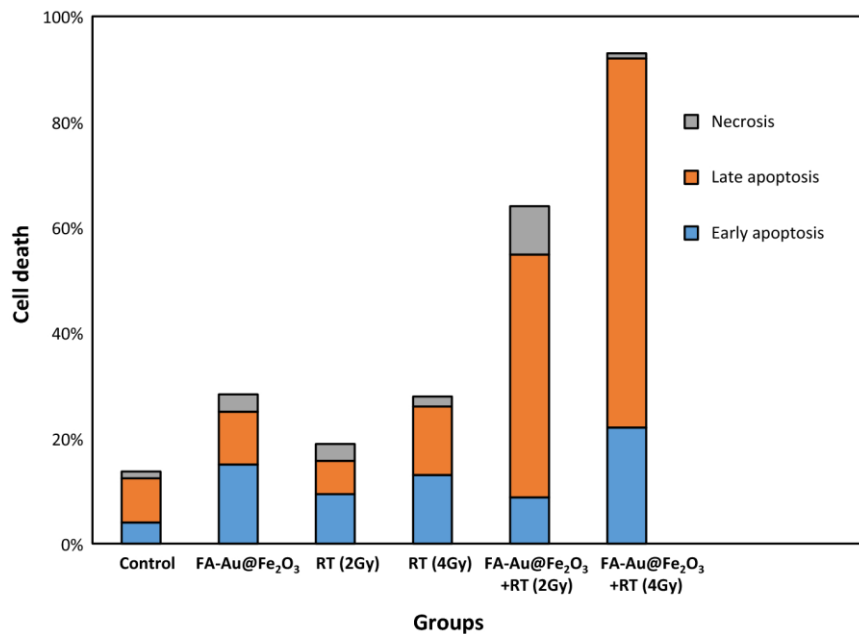


Figure 14: The percentage of necrotic and apoptotic KB cells after receiving various treatments⁵⁶

Considering the results of this study, it may be concluded that FA-Au@Fe₂O₃ NPs are suitable for cancer cells (with a wide range of folate receptors) radiosensitization.⁵⁶

3.10.1.4 Inhibition of the EGFR with nanoparticles enhances radiosensitivity in SCCVII cells

Head and neck cancer current treatment modalities, such as surgery and radiotherapy, have shown no significant increase in long-term survival over the past decades. Although radiation therapy has made important progress, patients still suffer from increased toxicity effects.⁵⁷

Epidermal growth factor receptor (EGFR) is a proto-oncogene that regulates many cellular processes, including proliferation, differentiation, survival, blood vessel formation, and DNA repair. The use of anti-EGFR therapies in cancer treatment depends on the role of the EGFR in oncogenesis. EGFR is over expressed or hyper activated, in many tumors, including squamous cell carcinoma of the head and neck. Anti-EGFR treatments combined with irradiation has anti-cancer effects in squamous carcinoma cells. EGFR inhibition can cause significant delay in tumor growth and can increase radiation sensitivity.⁵⁷

Yehui ping et al., in 2009 study, synthesized PLGA nanoparticles, to decrease expression of the EGFR in the SCCVII squamous cell line. The overall goal of this study was to confirm

the enhancement of radiosensitivity, in SCCVII cells (head and neck squamous cell carcinoma cell line) due to PLGA nanoparticles targeted delivery.⁵⁷

SCCVII cells were grown in minimal essential media and supplemented with 10% heat inactivated fetal calf serum, 100 IU/ml of penicillin and 100 lg/ml of streptomycin. PLGA nanoparticles were synthesized, containing antisense-EGFR-oligonucleotides. Solitary tumors were produced by subcutaneous inoculation of 10⁶ SCCVII cells into the floor of the mouth of 8-week old mice. Twenty-four hours before X-ray exposure, 2.5 mg/kg of nanoparticles containing EGFR ASOs were injected into the solid tumor. Injection of the same EGFR ASO dose was repeated immediately before X-ray exposure.⁵⁷

Cells were seeded in 96-well tissue culture plates, at a density of 2000 cells/well. Following treatment with nanoparticles carrying the antisense oligonucleotide for 24 h, the cells were irradiated at the dose of 2 Gy.⁵⁷

Tumor heterografts and cell lines were irradiated with a linear accelerator. Prior to irradiation, cells and mice were treated with nanoparticles. The dose of irradiation varied according to the need of experiment in vitro. A single 4 Gy dose was delivered for radiation therapy in vivo. The endpoint for tumor growth delay assays was applied after 7 days of irradiation.⁵⁷

To investigate whether antisense EGFR nanoparticles increase cell sensitivity to radiotherapy, antisense EGFR nanoparticles were combined with radiotherapy at the 2 Gy dose and cell viability was again measured in MTT assays. Combination of nanoparticles radiotherapy increased cell death at 48h post-transfection, compared with the control group. Similar results were observed by clonogenic cell survival analysis. Following irradiation, the ability of cells to form clonal colonies, after antisense EGFR nanoparticles treatment, decreased significantly along with the increase of irradiation dose. The combined treatment of cells with antisense EGFR nanoparticles and radiotherapy caused delay in tumor heterograft growth.⁵⁷

Antisense EGFR nanoparticle combining with radiotherapy treatment leads to cell cycle arrest at G1 and increase apoptosis in SCCVII cells. Treatment with antisense EGFR nanoparticles also led to increased apoptosis in these cells.⁵⁷

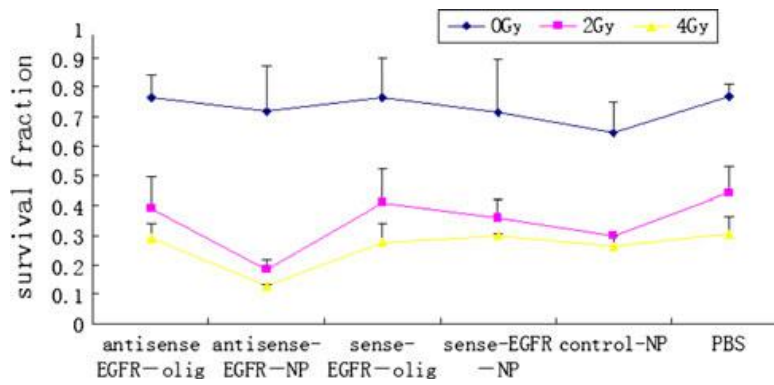


Figure 15: Survival curves for SCCVII cells after irradiation. Clonogenic cell survival analysis shows no difference in clone formation for all non-irradiated groups ($P > 0.05$). Following irradiation, survival of cell clones in antisense EGFR nanoparticle-treated group decreased significantly along with the increase dose ($P < 0.05$).⁵⁷

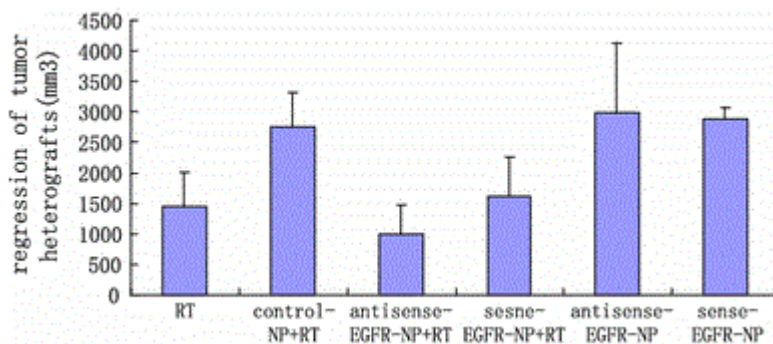


Figure 16: Combined treatment of cells with antisense EGFR nanoparticles and radiotherapy causes regression of tumor heterografts ($P < 0.05$).⁵⁷

Results from this study indicated that treatment with antisense EGFR nanoparticles downregulates EGFR expression and increases sensitivity to radiotherapy in SCCVII cell lines. It was also demonstrated that the SCCVII cells are sensitive to radiation damage when EGFR is inhibited by antisense EGFR NPs. Enhanced radiosensitivity may be associated with cell cycle redistribution and interruption of DSB (double-strand breaks) repair.⁵⁷

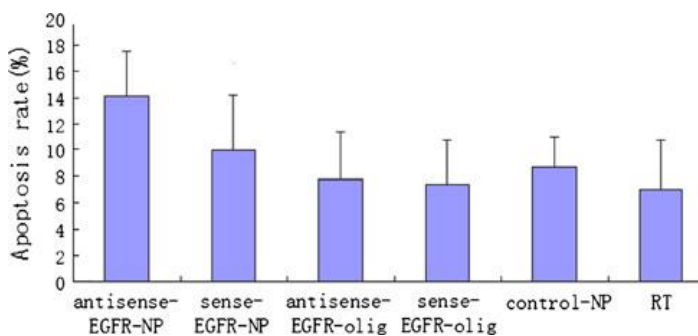


Figure 17: Apoptotic rate of SCCVII cells after 4 Gy irradiation. Antisense EGFR nanoparticles lead to increased apoptosis in treated cells ($P < 0.05$).⁵⁷

This study demonstrated that antisense EGFR nanoparticles enhance radiosensitivity by inhibition of EGFR-mediated mechanisms of radioresistance. Results are of great importance, regarding the clinical use of gene therapy and radiotherapy for head and neck squamous cell carcinoma, as combination of these NPs with radiotherapy may

improve therapeutic efficacy, even in the case of cancer cells resistant to anti-EGFR therapy.⁵⁷

3.10.1.5 Personalized targeted AuNPs impact on radiosensitivity & imaging of adenoid cystic carcinoma

Adenoid cystic carcinoma (ACC) is a malignancy arising usually in salivary and lacrimal gland. It usually has prolonged but progressive clinical course, with high tendency for distant metastasis. Tumor relapse is often, despite the meticulous surgical removal. Histologic grade, which is related with aneuploidy and genetic alterations in the tumor genome, determines the clinical outcomes. Treatment of choice, for salivary gland tumor, is usually surgery followed by post-operative radiotherapy. However, radiation efficacy is not established.⁵⁸

Personalized therapy refers to molecular profiling, using genomic characteristics of cancer cells in order to detect potential targets for treatment modality. Molecular alterations in ACC have an important role in the decision process of treatment strategy. However, there are no significant data that corroborate the worth of this approach to radiotherapy treatment.^{58,59-64}

Functionalization of AuNPs specifically to cancer biomarkers leads to accumulation of gold selectively into tumor site, thus enhancing the radiation effect on the target, while sparing the surrounding normal tissue. Hazkani et al., in a 2017 study, performed molecular profiling of a major salivary gland ACC, to identify potential biomarkers for targeted nano-radio-enhancers (NREs). The profiling revealed an anaplastic lymphoma kinase (ALK) mutation, which induces a constitutively activated tyrosine kinase receptor with pro-oncogenic effects.⁶⁵⁻⁶⁷ The presence of an ALK mutation in ACC is not common, and there are no data regarding the use of crizotinib (ALK tyrosine kinase inhibitor), as treatment for ACC.⁵⁸ The goals were:

- Clarification on whether functionalization of AuNPs with crizotinib can direct NPs to the tumor.
- Evaluation of targeted NPs enhancement of tumor visualization using CT.
- Investigation of the biological mechanisms underlying tumor reduction caused by the application of targeted nano-radio-enhancers.⁵⁸

In this study, ACC tumors were then subcutaneously injected into mice. Mice were treated 40-50 days after ACC implementation, until tumor size reached 10 mm in diameter. Mice were treated with radiation (single fraction of 18 Gy) or anti-ALK (crizotinib) alone, or a combination of treatments with or without targeted GNP.⁵⁸

Groups	Type of treatment
Group 1	Control (no treatment)
Group 2	Radiation alone
Group 3	Crizotinib alone
Group 4	Radiation + Crizotinib
Group 5	Crizotinib-AuNPs
Group 6	Radiation + Crizotinib-AuNPs

Table 1: Each group included three mice (except 1,6 groups with two mice each).⁵⁸

Groups 2, 4 and 6, were treated with radiation therapy, twelve hours after administration of AuNPs.⁵⁸

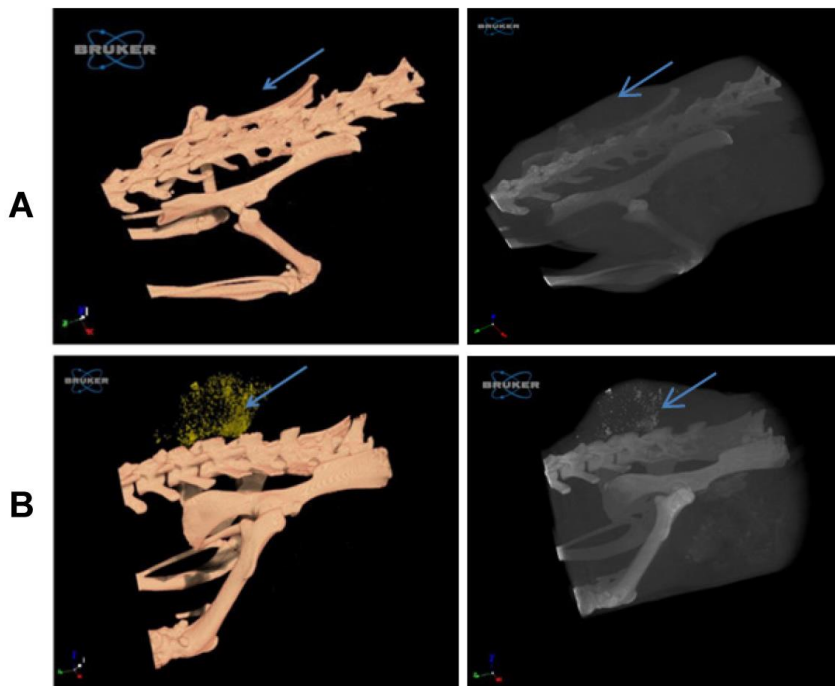


Figure 18: Imaging of the tumor with 3D whole-body volume rendering CT on day two. (A) In the control group, tumor was barely detected, while in targeted AuNP group (B), tumor is easily observed by the gold accumulation.⁵⁸

Tumor imaging (using CT) was performed two days after administration of treatment. Targeted NPs were easily identified, while there was difficulty in detection of the tumor in the control group.⁵⁸ CT imaging (figure 18) displays the accumulation of targeted AuNPs (with crizotinib) in the tumor site providing clear diagnosis.⁵⁸

Radiotherapy alone or crizotinib + radiotherapy hampered tumor growth, relative to untreated group, after 24 days (t-test, $p < 0.001$), but no significantly tumor reduction was observed in both treatment methods, below its size at T0 (t-test, $p > 0.05$). However, radiotherapy + crizotinib-AuNP significantly decreased tumor volume, to near disappearance, compared to before treatment size (t-test, $p = 0.007$).⁵⁸

Crizotinib-AuNP + radiotherapy effect on tumor volume reduction was considerable higher, compared to crizotinib + radiotherapy (without AuNP) (t-test $p < 0.01$) and radiation only ($p < 0.05$), 24 days after treatment. Administration of crizotinib without AuNP + radiotherapy did not cause any difference in tumor growth compared to radiation alone ($p = 0.966$).⁵⁸

Crizotinib alone or conjugated to AuNP, produced higher reduction of tumor volume after 24 days, as compared to untreated controls (t-test; $p < 0.001$ for both), despite the fact that these groups were not irradiated. However, crizotinib-AuNP decreased significantly the volume of the tumor, as compared to crizotinib alone (t-test, $p < 0.001$).⁵⁸

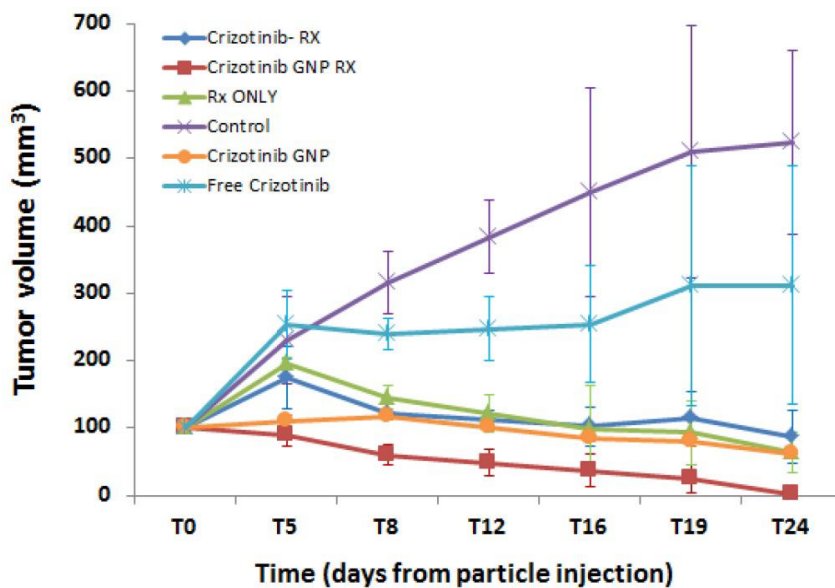


Figure 19: Average changes in tumor growth, 24 days after treatment. Tumor volume was monitored up to 24 days later. Results presented as mean \pm SEM (Standard Error of Mean). Rx: radiation.⁵⁸

Regarding the toxicity of treatment, the following results were observed. Four of 16 mice died before the conclusion of the study. Three of them were treated with crizotinib only and one, which died 24 days later, was treated with crizotinib-AuNP + radiation. Remaining mice did not show any obvious toxicity signs, judging by food intake, weight, and behavioral parameters.⁵⁸

Results from this study showed significant improvement of tumor radiosensitivity as evaluated by tumor volume reduction. Aggregation of crizotinib conjugated AuNPs in the tumor site, and effect of these NPs on tumor volume, are caused probably due to the EPR effect. The fact that smaller amount of NPs was present in the tumors of the irradiated group versus non-irradiated, indicates that AuNPs are effective in radiosensitization, as even half the amount of NPs is enough to produce a significant radiation effect.⁵⁸

This study also demonstrated that the functionalized NPs enhanced significantly tumor visualization, allowing clear detection of ACC. Furthermore, there were no NPs detected beyond the boundaries of the tumor region, indicating the accuracy enhancement by the NPs.⁵⁸

ALK mutation presence in the tumor was confirmed by similar findings on ALK staining between untreated control and radiation-treated groups. There was no degradation of ALK receptors by radiotherapy. Nevertheless, addition of crizotinib to AuNP or radiation amplified ALK staining. This finding was probably caused by crizotinib induction on stabilization and accumulation of ALK, inhibition of ALK phosphorylation and prevention of receptor ubiquitination.⁶⁸ The group treated with crizotinib-GNP + radiation, showed the weakest ALK staining, suggesting extensive tumor DNA damage. Weak staining, most likely produced by cells that did not present an ALK receptor and were not affected by treatment.⁵⁸

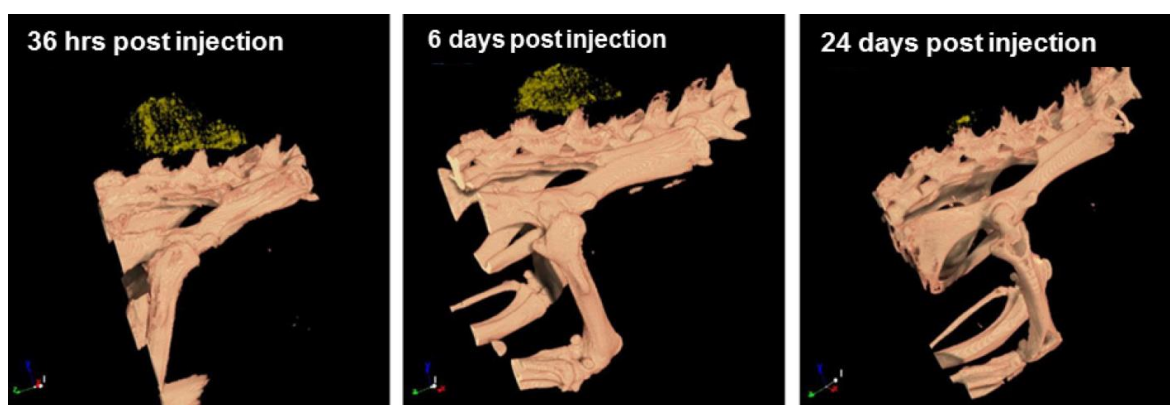


Figure 20: Post radiation targeted AuNP accumulation in the tumor. Accumulation of AuNPs (yellow dots) 36 hours, six days and 24 days post injection, indicating the gradual shrinkage of the tumor over time.⁵⁸

3.10.2 Nanoparticles alternatives to AuNPs

Alternatives nanoparticles to AuNPs are being sought, which may be more effective less costly. Iron oxide nanoparticles (IONs) have potential as MRI contrast agents as well as in photothermal therapy (PTT), photodynamic therapy (PDT), magnetic hyperthermia and chemo/biotherapeutics. Although iron's atomic number (Fe, Z=26) is relatively low, IONs can be used in combination with low LET X-rays. Aminosilane-type shell-coated SPION combined with thermotherapy and X-ray irradiation, in an orthotopic rat model of prostate cancer, produced, more effectively, tumor growth reduction than radiation alone.¹² Other studies have shown that X-ray radiosensitization by IONs might result ROS production, due to IONs' surface-catalyzed Haber-Weiss cycle and Fenton reaction.^{12,69,43,70} Several studies have shown the toxic effects of IONs.⁷¹ To overcome toxicity of IONs, surface modification and functionalization with various molecules and ligands could contribute to addressing clearance from the circulation and retention in the mononuclear phagocyte system (MPS) as well as improving tissue targeting, biocompatibility, and stability.⁷²

Hafnium oxide is a new class of material, with high electron density, designed in the form of crystalline 50nm-particles (HfO₂-NP). Combined with radiotherapy, Hafnium oxide NPs enhance radiation dose deposited from within the tumor cells. Preclinical studies demonstrated that HfO₂-NPs exposed to RT, increase cancer cells death in vitro and antitumor efficacy in vivo, when compared to RT alone. Assessment of hafnium oxide nanoparticles efficacy, in cancer epithelial and mesenchymal tumor models and on patient-derived tumor xenografts in nude mice, have shown superior anti-tumor effects over radiation therapy alone, in terms of complete response and overall survival.⁷³

Currently, several multinational phase I/II trials and one phase II/III trial are ongoing and recruiting participants for the treatment of head and neck cancer (squamous cell carcinoma), rectal cancer, hepatocellular carcinoma (liver cancer), prostate cancer, and adult soft tissue sarcoma.^{12,73}

Bismuth (Bi, Z=83) and platinum (Pt, Z=78) have the potential to yield a dose enhancement factor higher than Au, with Bi being the highest. The smaller the nanoparticle size is, the greater the dose enhancement is predicted to yield, because

smaller nanoparticles accumulate closer to the nucleus, where they can cause the greatest damage. In a 2014 study, Zhang et al., investigated the toxicity, biodistribution, and radiation effects of bismuth selenide (Bi_2Se_3) nanoplatelets in cell lines and mice. There was no significant toxicity to either cells or mice and 93% of Bi cleared from the body, 90 days after treatment. After irradiation doses of up to 8Gy, a significant radiation dose enhancement was observed.⁷⁴

Gadolinium (Gd, Z = 64) is another alternative to AuNPs. In addition to having a relatively high atomic number, Gd is already used as a contrast agent in MRI. Gd_2O_3 core nanoparticles encapsulated in a polysiloxane shell have shown potential as an image guided radiotherapeutic tool in a gliosarcoma rat model (Le Duc et al., 2011).⁷⁵ Accumulation in the tumor after saphenous vein injection was demonstrated using MRI, and the tumor-bearing rats were treated with microbeam radiation therapy, with a significant increase in survival in the nanoparticle-treated group. Another study of 2013, Milaldi et al., using a rat brain tumor model confirmed that ultra-small Gd-based nanoparticles accumulate in brain tumors after IV administration.⁷⁴

3.10.3 Particle therapy and nanomedicine

Nanoparticles have been used in clinical studies as an efficient agent to improve the concentration of active products in the tumor region and restrict radiation effects to cancer cells, thus sparing normal tissue. The selective delivery of NPs is due to the enhanced permeability and retention effect (EPR) when NPs are small enough (<200 nm) to permeate through the aberrant tumor blood vessel walls. Selective accumulation of NPs can also be achieved through functionalization of the surface of NPs with tumor specific ligands (antibodies or other peptides). Thus, the combination of radiotherapy with nanoparticles, enhances the therapeutic effects and opens a new range of treatments. Furthermore, conventional radiotherapy is not able to eradicate aggressive radioresistant tumors.⁷⁶

Treatment by high-energy ions such as protons (proton therapy) and carbon ions (carbon therapy) may be used as an alternative treatment in cases, which are not responding to conventional RT. The advantage of ion beams is based on their property to penetrate tissues over several centimeters and deposit the maximum energy at the end of their

track, where the ionization cross section of the medium is extremely large and at a depth dependent from their initial energy (Bragg peak). In this way, the beam can be tuned, by modulating its energy, to target the tumor without damaging the tissues located deeper position. Furthermore, because of the larger relative biological effectiveness (RBE), compared to X-rays, ion beam radiation can provide greater cell killing for the same amount of delivered dose. Carbon ions have the potential to be four times more efficient than photon beams.⁷⁶

There are two different modalities for particle therapy delivery. The first is the passively modulated broad beam modality, consisting of a beam shaped to the target with a spread out Bragg peak (SOBP). The second is the pencil beam active scanning mode, where a beamlet of a few mm is scanned, spot by spot, on the tumor region, modulating the energy for each depth slice.⁷⁷ Due to its larger degradation of the beam through the beamline materials, the broad beam modality provides a larger entrance channel dose, in comparison to the pencil beam.⁷⁸ As such, low but significant dose deposited in the tissues, located before reaching the tumor region, is unavoidable. Furthermore, damage to surrounding tissues may be caused by motion and other uncertainties.⁷⁶

Addition of “nano-radio-enhancers” (NREs) to the tumor region is proposed as a way to overcome the above-mentioned limitations. Use of contrast agents offers the possibility to image the biodistribution of the agent and the tumor prior to or during the treatment.⁷⁶

3.10.3.1 Proton radiotherapy combined with nanoparticles

Effectiveness of high-Z nanoparticles to enhance the effects of proton radiation was first demonstrated by Kim et al. (2010).⁴¹ It was shown that small gold or iron nanoparticles (1.9–14 nm), enhanced the regression of CT26 mouse tumors treated by fast protons (45 MeV-beam) and cell killing was enhanced when CT26 cells were loaded with NPs. Concerning the mechanism of enhancement, it was argued that proton induced X-ray emission (PIXE) cannot account as the major process in the radiation-enhancement (Dollinger 2011).^{76, 79}

Enhancement of the effects of proton radiation by gold was demonstrated in vitro by Polf et al. (2011).⁸⁰ Significant increase of tumor cell mortality was observed, when loaded

with gold containing phage-nanoscaffolds (44 nm diameter, 1 ng gold per cell) and irradiated by 160 MeV protons. Kim et al. (2012)²⁴ later confirmed that the amplification of tumor regression and mice survival was related to ROS generation in tumor cells.⁷⁶ Recent experiments performed with platinum and gadolinium NPs, irradiated with 150 MeV protons, demonstrated the amplification of nanosize biodamage (Schlathölter et al. 2016).⁸¹ The role of the generated hydroxyl radicals was again shown, but more importantly, the radio-enhancement effect was found to be greater at the end of the ion track. The above-mentioned studies have shown the potentiality of the use of NREs to concentrate the effects of proton radiation (at the track end) in the tumors.⁷⁶

3.10.3.2 Carbon ions radiotherapy combined with nanoparticles

Nanoparticles may be activated through Coulombic interaction (including ionization and surface plasmon excitation channels) by charged particles (incident ions or secondary electrons of the track). Radicals production occurs due to the interaction of electrons emitted by the nanoparticles, as well as the radiolysis of the surrounding water molecules.⁷⁶

In a 2013 study, Kaur et al.⁸² observed the enhancement of the effects of carbon ion radiation in tumor cells (HeLa) loaded with AuNPs. A dose enhancement factor (DEF) close to 40% RBE was obtained using 62 MeV carbon ion beam irradiation. The effect was higher than the one achieved with proton beam irradiation observed by Polf et al. (2011).⁸⁰ However, since these two studies used different cell models, cell uptake and cell sensitivity may have contributed to the results.⁷⁶

Enhancement of carbon radiation effects was then demonstrated with the use of gadolinium-based nanoagents (AGuiX from Nano-H, Lyon, France). These theranostic agents have unique multimodal properties, such as improvement of MRI contrast and enhancement of radiation effects (Porcel et al. 2014).⁸³ In this study, it was showed that cell killing, induced by carbon ion radiation, was enhanced by a low concentration of gadolinium. It was the first study that introduced the opportunity of application of theranostics in carbon therapy.⁷⁶

3.10.3.3 Proton therapy enhanced by metal-containing nanoparticles

Gadolinium-based NPs (GdBNs) are MRI active agents. However, application of GdBNs, excited by high-energy photons and carbon ions (as incident radiation), can lead to amplification of cell killing.^{83,75,84,85} These properties of the multimodal compounds offer promising perspectives to implement theranostics (therapy and diagnosis based on a single NP) in cancer radiotherapy.⁸¹

The main advantage of ions, compared to photons, derives from their characteristic dose–depth distribution, which peaks in a well-defined depth at the end of the particle tracks (Bragg peak), producing superior dose deposition in the tumor region. Tissues, in front of and behind of the site of interest, receive low doses. Energy modulation of ion beam is required to produce a spread-out Bragg peak, that results in constant physical dose over the total tumor volume. However, this energy modulation increases the dose deposition in tissues in front of the tumor. Accumulation of NPs in the tumor site, can enhance selective cell killing, thus overcome limitations of hadron therapy. Particle therapy studies have demonstrated the efficiency of high-Z NPs to amplify the effects of fast protons.⁸¹

Schlathölter et al. performed a study in 2016, to evaluate the efficacy of 3 nm platinum (Z=78) and 5 nm gadolinium (Z=64) based NPs to enhance nanosize lesions, caused by proton irradiation. Plasmid pBR322 was used as a molecular probe to quantify simple and complex damages in biomolecules. Ion beams were implemented, which mimic the beam at the entrance of the ion track (LET=0.44 keV/μm) and the beam at the end of the track (LET =3.6 keV/μm).⁸¹

Before irradiation, plasmids were 95% supercoiled and 5% circular conformed, indicative of a single-strand break (SSB). Linear conformation, indicative of double-strand breaks (DSBs), was absent. Thus, production of DSB was used as markers of nanosize molecular damage (complex damage) induction.⁸⁶

Experiments were performed, using four samples containing:

1. Metal-free plasmid samples used as controls
2. Plasmids and PtNPs (platinum NPs)
3. Plasmids and GdBNs (gadolinium-based NPs)
4. Plasmids and DMSO (dimethyl sulfoxide, with or without NPs)

Doses ranged from 0 to 350 Gy for most experiments and up to 800 Gy in the presence of DMSO. The dose rate was close to 30 Gy/min.⁸¹

Contributions of hydroxyl radicals were higher than 90% for PtNPs and GdBNs, indicating that production of these radicals is a key step in enhancing of radiation effects by the NPs.⁸¹

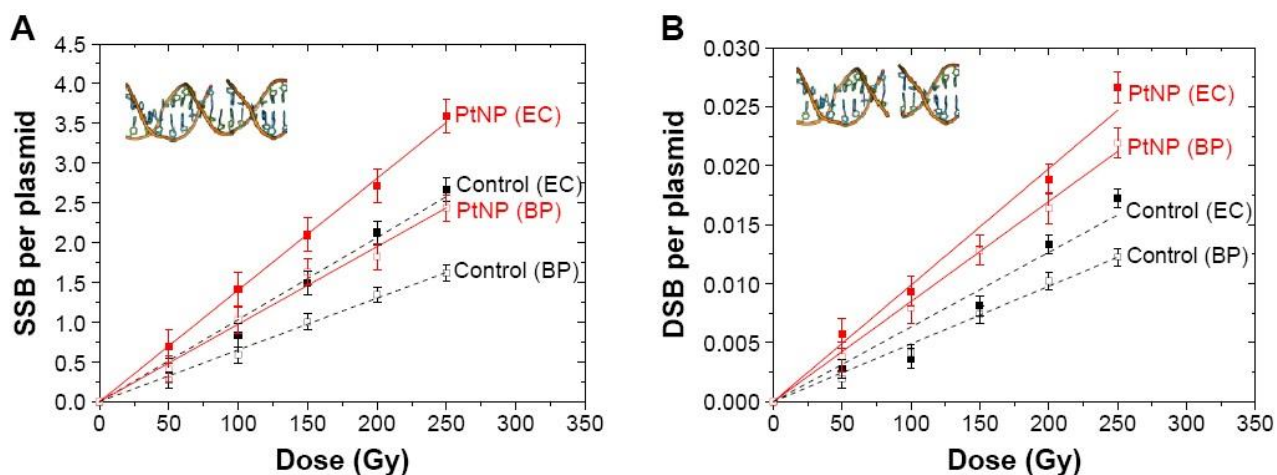


Figure 22: SSBs (A) and DSBs (B) in DNA plasmids, in the presence of PtNPs (red) and in the control (black) irradiated by protons at the EC and at the BP (BP: Bragg peak, DSB: double-strand break, EC: entrance channel, PtNP: platinum nanoparticle, SSB: single-strand break)⁸¹

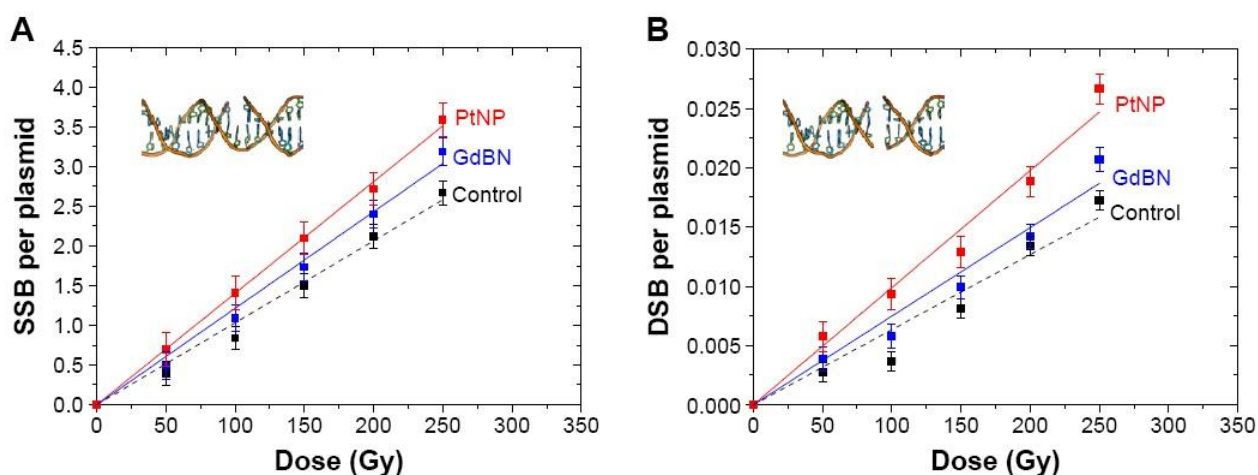


Figure 23: SSBs (A) and DSBs (B) induced by protons at the entrance channel (0.44 keV/ μ m) in plasmids in the presence of PtNPs or GdBNs and in the control (DSB: double-strand break, GdBN: gadolinium-based nanoparticle, PtNP: platinum-based nanoparticle, SSB: single-strand break)⁸¹

This study indicated that amplification effect by NPs, activated by protons, is due to nanoscale processes that produced severe damage in biomolecules. The effect is more distinct in the Bragg peak region than in the entrance region, which increases the potential of NPs even more. It was demonstrated that NPs enhanced the yield of complex

nanosize molecular damages. These damages can be attributed to production of free radical, as a result of NPs activation. The stronger radiation damage amplification from Pt-based NPs, than Gd-based NPs, can partly be attributed to the differences in atomic number between the two elements. Collective electronic excitations (plasmons) most likely play an important role in high energy proton-NP interactions (as recently predicted theoretically), which are responsible for the superior efficiency of PtNPs. This study demonstrated that combination of proton therapy with administration of PtNPs or GdNPs can significantly improve proton therapy efficacy. In addition, combination of platinum and gadolinium could offer theranostic perspectives in proton therapy.⁸¹

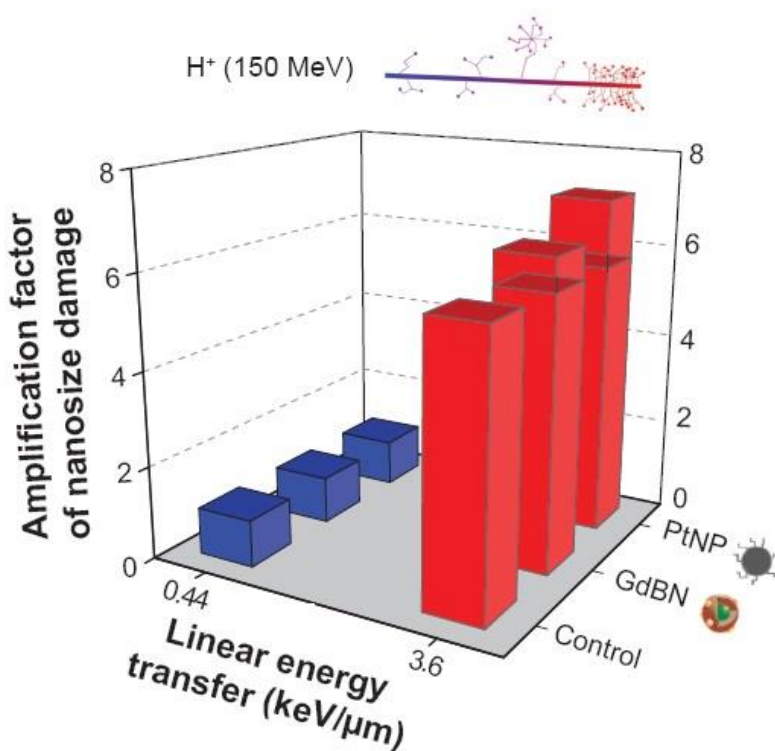


Figure 24: Amplification factor of nanosize molecular damage induced along a 150 MeV proton track in presence of metal containing nanoparticles (GdBN: gadolinium-based nanoparticle, PtNP: platinum nanoparticle)⁸¹

3.11 Challenges & Contradictions of Metal-NP applications as Nano-Radio-Enhancers

Many strategies are currently being developed to improve radiotherapy outcome. Some examples are spatial and time dose fractionation, micro/mini-beam irradiation, heavy-ion irradiation, application of normal cell radio-protectants and/or tumor cell radiosensitizers. One of the radiosensitizing approaches, as mentioned above, is to enhance radiation effect by metal nanoparticles. Due to their high electron content and photoelectric absorption cross-section, metal (consisted of high-Z elements) nanoparticles emit showers of

secondary electrons, after been excited by irradiation.^{87,88} This secondary energy produces clouds of high ionization densities, thus enhancing radiation-induced cell damage.⁸⁹

The downside of current methods is that nanoparticles, although their very small dimensions, penetrate the cells but not the cell nucleus, unless they are specifically modified for this purpose. Nanoparticles, entering the cells, remain retained inside the cytoplasm, where they accumulate mainly in endoplasmic vesicles (endosomes) and lysosomes. In some cases, nanoparticles may co-localize preferentially within the endoplasmic reticulum (ER) and Golgi apparatus. However, they don't accumulate in mitochondria, the only organelles containing their own DNA. These findings indicate that there are various cellular processes, which may participate in nanoparticle-mediated tumor cell radiosensitization. As such, not all nanoparticles share a common mode of action, in terms of the cell damage type and its underlying mechanism.⁸⁹

Pagáčová et al. performed a study in 2019, investigating whether extra-nuclear presence in cells, of different metal nanoparticles, has the potential, with or without irradiation, to enhance damage of nuclear DNA. The effect of nanoparticles on kinetics and efficiency of DNA repair was also studied, after cells irradiation with low LET ionizing radiation (γ - and X-rays).⁸⁹

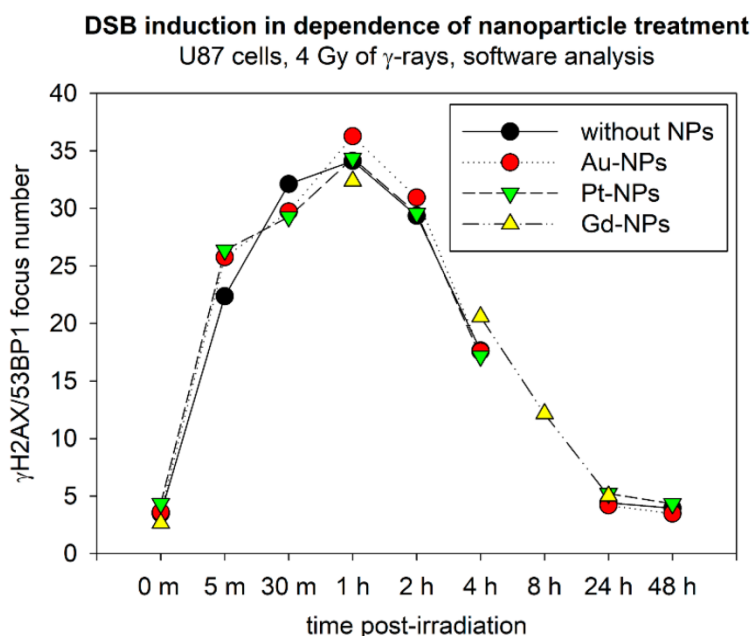


Figure 25: Comparison of H2AX/53BP1 focus (DSB) formation and repair in U87 cells irradiated with 4 Gy of γ -rays in absence or presence of 2.6 nm Pt-NPs, 2.4 nm Au-NPs or 2.0 nm Gd-NPs. Results are shown as mean numbers of foci per nucleus measured at the indicated periods of time PI. Black circles—without NPs, green triangles Pt-NPs (0.5 mM, 6 h-incubation), and red circles—Au-NPs (0.5 mM, 6 h-incubation; preliminary results). The data are also compared to our earlier results for Gd-NPs (1mM for 1h, ⁶⁰Co-irradiation, 4Gy) (yellow triangles). X-axis: m=minutes, h=hours; 0min=non irradiated samples.⁸⁹

Pagáčová et al. investigated how platinum (Pt) and gold (Au) nanoparticles influence DNA DSB induction and repair in three different cancer cell types (U87 glioblastoma cells, HeLa

cervix cancer cells and SkBr3 breast cancer cells), exposed to γ -(^{137}Cs) or X-radiation. U87 glioblastoma cells were selected for their high resistance to radiotherapy. HeLa cells, showing relatively lower resistance to radiation, were then involved into the study to explore how tumor cell types of different radiosensitivities and origins respond to nanoparticle uptake and nanoparticle uptake followed by irradiation. The SkBr3 model is more radioresistant than HeLa cells. It was shown that ultrafine AuNPs, as well as the larger AuNPs, efficiently penetrate into cytoplasm but remain restricted from nucleus. Even short (2h) incubation with nanoparticles was shown to be sufficient for their internalization and cell radiosensitization.⁸⁹

As indicated from figure 25, the differences in DNA damage and repair, between U87 cells exposed to 4 Gy of γ -rays after being or being not incubated with nanoparticles, are small for all nanoparticles (platinum, gold, and gadolinium). This shows that 2.6 nm Pt, 2.4 nm Au and 2.0 nm Gd nanoparticles of given composition neither intensify DSB induction by ionizing radiation, nor affect consequent repair of these lesions.⁸⁹

There are, however, some indications showing a delay in DSB repair, which could be theoretically explained by a higher complexity of DSBs generated, in presence of NPs. The reason that the complexity but not the extent of DSB damage increased in presence of NPs, is unclear. A possible explanation is that cytoplasmically located NPs may enhance radiation damage to the cytoplasm, leading to a suboptimal condition of cells, which may indirectly decrease DSB repair. This could be supported by the observation that potential indications of a slower repair in nanoparticle-treated cells appeared only in later periods of time, post-irradiation.⁸⁹

This study demonstrated that cell's nucleus is inaccessible even for nanoparticles of ultrafine dimensions (2.5–10 nm). However, the action radius of most secondary electrons produced from cytoplasmically located nanoparticles is quite short. Since some amounts of nanoparticles accumulate around the cell nucleus or are directed to the endoplasmic vesicles and reticulum, some secondary energy may reach and damage the chromatin.⁸⁹

Moreover, accumulation of nanoparticles in endosomes and lysosomes could result in damage of these structures with important consequences. Recent studies involve lysosomes in important cell signaling pathways, eventually initiating apoptosis. In

addition, even simple disruption of a larger amount of lysosomes due to their membrane damage by locally amplified radiation effects, mediated by intra-lysosomal nanoparticle accumulations, may result in massive leakage of lytic enzymes and extensive cytoplasmic damage, which could initiate cell death.⁸⁹

Cytoplasmically located nanoparticles may also affect organelles or structures which they do not co-localize with. ROS generated by nanoparticles, when irradiated, may damage organelles located in close proximity, like mitochondria. Among other cytoplasmic targets, mitochondria are critical for cell survival. Furthermore they are the only extra-nuclear structures with their own DNA. Therefore, nanoparticle-mediated fragmentation of mitochondrial DNA, may represent an elegant modification of the “classic” DNA damage-based hypothesis on cell radiosensitization by nanoparticles. In addition, ROS generation could potentially affect biochemical cellular pathways.⁸⁹

The endoplasmic reticulum (ER) may also be a potential target for nanoparticle effects. ER functions are essential for most cellular activities and survival. In addition, ER has an important role in the response to oxidative stress-induced damage and is sensitive to ROS. As such, irradiated nanoparticles can induce cytotoxic effects by affecting ER functions. In a 2011 study, Zhang et al. demonstrated that implementation of Ag-NPs resulted in cytotoxicity and cell death by apoptosis, associated with secondary DNA fragmentation.⁹⁰ It was indicated that nanoparticles may initiate cell death through disturbing functions of ER, and also the importance of time in interpretation of nanoparticle-mediated DNA effects. Thus, it can be assumed that in various studies the nanoparticle-mediated effects on DNA can rather reflect this secondary apoptotic DNA fragmentation than primary enhancement of DSB induction by radiation. Szegezdi et al., in their 2006 study, described the mechanism of ER stress-related apoptosis.⁹¹ Disruption of ER function leads to accumulation and aggregation of unfolded proteins accompanied with stress signaling. These signals are detected by transmembrane receptors, which in turn initiate the unfolded protein response (UPR), to restore normal ER functions. If the stress persists, it can lead to apoptotic cell death.⁸⁹

Altogether, it was concluded that, while nanoparticle-mediated radiosensitization has been related to DNA damage, results of this study, regarding ultrafine Pt and Au

nanoparticles and also Gd nanoparticles (from earlier data), do not support this theory as a general mechanism responsible for the radiosensitizing effect.⁸⁹

4. Hyperthermia

Hyperthermia (HT) is a treatment modality for the therapy of a wide range of lesions with minimal adverse effects and adjacent tissue damage. Currently, hyperthermia has been regarded as an additional therapeutic method for cancer treatment. It has the potential to improve clinical response and reduce toxicities of radiotherapy and chemotherapy. However, the combination of hyperthermia with radiotherapy and chemotherapy has not yet been formally implemented in every day clinical application. A major problem is the limitation of current techniques on accurate positioning and temperature equilibrium control. Lately, with the emergence of nanotechnology and the development of photothermal therapy (PTT) and magnetic hyperthermia, a promising new approach has been offered, which initiates a resurgence of hyperthermia.⁹²

In application of hyperthermia, the raising of temperatures can be locoregional, or systemic heating, depending on the method used and the goal of the treatment.⁹³ Local HT can selectively heat the tumor to treatment temperature (39-45°C) by the use of a physical heating device.⁹² Local hyperthermia may be external, interstitial or endocavitary.⁹³

Local hyperthermia is appropriate for head and neck cancers, because of their superficial anatomic sites. Its application can be performed through placing a contacting medium on tumor surface. Single or confined tumor mass are heated by antennas or applicators.⁹³ The methods of implementation of local hyperthermia are radiofrequency (RF), microwave, ultrasound and near-Infrared photothermal therapy (PTT).^{92,93}

These methods are based on three physical mechanisms for delivering heat energy to the body:

- Thermal conduction of heat (heat flows from higher to lower temperature)
- Resistive or dielectric losses from applied electromagnetic field (radiofrequency waves and microwaves)
- Mechanical losses caused from molecular collisions from an ultrasound pressure wave.⁹⁴

4.1 Hyperthermia Techniques

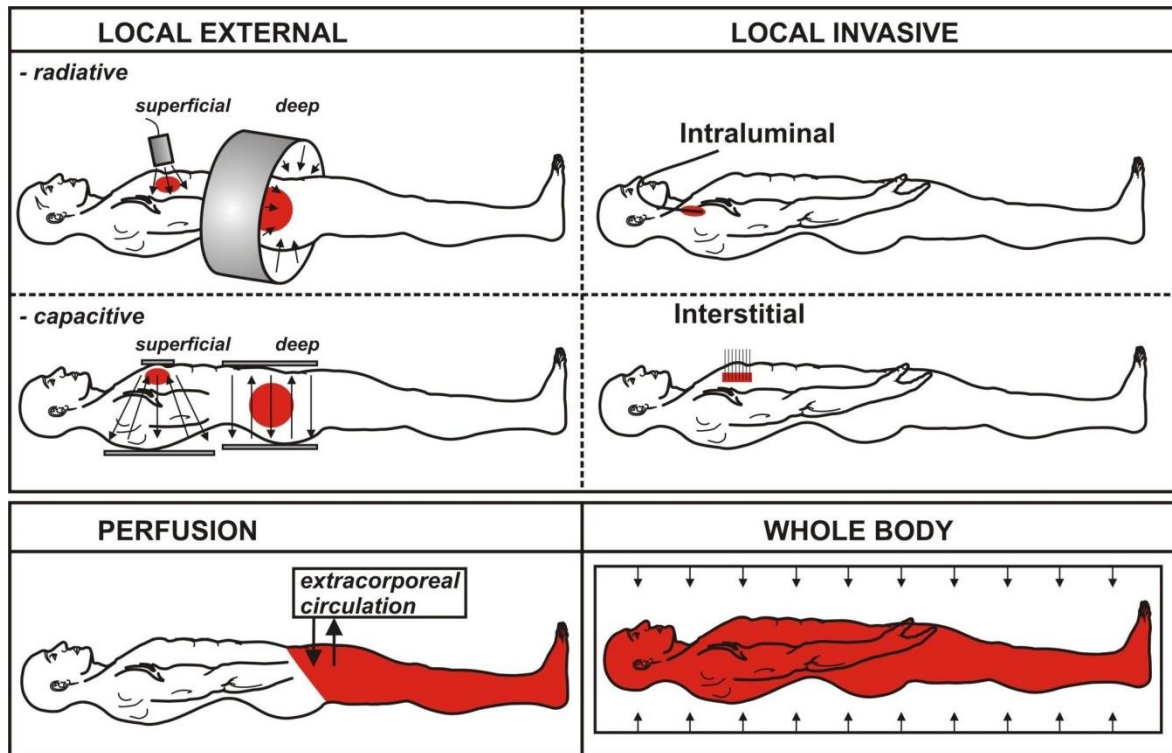


Figure 26: Hyperthermia therapy techniques⁹⁵

4.1.1 Radiofrequency (RF)

Radiofrequency refers to alternating electric current that oscillates in high frequency. It is electromagnetic energy, formed from waves moving together (or radiating) through space at the speed of light. Unlike ionizing radiation, electromagnetic energy is non-ionizing. It is not strong enough to ionize atoms and molecules. Radiofrequency energy is safer, as it is absorbed by tissue as simple heat.⁹⁶

Radiofrequency effect is based on radiofrequency current (460 kHz) passing through the target tissue, from the tip of an active electrode towards a dispersive electrode. The dispersive electrode has a much larger area than the active electrode. Since the active electrode has a far smaller cross-sectional area than the dispersive electrode, the current density in amperes per square meter is far greater, resulting in difference in current density between the two electrodes, thus, the energy at the tip of the probe leads to ionic agitation with subsequent conversion of friction into heat, depending on the electric permittivity of the tissues. Tissue ions are agitated as they attempt to follow the changes

in direction of alternating electric current. The agitation results in frictional heat.^{93,96} Cells die when they reach a certain temperature. The main tumoricidal effect of RF ablation occurs when the absorption of electromagnetic energy induces thermal injury to the tissue. However, RF energy and generated heat does not alter cell's chemical structure.⁹⁶

4.1.2 Ultrasound

Ultrasound is a mechanical wave, which involves the propagation of sound waves, generating heat through mechanical friction. It has the advantage of having adequate tissue penetration at wavelengths that permit beam shaping and focusing. Penetration depth can be adjusted from less than 1 cm up to 20 cm, allowing treatment of both superficial and deep regions. The main disadvantages of this technique are high bone absorption and inability to penetrate through air-containing tissues (respiratory tract, gastrointestinal tract).⁹⁴ Ultrasound uses frequencies between 0.5-10 MHz. Clinically, 1 MHz ultrasound is often used.⁹²

4.1.3 Microwave

Microwave energy is a promising technique and effective in heating cancerous tumors, because of the high water content. One or more microwave antennas can be used to treat the tumor, depending on tumor size and location in the body. Heating occurs when alternating electromagnetic (EM) field is applied to an imperfect dielectric material. In tissue, heating is generated because the EM field forces water molecules to oscillate. The bound water molecules tend to oscillate out of phase with the applied fields, thus part of the energy is absorbed and converted to heat. The more water is contained (e.g., most solid organs), the more energy is absorbed.^{97,98}

The frequency of microwave HT ranges from 430 to 2450 MHz, and the higher frequency, the more shallow tissue penetration. The maximum penetration depth is 3-4 cm, using 915 MHz microwave frequency. From simulation studies of head and neck hyperthermia, imposed the required positioning accuracy to be within ± 5 mm, and the water bolus shape, and stability and skin contact have an important impact on treatment quality.^{97,92}

The major difference between microwave and RF technique is that microwave heating occurs in a volume around the applicator antenna, while RF heating is limited to areas of high current density. RF heating requires an electrically conductive path. On the other hand, microwaves are capable of propagating through materials with low or zero conductivity. This means that low conductivity tissues inhibit RF current flow but allow better microwave propagation.⁹⁸

4.1.4 Near-Infrared Photothermal Therapy (PTT)

PTT involves the implementation of light-absorbing photothermal agents, to treat tumors by light-induced-heating. PTT agents convert light at certain wavelengths into heat, to induce cancer cells necrosis. In this way, PTT has the potential for enhancing the specificity of HNSCC treatment through localizing laser irradiation and improving the accumulation of PTT agents, and minimizing comorbidities to surrounding healthy tissues.⁹²

The laser power threshold for photothermal-induced destruction of cancer cells, after nanoparticle treatment, is found to be 20 times lower than that required to destroy human oral squamous carcinoma (HSC) cells in the PTT, without implementation of nanoparticles. Currently, nanoparticle (NP)-enabled near-infrared photothermal therapy is a promising approach of HT treatment for malignancies.⁹²

4.2 Biological effects of Hyperthermia

Intrinsic characteristics of cancer cells and surrounding environment determine the biological response of the tumor to heat. Modifications of the tumor microenvironment may increase or decrease the response of the tumor to heat. In temperatures between 40°C and 43°C, most tumor cells tend to die, while healthy cells tend to survive. When cancer cells are subjected to these temperatures, they are being damaged irreversibly, in a time and dose dependent way.⁹³

The most serious cell damage, by heating, occurs to cells in the S phase of cell cycle (synthesis phase), due to impairment of chromatin structure and inactivation of replication protein. The factors of the intratumor microenvironment, that have a

significant impact on tumors' response to HT, are perfusion, permeability, pO₂, pH and pressure.^{92,99-101}

The biochemical processes affected by heat are several:

- DNA, RNA synthesis, DNA repair mechanism and cell respiration are inhibited.
- Tumor cell membranes become more permeable and fluid (which partially explains the increased uptake of drugs).
- DNA polymerases-β key enzymes in multistep repair system and are strongly inhibited.
- Mitochondria suffer different alterations in their cristae.
- Enhanced production of heat shock proteins (HSP) is common and this affects thermo-tolerance and tumor immunogenicity.
- Heat increases the influx of reactive oxygen radicals which contribute to cytotoxicity.
- Hyperthermia, combined with drugs promoting apoptosis, has synergistic effect.⁹³

Hyperthermia as demonstrated by Ahmed and Zaidi, can enhance apoptosis, through several biological effects as increased tumor membranes permeability, increased production of ROS, inhibition of DNA repair and alteration of cellular cytoskeleton.^{102,103} In a 2007 study, Liang et al. demonstrated that hyperthermia can alter the expression of apoptosis genes, such as p53, Bcl-2 and Bax, thus enhancing the effects of chemo- and radiotherapy.¹⁰⁴

Hyperthermia has the potential of radiosensitization. Local HT activates HIF-1 and its downstream targets, such as vascular endothelial growth factor (VEGF) and pyruvate dehydrogenase kinase 1 (PDK1) and modifying tumor cell metabolism signaling pathways. This effect results in increase of vascular permeability which leads to increased oxygen pressure levels in the tumor microenvironment. This alteration enhances the radiosensitivity of the tumor. Radiosensitization may also be a result of DNA inhibition of repair, alteration in nuclear protein aggregation and higher order chromatin organization.⁹²

Another important anti-tumor effect of HT is the capacity to inhibit angiogenesis. In 1988 Fajardo et al. showed that capillary endothelial cells were thermosensitive. The extent of inhibition was inversely proportional to temperature. Another study in 2003 by Roca et al., demonstrated that hyperthermia inhibited angiogenesis in vitro and in vivo by

controlling extracellular matrix degradation through the induction of Plasminogen activator inhibitor-1.^{105,93}

Hyperthermia (HT)	Radiotherapy (RT)
Hypoxic cells are more thermosensitive.	Hypoxic cells are more radioresistant.
Low extracellular pH in the tumor microenvironment favors the toxicity of HT.	Low extracellular pH in the tumor microenvironment does not favor the toxicity of RT.
HT mainly acts in phase S of cellular cycle, which is the most radio-resistant.	RT acts in phases G/M of cellular cycle, which are the most thermo-resistant.
The hypoxic center of the tumor with low blood circulation is the best target for HT, due to temperature rise in toxic levels.	The hypoxic center of the tumor is the most radioresistant region.
Blood flow at the tumor vessels is not raising during HT, while it is raising in normal surrounding tissues. The cancerous tissue is heating ectectically, while the blood flow in healthy tissues decreases the local temperature.	No change in blood flow during RT.

Table 2: Role of Cell Cycle in mediating sensitivity to Hyperthermia & Radiotherapy⁹⁵

4.3 Local Hyperthermia application in Head and Neck Cancer

Combined treatment with hyperthermia and radiotherapy demonstrated local control and survival in several phase II studies and randomized trials for patients with head and neck cancers. Jones et al. tested, in a 2005 randomized trial, the clinical value of hyperthermia delivered within a defined thermal dose range based on dosimetric principles, established in the preclinical setting and retrospective analysis of human phase II trials. This study concluded that adjuvant hyperthermia, with a thermal dose more than 10 CEM 43°C T₉₀ produced a significant improvement in local control, in patients with superficial tumors, which were submitted to radiation therapy.¹⁰⁶

In another study of 2013, Kouloulis group evaluated the correlation between the thermal parameters of hyperthermia and the clinical results in patients with superficial

tumors. This study showed that 60% of the patients with superficial tumors, including submandibular lymph nodes from head and neck cancers, had a complete response and indicated that microwave heating should be over 44 °C for favorable treatment response, when combined with radiotherapy.¹⁰⁷

4.4 Nanotechnology-based Hyperthermia in Head and Neck Cancer

Conventional hyperthermia generates a temperature gradient with a maximum on the surface of the body that decreases with distance from the source.¹⁰⁸ As a non-selective tissue heating method, it cannot distinguish between cancer tissue and the surrounding healthy tissue, thus it can lead to serious side effects. Recent development in the field of nanomedicine, has led to novel methods and solutions, in order to overcome this disadvantage of hyperthermia techniques. Nanomaterials have shown great potential in targeted hyperthermia-based therapy methods.⁹²

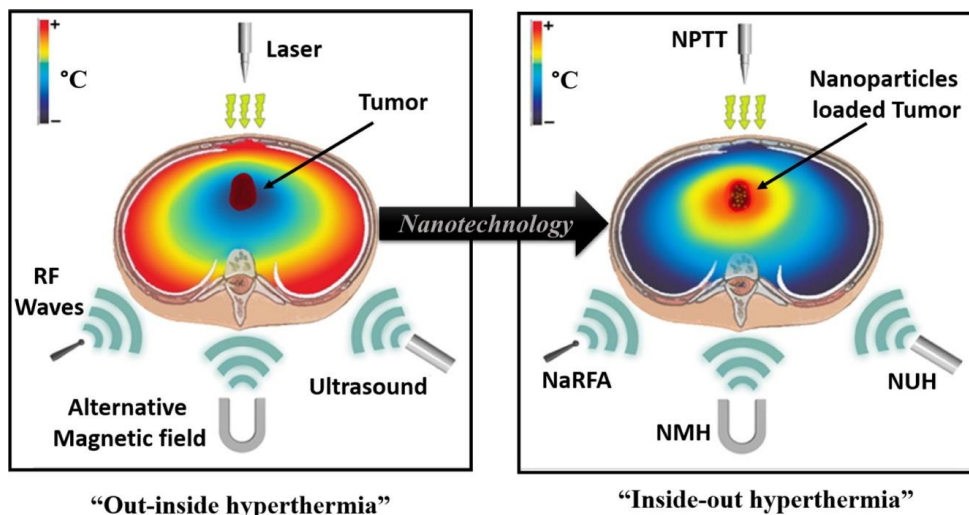


Figure 27: NPs accumulated inside the tumor, can absorb energy, to enhance the effects of hyperthermia. NPTT: Nano-Photo-Thermal Therapy, NMH: Nano-Magnetic Hyperthermia, NaRFA: Nano-Radio-Frequency Ablation, NUH: Nano-Ultrasound Hyperthermia.¹⁰⁸

Nanoparticles have the capability to absorb the energy produced by an external source and enhance the effects of hyperthermia. As such, nanoparticles can function as the primary source of heat and reverse the direction of heat loss, as shown in figure 27 (inside-out hyperthermia). In this way, NPs focus the energy on the target, to maximize the effects on tumor region, while minimizing the adverse effects on healthy tissues.¹⁰⁸

4.5 Types of nanoparticle-enhanced Hyperthermia

4.5.1 Nano-Photo-Thermal Therapy (NPTT)

NPTT method can selectively kill cancer cells by targeting the nano-photosensitizer towards them and then implement laser light to target region (Fig. 4). Implementation of nanoparticles has the potential to alter the photothermal properties of the medium and enhance the local conversion of optical energy into heat, thus localizing hyperthermia effects selectively in cancer cells. Gold nanoparticles (AuNPs), as well as other nanostructures responsive to laser radiation, have also been developed for targeted photothermal therapy. Carbon-based nanomaterials (carbon nanotubes, fullerene, graphene) have shown great potential in enhancing photothermal therapeutic modality.^{108,109-111}

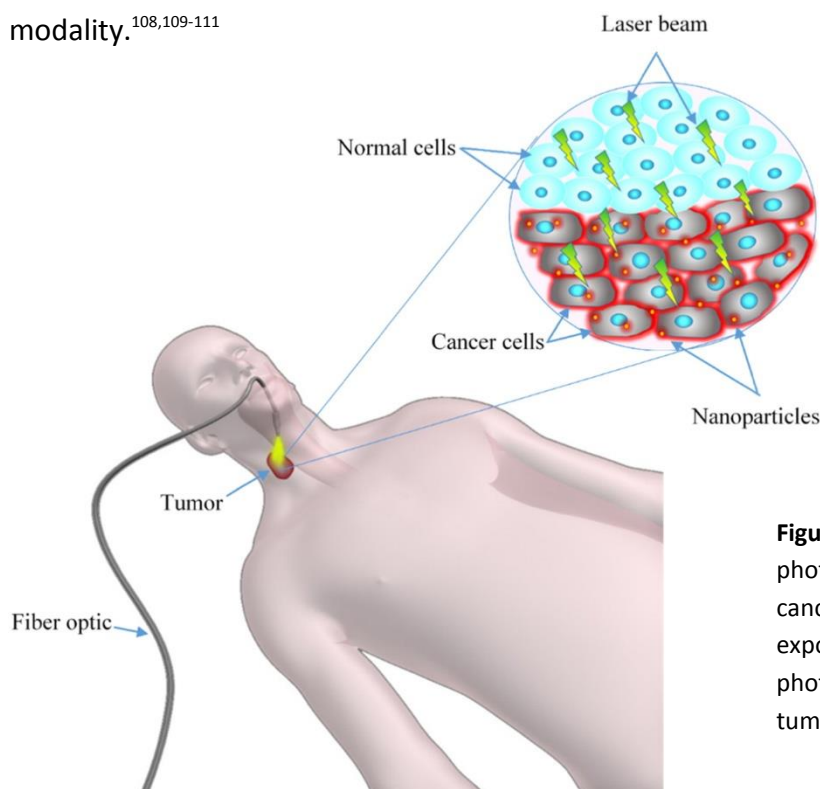


Figure 28: Targeted NPs as photosensitizing agents towards cancer cells, and laser light exposure to induce selective photothermal ablation of the tumor.¹⁰⁸

Surface plasmon resonance (SPR) is defined as the resonant oscillation of free electrons on the particle surface induced by incident light. The interaction of NPs with the laser light results in the absorption of laser photons by the electrons in atoms of the NP and the subsequent excitation to higher energy levels. Through electron-phonon relaxation, the absorbed energy is converted to heat and is transferred into the particle lattice. The photothermal conversion efficacy depends on the absorption cross-section of each

particle and the laser fluency.^{108,112} Various temperature increments, thermodynamic and thermo-biological responses can occur in the target tissue, depending on the laser fluency. Phase change of the medium, protein denaturation, acoustic wave formation due to particle expansion, water vapor bubble formation, particle melting and vaporization, plasma generation and fragmentation of the particle are the thermodynamic and thermo-biological outcomes that could be produced by the interaction of the laser beam with nanoparticles.¹⁰⁸

4.5.1.1 EGFRmAb–AuNPs enhanced photothermal therapy induces apoptosis in hypopharyngeal_cancer cells

Hypopharyngeal cancer (HC) is a tumor of the upper aerodigestive tract. HC belongs to the category of head & neck squamous cell carcinomas (HNSCCs). Current therapeutic modalities result in poor results, regarding the survival rates and the quality of life of these patients. HC usually develops in the piriform fossa. Patients are often asymptomatic and most of them are diagnosed at late stages.¹¹³

Gold nanoparticles (AuNPs) can be used for plasmonic photothermal therapy (PPTT), usually in near infrared (NIR) region. NIR range radiation can penetrate deeply into tissues, with little effect of the fluorescence on the tissue. AuNPs have the potential to absorb and convert light in NIR range into a heat, quite effectively. This effect is due to the surface plasmon resonance (SPR) and leads to a selective heat-induced apoptosis in tumor cells. Furthermore, conjugation of AuNPs with tumor targeting antibodies produces higher selectivity and efficacy of the therapy method.¹¹³

EGFR (epidermal growth factor receptor) is overexpressed in around 90% of HNSCCs. Mutations affecting EGFR expression or activity, result in proliferation and invasion of various cancer cells. It has been shown, in many studies that anti-EGFR monoclonal antibody (EGFRmAb), conjugated to AuNPs (EGFRmAb-AuNPs), have the potential to induce apoptosis of HSC and HOC malignant cells¹¹⁴ and Hep-2 laryngeal cancer cells.¹¹⁵

In the 2018 study by Zhang et al., there was an evaluation of the application of EGFRmAb-AuNPs conjugates, as photothermal enhancers in FaDu HC cells treatment (human hypopharyngeal squamous cell carcinoma).¹¹³

The two cell lines that were used in this study were the FaDu cell line and the human kidney epithelial 293T cell line. The AuNPs had dimensions of 50 x 12 nm. Polyethylene

glycol was used to conjugate the EGFRmAb to the AuNPs. Confocal microscopy showed that EGFRmAb with AuNPs conjugation improved accumulation into FaDu cells. Cellular uptake of the EGFRmAb–AuNPs in FaDu cells was increased compared to AuNPs alone. However, the level of cellular uptake of the EGFRmAb–AuNPs in 293T cells was significantly reduced compared with AuNPs alone.¹¹³

The cytotoxicity of EGFRmAb–AuNPs was tested by measuring the release of LDH using an LDH activity assay. AuNPs only treatment was cytotoxic to FaDu cells and 293 T cells. EGFRmAb-AuNPs conjugates had significantly lower cytotoxicity compared with EGFRmAb alone in both FaDu and 293T cells. Exposure of groups to NIR radiation induced the cytotoxicity of EGFRmAb-AuNPs group in FaDu cells compared with the same treatment group in 293 T cells.¹¹³

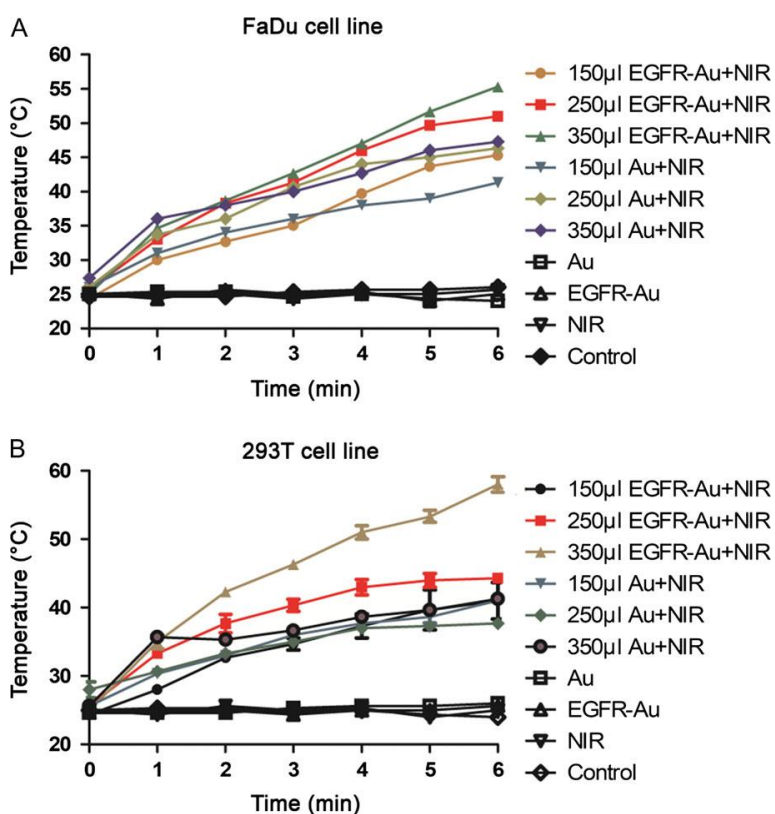


Figure 29: Temperature changes in the cell culture media following treatment with NIR radiation. Following 6 min of irradiation at 808 nm with a near infrared laser: (A) temperature of FaDu cell culture media increased as concentration of AuNPs increased. AuNPs coated with the EGFRmAb produced more heat than uncoated AuNPs. (B) Temperature of the 293 T cell culture media increased as the concentration of the AuNPs increased. AuNPs coated with the EGFRmAb produced more heat than uncoated AuNPs. Data are presented as the mean \pm SD from three independent experiments. EGFR-Au, EGFRmAb-AuNPs, Au, AuNPs¹¹³

AuNPs have been shown to be effective for plasmonic photothermal therapy (PPTT). However, AuNPs have poor specificity for tumor cells and a high cytotoxicity in normal tissues, as shown. Conjugation with EGFRmAb reduced the cytotoxicity to normal tissue. The NIR-induced temperature elevation was correlated with the NIR treatment time and the EGFRmAb-AuNPs concentration. Conjugation with the EGFRmAb increased the temperature in the presence of NIR in both FaDu and 293 T cell cultures. EGFRmAb

conjugation promoted also the uptake of conjugated AuNPs into FaDu cells. Implementation of EGFRmAb-AuNPs with NIR exposure induced FaDu cell apoptosis. Furthermore, conjugation with EGFRmAb enhanced cell selectivity as well as efficacy of AuNPs in FaDu cells.¹¹³

This study also indicated that expression of apoptosis inhibitor Bcl-2 was decreased, while expression of the apoptosis promotor Bax was increased, in FaDu cells treated with EGFRmAb-AuNPs + NIR.¹¹³ Apoptosis was also observed in cells treated with unconjugated AuNPs, possibly because they increase oxidative stress and can potentially bind to the major groove of DNA. After exposure to NIR radiation, these effects of AuNPs can disrupt genome integrity and cause apoptosis. Finally it was demonstrated that a significant amount of EGFRmAb-AuNPs can enter the nucleus.¹¹³

4.5.1.2 Platelet-facilitated Photothermal Therapy

A different approach to the implementation of NPTT is the use of platelets as delivery systems. Platelets (PLTs) accumulate in injured tissues to trigger repair processes. PLTs can evade phagocytosis and also target injured, by PTT-mediated heat, tumor tissues. PLTs can be used as carriers for targeted delivery of AuNRs to tumor tissues, in order to enhance the PTT effect, which leads to further accumulation of PLTs in a feedback manner.¹¹⁶

AuNR-loaded PLTs (PLT-AuNRs), which inherited the long circulating and injury targeting properties of PLTs, were used in a 2018 study, by Rao et al., as PTT enhancement agents. In order to improve AuNRs biocompatibility, they were conjugated with bovine serum albumin (BSA). A cell viability test showed reasonable biocompatibility of AuNRs which was improved when they were loaded into PLTs.¹¹⁶

Interaction of PLTs with circulating tumor cells (CTCs) has shown their targeting potential due to their significant interplay and involvement in tumor metastasis. Further in the experiment, conditional knockout (2cKO) mouse model was employed to further evaluate the in vivo performance of PLT-AuNRs. The mice, bearing HNSCC, which were treated with PLT-AuNRs exhibited the best performance in terms temperature increase, which could be result of the long blood circulation and good cancer targeting capabilities of PLT-AuNRs. Successive temperature increase was observed, after each treatment, showing

that PTT-ablated tumor tissues attracted additional PLT-AuNRs, which enhanced PTT in a feedback manner.¹¹⁶

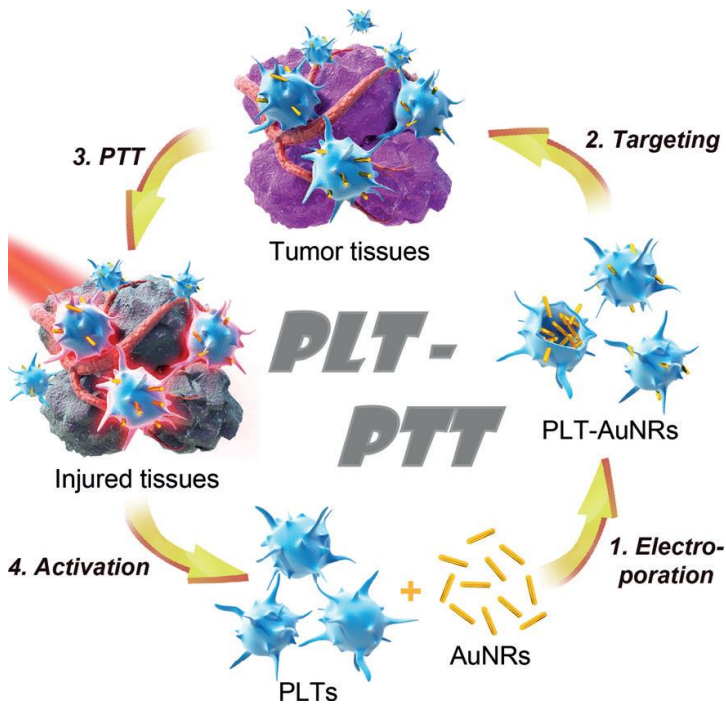


Figure 30: Platelet-facilitated photothermal tumor therapy (PLT-PTT). Platelets (PLTs) were first separated from blood and mixed with gold nanorods (AuNRs). After an electroporation process, AuNRs were loaded into PLTs. The AuNR-loaded PLTs (PLT-AuNRs) were used to enhance photothermal tumor therapy (PTT). Moreover, PTT, which injures the tissues adjacent to tumors, would activate PLTs, which accumulate to tumor sites and enhance PTT effect in a feedback manner.¹¹⁶

The mice received PTT treatment every other day over a period of 15 days and the effects in each group were investigated by measuring the tumor volumes after the various treatments. The mice treated with PBS or AuNRs + Laser, exhibited thriving tumor growth, while PLT-AuNRs + laser treatment method showed significant delay of tumorigenesis in head and neck region.¹¹⁶

This study concluded that PLT-AuNRs enhanced PTT, improved greatly the PTT effects, indicating the efficacy of this method in the treatment of head and neck cancer. Autologous administration of PLTs, which are separated from cancer patients, can be used to develop PLT-AuNRs for personalized cancer therapy.¹¹⁶

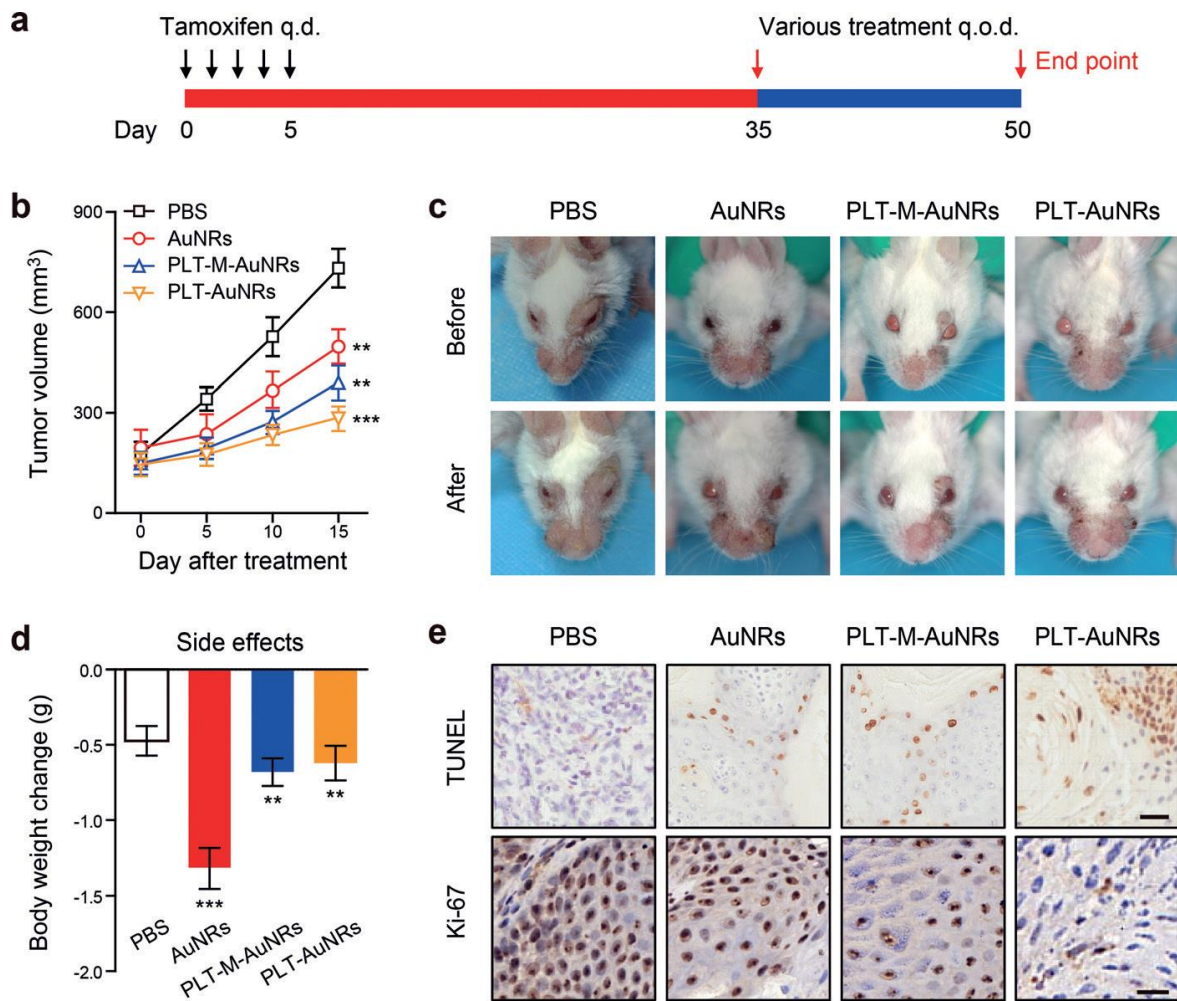


Figure 31: In vivo anticancer effect evaluation. a) Schematic diagram of therapy strategy. HNSCC bearing (2cKO) mice first received (orally) tamoxifen every day for 5 days and then injections of various NPs and laser irradiation or phosphate buffer solution (PBS) only every other day for a period of 15 days. b) Tumor volume curves after various treatments. c) Representative photos of HNSCC bearing mice before and after various treatments. d) Treatment side effects were assessed by mice body weight. e) Representative TUNEL- and Ki-67- stained tumor slice images of mice after various treatments. Scale bars: 50 and 25 mm in TUNEL and Ki-67-stained slices, respectively. Data represented as mean \pm SEM (n=6). Compared with the PBS group, ** and *** individually indicates $P < 0.01$ and $P < 0.001$.¹¹⁶

4.5.2 Nano-Magnetic Hyperthermia (NMH)

Conventional hyperthermia has a heat distribution profile which is characterized by inhomogeneity and can produce hot spots in normal tissue. This inhomogeneity can also result unheated regions in the tumor region, which can lead to relapse. As such, thermal differentiation between cancer and healthy tissue is necessary for a successive treatment. Nano-magnetic hyperthermia (NMH) is a treatment modality, which is based on the ability of magnetic nanoparticles (MNPs) to accumulate in the sites of interest, to achieve

differentiation between the heat distribution in the tumor region and the healthy tissues.¹⁰⁸

NMH is based on the implementation of magnetic nanoparticles in the presence of an alternating magnetic field (AMF). The frequency of the field used ranges from several KHz to 10 MHz, which has an adequate penetration depth. Many factors determine the NMH efficiency, like AMF frequency and amplitude and size of the NPs, which affects their properties. The generation of heat in NMH, is based on two mechanisms, hysteresis losses and relaxation losses. Hysteresis losses occur in particles with multi-magnetic domains, and relaxation losses (Néel or Brown relaxation, figure 32) occur in superparamagnetic or single-domain particles.¹⁰⁸

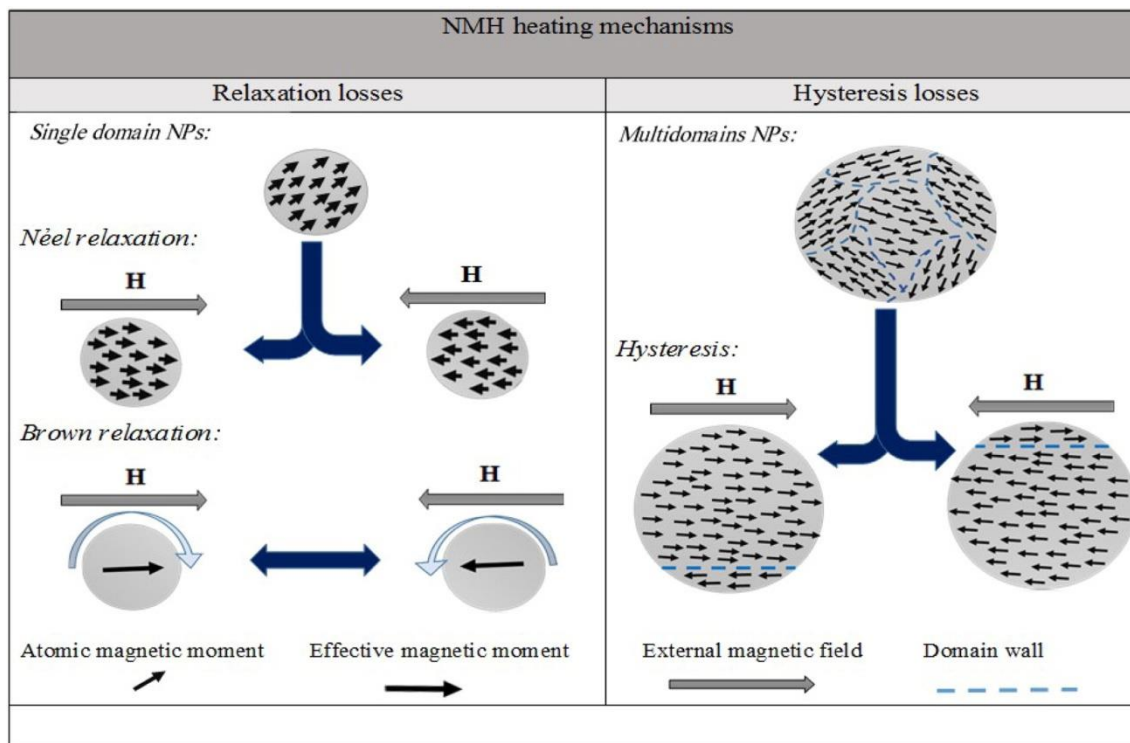


Figure 32: Mechanisms of heat generation via magnetic nanoparticles under AMF.¹⁰⁸

When MNPs are implemented in clinical applications, the magnetic core is modified with a specific coating layer, for the following reasons:

- Prevention of nanoparticle agglomeration within the magnetic fluid (stabilization).
- Minimization of the systemic toxicity of MNPs (biocompatibility).
- Bonding of different functional ligands on the particle surface (functionalization).¹⁰⁸

4.5.2.1 Polyphosphate Magnetic Nanoparticles enhanced Hyperthermia for Oral Cancer Treatment

Hyperthermia therapy aims to produce damage to the cytoskeleton, cytoplasm, and organelles membrane of cancer cells, causing cell death by apoptosis or necrosis. Magnetic HT can be implemented using biocompatible magnetic nanomaterials and a proper magnetic field. The study of Candido et al., in 2014, used the hamster buccal pouch (HBP) carcinogenesis model, to evaluate oral cancer development and efficacy of nano-magnetic hyperthermia. The magnetic nanoparticles (MNPs) used were iron oxide maghemite phase particles ($\gamma\text{-Fe}_2\text{O}_3$), functionalized with tripolyphosphate anions. Human cancer UM-SCC14A cells from the floor of mouth were added to the culture medium (at concentrations of 0.35, 0.7 and 1.4×10^{15} particle/mL), for the incubation with MNPs.¹¹⁷ The animals (hamsters) were divided into five groups (n=6) and were used as animal models of oral cancer, with the exception of the control group. Tumors reached the size of 200-250 mm³.¹¹⁷ The groups are listed in the following table.

Table 3	Experimental Group	n
	Normal group	6
	Cancer group (no treatment)	6
	MNP group	6
	MNP + AMF1 group	6
	MNP + AMF7 group	6
MNP: polyphosphate-coated magnetic nanoparticles AMF1 and AMF7: data collected one day and seven days, respectively, after NMH ¹¹⁷		

The two last groups received a combined treatment of MNPs and exposure to an alternating magnetic field (AMF) at a frequency of 1MHz and 40 Oe field amplitude. There was no significant difference in cytotoxicity for MNPs up to 0.7×10^{15} particle/mL, showing no toxicity by MNPs at these concentrations. At the 1.4×10^{15} particle/mL concentration, there was an increase in cytotoxicity, verified by the decrease in cell viability.¹¹⁷

Histopathologically, in the cancer group (no treatment), cellular pleomorphism with many atypical mitoses, were observed. Regarding the tissue arrangement, hyperplasia,

hypergranulosis, hyperkeratosis, parakeratosis and acanthosis in the basal layer, were present.¹¹⁷

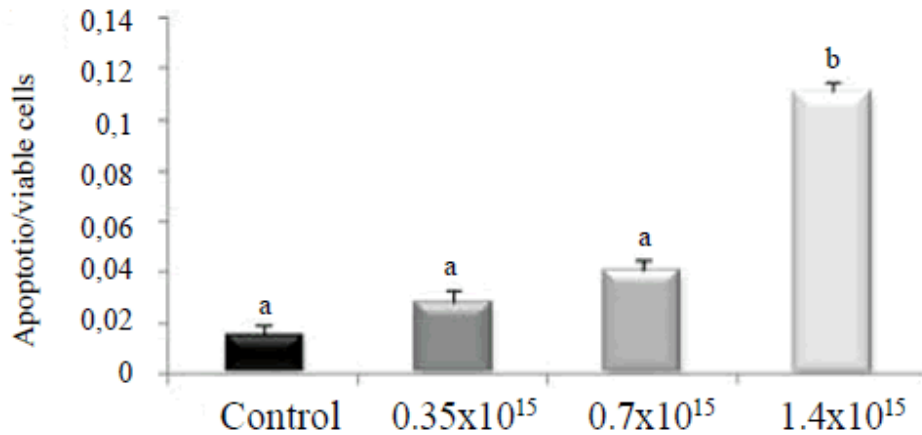


Figure 33: Effect of MNPs on apoptosis. Cells incubated with 0.35×10¹⁵, 0.7×10¹⁵ and 1.4×10¹⁵ particle/mL¹¹⁷

These features were observed to a lesser extent, in animals treated with MNPs. There was a slight recovery in the tumor size of group MNP but without complete regression. In animals that received combined treatment with MNPs and hyperthermia (MNP+AMF1 and MNP+AMF7 groups), a significant regression of the cancer was observed. Response to the combined therapy was time-dependent (more satisfactory for animals euthanized seven days after, than one day after).¹¹⁷

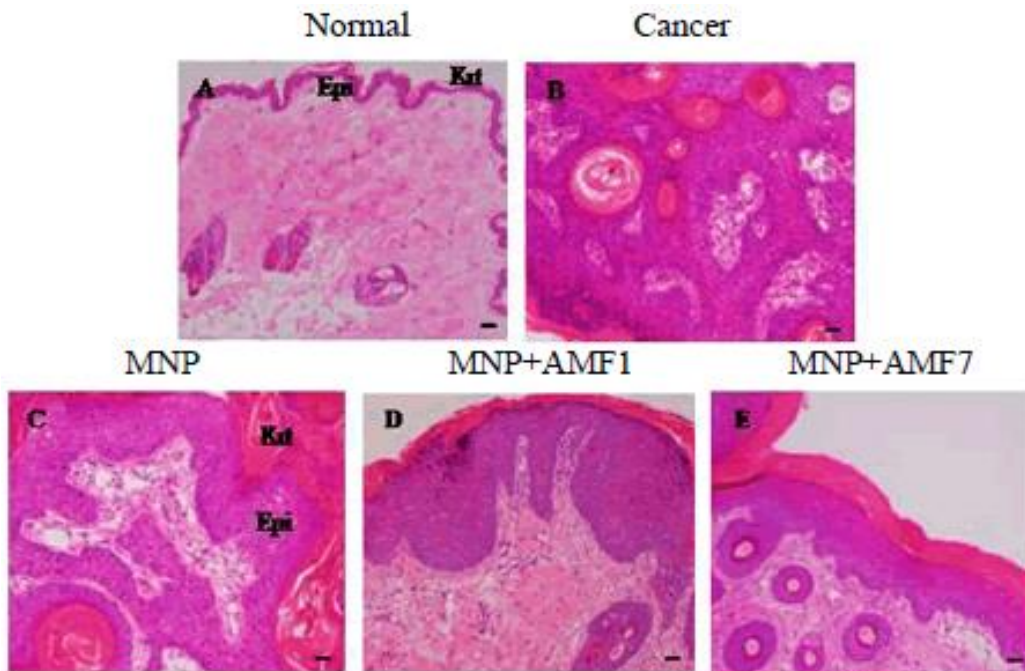


Figure 34: Histopathological sample of right buccal pouch in the (A) Normal, (B) Cancer, (C) MNP, (D) MNP+AMF1 and (E) MNP+AMF7 groups. Tissues were stained by HE. Scale bars represent 20 µm. Epi: epithelium. Krt: keratin.¹¹⁷

MNPs were present at high levels in the spleen. This finding indicated that biodistribution of MNPs passed through the spleen before being removed, though it was also shown that there was no accumulation of MNPs in the body after a few days.¹¹⁷

NMH treatment resulted in two significant effects. The first effect was intense apoptosis and fibrosis in the tumor area and the second was the inhibition of cell proliferation. These two effects indicated that the NMH induced cell death in the tumor tissue. Another important finding of this study was that the functionalized iron oxide MNPs not only demonstrated the characteristics of a magnetic NP, but, moreover, the biocompatibility and biodegradability of functional organic materials.¹¹⁸ The use of MNPs at concentration of 0.7×10^{15} particle/mL was free of adverse effects significant cytotoxicity in vitro. Finally, it was demonstrated that NMH led to lysis of OSCC, in vivo, showing the effectiveness of this treatment method.¹¹⁷

4.5.3 Nano-Radio-Frequency Ablation (NaRFA)

Radiofrequency (RF) waves can penetrate deep into tissues inside the body and reach deep-seated tumors. However RF ablation is an invasive, non-specific and non-uniform heating method, which can produce adverse thermal effects on healthy tissues. Moreover, current RF ablation techniques are characterized by inaccuracy and incomplete treatment, especially in large tumors.¹⁰⁸

Nano-Radio-Frequency Ablation (NaRFA) is a non-invasive technique, which has the potential to improve the efficacy of the treatment, maximizing the effect on tumor tissue and minimizing heat deposition to healthy one. This can be achieved by accumulation of nanoparticles in the tumor, which absorb the RF electric field and release heat selectively in cancer cells.¹⁰⁸

In 2011, Kruse et al. evaluated the effects of particle size in RF treatment-induced heating rate. AuNPs with diameters of 5, 10, 20 and 50 nm were exposed to RF waves (at 125W). 5 nm AuNPs produced the highest heating rate. It was concluded that smaller NPs were more efficient RF sensitizers.¹¹⁹ This effect was attributed to the higher resistivity of a smaller nanostructure. Higher resistivity, according to the joule heating principle, leads to more efficient heat dissipation.¹²⁰ Kruse et al. also evaluated the AuNP concentration effect on RH heating rate. The temperature rise versus concentration profiles showed

that the temperature increases directly with the AuNP concentration up to a specific range and eventually saturates, when further increases in concentration had no effect on temperature changes.¹²⁰

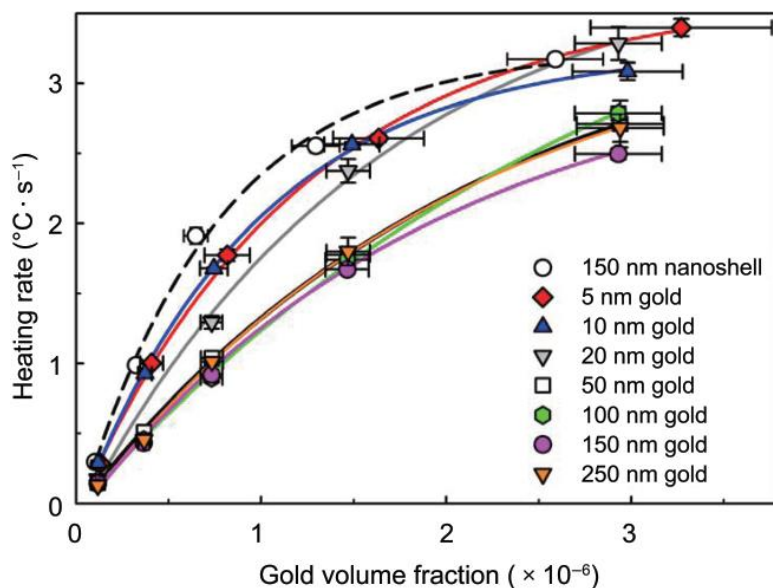


Figure 36: Size-dependent RF heating rates of AuNPs versus gold volume fraction. A size-dependent clustering of RF heating rates is shown.¹²⁰

4.5.4 Nano-Ultrasound Hyperthermia (NUH)

Ultrasound can offer advantages over other heating methods. It can focus heat at any depth, with minimal thermal damage to surrounding tissues. High intensity focused ultrasound (HIFU) is a non-invasive method, implemented in benign and malignant diseases.¹⁰⁸ HIFU shows high spatial accuracy, thus having great potential as a targeted thermal therapy, however it has some drawbacks. Small volume of ablated tissues is produced in the focal region of a focused acoustic field, which leads to elongation of exposure time, in order to effectively treat large tumor regions. As a result, elongation of treatment time can result in thermal injuries of healthy tissues, as well as inaccuracy, caused by organ motions.^{121,108}

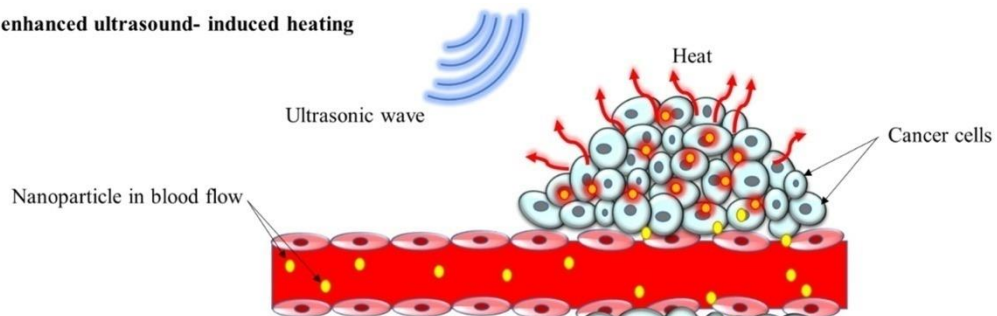
Nanoparticles can, also in this technique, enhance the absorption of energy of ultrasound waves producing heat. NPs implementation modifies thermal and mechanical interactions of ultrasound with tissues, improving the effects of ultrasound-induced heating and cavitation (figure 37).¹⁰⁸ Thermal interactions depend on:

- a) Ultrasound attenuation coefficient: Through absorption and scattering of ultrasound waves, additional attenuation of the acoustic waves by NPs is induced, causing

additional thermal dissipation. Larger NPs attenuate acoustic waves more extensively than small ones. Furthermore, NPs attenuate more extensively the higher ultrasound intensities and frequencies.¹⁰⁸

b) Thermal conductivity: Due to their high thermal conductivities, metallic NPs can enhance the effective thermal conductivity of a tumor loaded with these NPs, exhibiting increased heating rate, relative to surrounding tissues. Smaller NPs have higher thermal conductivity due to their higher surface to volume ratio.^{108,122}

a) Nanoparticle enhanced ultrasound- induced heating



b) Nanoparticle enhanced ultrasound- induced cavitation

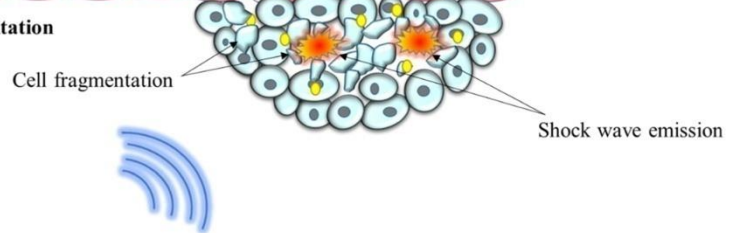


Figure 37: Thermal and mechanical interactions of ultrasound with tissues.¹⁰⁸

c) Mechanical interactions: The implementation of HIFU can also result in non-thermal effects, such as acoustic cavitation, microstreaming and radiation forces,¹²³ which produce jet formation and shock wave and consequent shear stress, membrane damage and cell death.^{108,123} By modification of exposure time, number of pulses and duty cycles, it is possible to produce predominantly thermal or non-thermal effects in the focal region.¹²³

Production of elevated temperatures in the tumor, when the target site is located deep inside the body or if it's hypervascularized, can be problematic. Enhancement of the acoustic power or the exposition time can produce the desired effects, but it increases the risk of side effects. Nanoparticles or micro- and nano-bubbles can enhance HIFU mechanical effects, inducing cavitation nuclei. Moreover, they increase acoustic attenuation which leads to temperature rise, reducing the required ultrasound intensity

and exposure time, to achieve the desired outcomes, thus decreasing adverse effects probability.¹²³

4.6 Combination of Nanoparticle Enhanced Hyperthermia and Radiotherapy

As mentioned above, hyperthermia has radiosensitizing effects. Considering this property, the synergistic effects of hyperthermia and radiotherapy can potentially overcome the limitations of each single therapeutic modality and result in an effective treatment for radioresistant tumors.¹²⁴

Exposure to temperatures above 41°C, results in protein denaturation and temporary cell inactivation. Surviving cells appear resistant to further exposure, due to thermotolerance. Increased thermotolerance limits the efficiency of hyperthermia, though it can be an advantage for radiation therapy. In some cases, thermotolerance comes along with a modification of cellular response, increasing sensitivity to X-ray irradiation. Furthermore, photo-thermal therapy can enhance radiotherapy effects, by attenuating the repair of DSBs induced by RT. Cells in S-phase and in hypoxic, low pH regions, have increased radioresistance. Hyperthermia increases blood flow, which results in improved tissue oxygenation, causing increased radiosensitivity, temporarily.¹²⁴

Furthermore, the enhancement of these combined modalities with appropriate nanoparticles, has the potential to achieve improved therapeutic outcomes with a reduced X-ray dose.¹²⁵

4.6.1 Nano-Photo-thermal therapy and radiotherapy enhanced by folate conjugated gold nanorods (AuNRs) on KB nasopharyngeal carcinoma cells

Gold nanoparticles (AuNPs) bring together a wide range of attractive properties, such as their biocompatibility and low toxicity, their high atomic number (Z=79) and ability to absorb both ionizing and non-ionizing radiation, as well as their ability for surface functionalization. These properties of AuNPs, makes them ideal candidates for nano-photothermal therapy (NPTT) and enhanced radiotherapy (RT).¹²⁶

There is variability in AuNPs types, such as nanorods, nanocages, nanoshells. Nanorods (AuNRs) are characterized by small diameter and high heat conversion efficacy. When AuNRs are irradiated by NIR laser, with a wavelength at their Longitudinal Plasmon Resonance (LPR), induce photothermal damages to cancer cells. Furthermore, the high-Z

number and high electron density of gold, result in strong X-ray attenuation, thus an effective radiosensitizing agent. The radiosensitization of tumors to radiotherapy, by gold NPs, is induced by the production of reactive oxygen species (ROS), which cause cytotoxicity via apoptosis. As such, AuNRs are effective radiosensitizing and photosensitizing agents.¹²⁶

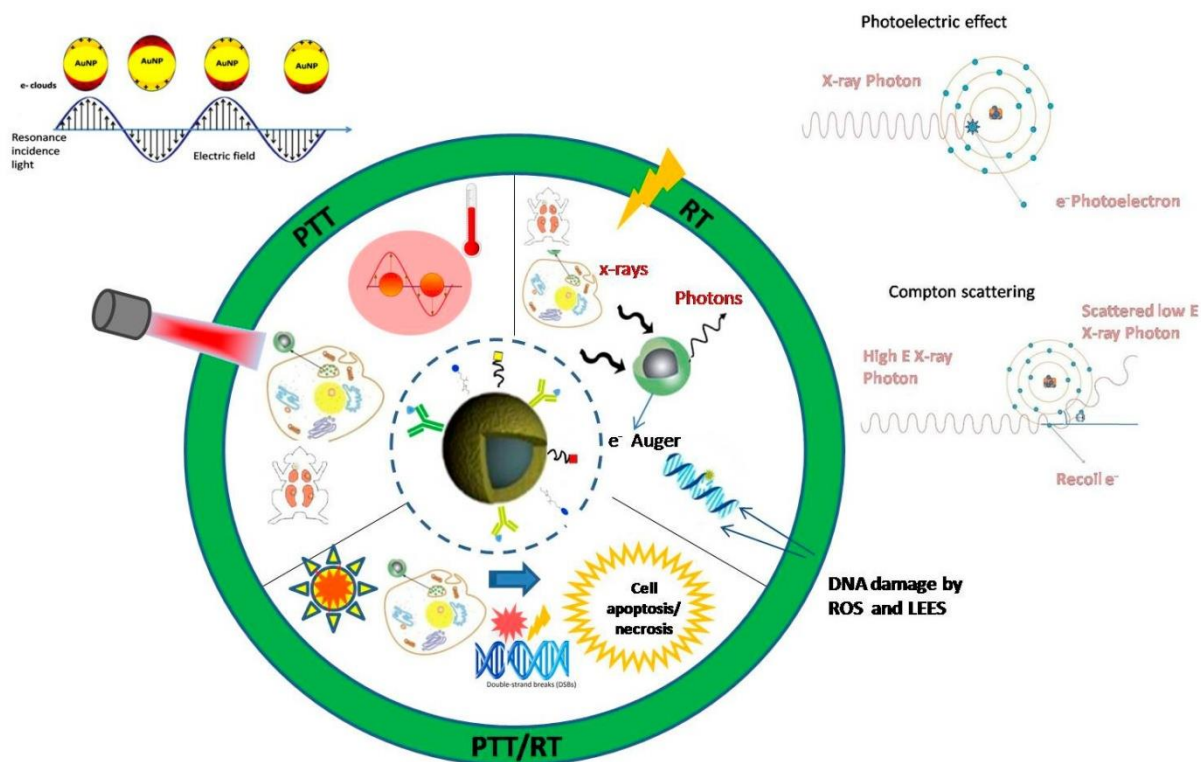


Figure 38: Basic mechanisms of action of photothermal therapy and ionizing radiotherapy and combination of both, enhanced by nanoparticles.¹²⁴

In addition, there are many types of functionalization of AuNRs, among which, folic acid appears to be ideal candidate, due to its low cost, non-immunogenic properties and easy conjugation. Cancer cell overexpress folate receptors, as folate is necessary for DNA nucleotide synthesis and cell division. Therefore, folate conjugated AuNRs are suitable for active targeting in head and neck cancer.¹²⁶

Movahedi et al. reported, in 2018, a study concerning the use of folate (FA) conjugated gold nanorods (AuNRs), as thermo-radiosensitizing agents, in the treatment of KB nasopharyngeal cancer cells. They prepared and characterized FA-conjugated and non conjugated AuNRs, with the use of UV-visible (UV-vis) spectroscopy, dynamic light

scattering (DLS) and transmission electron microscopy (TEM), to analyze the morphology, size distribution and effective diameter of nanoconjugates.¹²⁶

The KB human nasopharyngeal carcinoma cells were grown in a culture medium. 10,000 cells/well in 96 well plates were cultured and treated with nanoparticles (5,10 and 15µg/ml incubated for 4h), to evaluate cytotoxicity of AuNRs and AuNRs-FA (figure 39).¹²⁶ KB cells, with or without NPs, were exposed to laser radiation at wavelength of 808 nm, for 5, 10, 15 min. After laser exposure, treated cells were submitted to 2 Gy of 6 MV X-ray, with a dose rate of 2 Gy/Min.¹²⁶

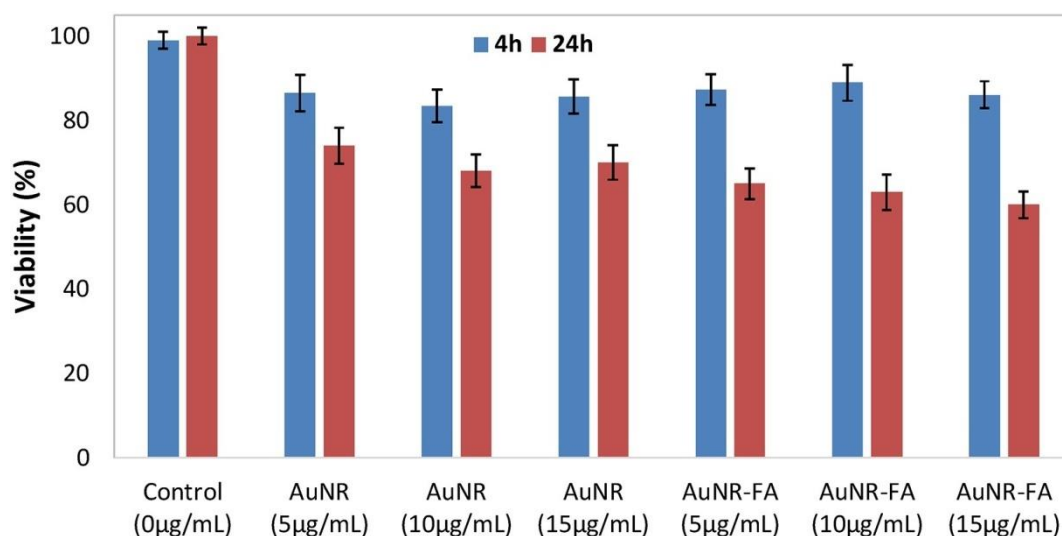


Figure 39: The viability of the KB cells treated with different concentrations of AuNRs and AuNR-FA (incubation time: 4 h and 24 h). All groups had significant cytotoxicity compared with control group ($P < 0.03$), but with no significant differences with each other ($P > 0.05$). At the same concentration, cell viability for 24 h incubation was significantly lower than that observed for 4 h ($P < 0.02$).¹²⁶

Treatment of KB cells with nanoconjugates resulted in significant damage to mitochondria and swelling of the nucleus membrane. Combined treatment with nanoconjugates + laser + radiotherapy induced intensive damage to KB cells: autophagic vacuoles, damaged mitochondria, chromatin condensation, plasma membrane

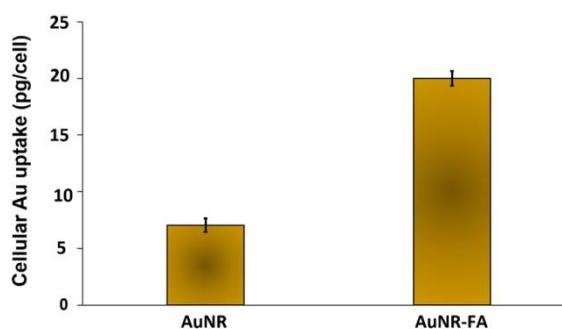


Figure 40: Au content of KB cells, following treatment with targeted and non-targeted AuNRs (15 µg/ml; 4 h).¹²⁶

blebbing and disruption of the plasma membrane (figure 41).¹²⁶

Figure 41: Ultrastructure of KB cells after receiving combinatorial treatment (AuNR-FA + laser + RT). Arrows show the presence of nanoconjugates inside the KB cell. aV: autophagic vacuoles, M: mitochondria, CC: chromatin condensation, b: plasma membrane blebbing.¹²⁶

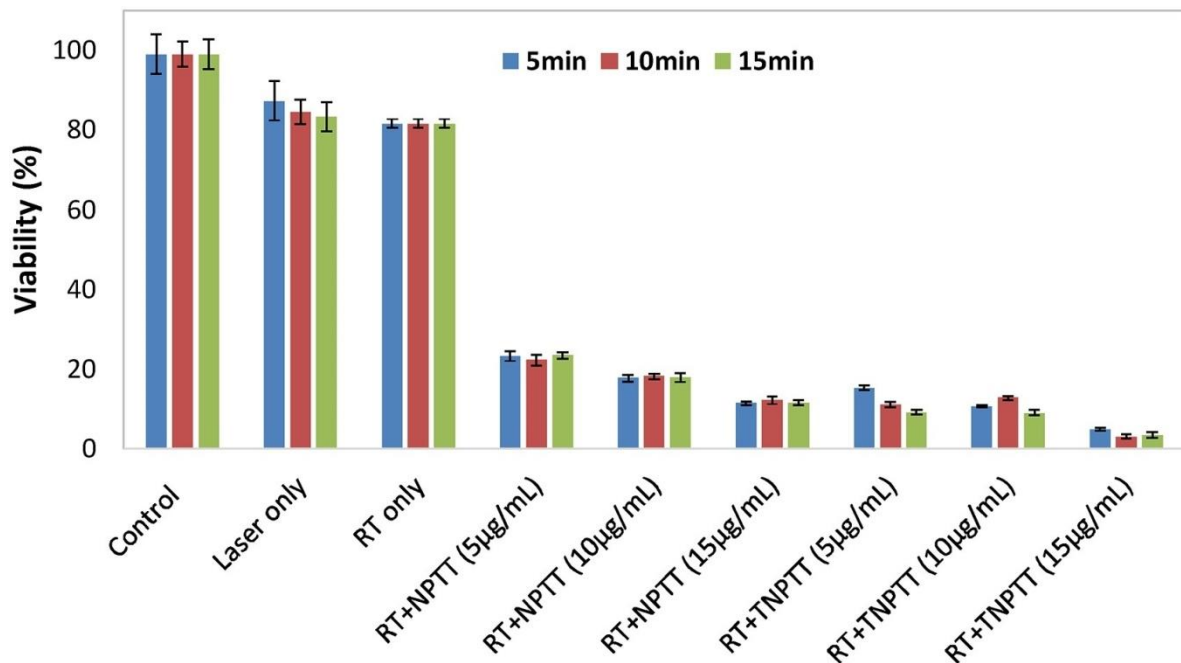
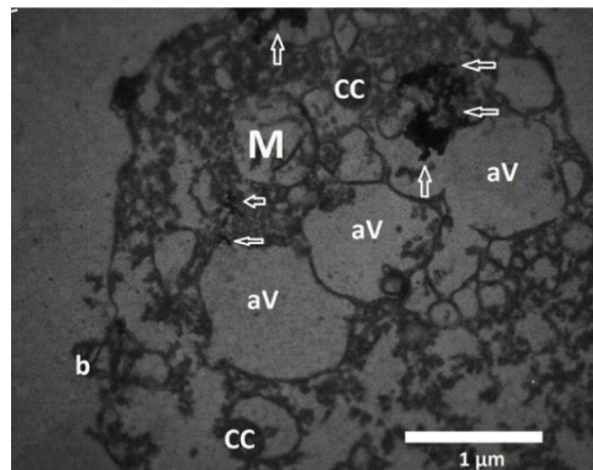


Figure 42: Viability of KB cells received various combinatorial treatments of nanoparticles, X-ray and laser exposure. All groups had significant cytotoxicity compared with control group ($P < 0.03$). At the same concentration, cell viability for RT+TNPTT groups were significantly lower than RT+NPTT groups ($P < 0.05$). Also, at the same concentration of nanoparticles, laser irradiation time had no significant effects ($P > 0.05$). RT: radiotherapy, NPTT: nano-photo-thermal therapy, TNPTT: targeted nano-photo-thermal therapy¹²⁶

The group treated with the combination of targeted AuNRs-FA, RT and NIR laser, shown substantially decrease of cell viability to 3.5% (figure 42), indicating that targeted nanoparticles demonstrated an excellent photo-thermo-radiosensitivity. The mechanism of this successful enhancement, may be related to the high level of cell uptake for AuNR-FA nanoconjugates.¹²⁶

Radiotherapy's goal is the destruction of tumor cells, while preserving healthy tissue. However, the radioresistance of tumors is related with relapse of cancer. Moreover,

increased radiation dose, in order to achieve an effective treatment, causes severe side effects to patients with head and neck cancer. The combination of radiotherapy with hyperthermia offers the possibility of an effective treatment, because of the radiosensitizing effects of hyperthermia treatment modalities.¹²⁶

The implementation of nanoparticles in cancer therapy, has beneficial outcomes, when combined with the above mentioned therapy methods. This study demonstrated that AuNRs' ability to absorb NIR laser radiation (caused by the surface plasmon resonance effect), produces significant enhancement in photo-thermal treatment. In addition, the strong X-ray attenuation of gold (due to the high-Z number of Au), renders AuNRs as effective radiosensitizing agents. These unique properties of gold nanoparticles, along with their ability for active targeting (by surface functionalization) and their low toxicity, enable them as ideal enhancers for the combined use of hyperthermia and radiotherapy.¹²⁶

The conclusions of this study are in good agreement with other relative publications.¹²⁶

4.6.2 Treatment of HNSCC with nano-Quadrapeutics

An interesting multidisciplinary approach study, regarding the treatment of patients with aggressive types of HNSCC, was published in 2015, by Lukianova and Lapotko. The goals of this approach were the selective destruction of drug-resistant residual cancer cells, while preserving functionality of healthy tissue and the reduction of nonspecific toxicity and duration of the therapy.¹²⁷

Lukianova and Lapotko reported their findings regarding the implementation of "Quadrapeutics" in the treatment of HNSCC. Quadrapeutics is defined as a cell-level on-demand therapeutic technology, self-regulated in cancer cells' therapeutic strength and amplified with cancer's aggressiveness.¹²⁷

Quadrapeutics treatment is based on the administration (systemically) of AuNPs and a liposomal drug (both conjugated to a HNSCC-specific standard antibody), aggregate into an intracellular nanocluster via receptor-mediated endocytosis. The largest nanoclusters form in aggressive cancer cells, while the smallest form in healthy ones. A low energy NIR laser pulse is then applied. The laser's energy is converted to heat through the plasmon resonance effect in the AuNPs, leading to the evaporation of the surrounding liquid,

forming an expanding-collapsing (lasting nanoseconds) vapor nanobubble (plasmonic nanobubble – PNB). The laser pulse generates PNBs only around large nanoclusters (internalized in malignant cells), because they have a high PNB generation threshold energy. Finally, low dose of radiation is applied.¹²⁷

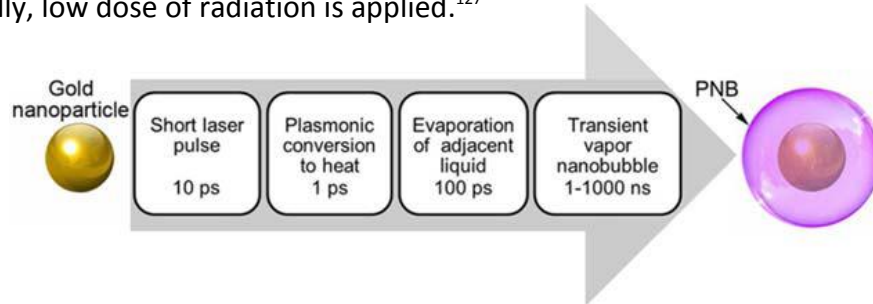


Figure 43: Plasmonic nanobubble (PNB) generation. Absorption of a laser pulse by NP and plasmonic conversion of light to heat, results in rapid explosive evaporation of the surrounding liquid. This vapor expands and collapses in nanoseconds. This non-stationary effect is named PNB.¹²⁷

This process results in the following synergistic events:

- The large PNBs eliminate malignant cells.
- If some PNBs are not large enough to destroy cancer cell, they produce rupture of the colocalized liposomes/endosomes, causing the release of the encapsulated drug into the cytoplasm, which kills the cell.
- Lastly, the low energy radiation is selectively enhanced by the large nanoclusters in cancer cells, producing the emission of secondary electrons.¹²⁷

The PNB generation threshold energy depends on NP size and aggregation state and rapidly decreases with NP diameter or with nanocluster size (when NPs aggregate into clusters).¹²⁷

The quadrapeutics has been evaluated, both in vitro (for two HNSCC cell lines and normal

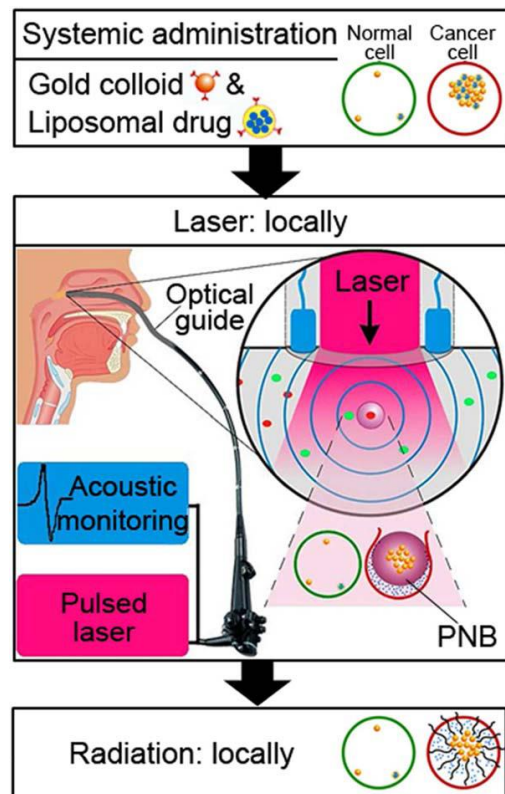


Figure 44: Quadrapeutics: Functionalized AuNPs and liposomal drugs are delivered systemically to form nanoclusters in cancer cells. Laser pulse is applied locally via an endoscope to selectively generate PNBs, which destroy cancer cells and release liposomal drug. The same nanocluster selectively enhances the radiation. These events produce an intracellular synergistic effect, only in malignant cells.¹²⁷

epithelial cells) and in vivo (HNSCC in xenograft animal models), for combined diagnosis and treatment (theranostics). PNBs were detected in vivo via acoustic traces. Also, the PNBs were evaluated for intraoperative detection of microscopic residual disease. After tumor removal, the surgical margins were scanned with a NIR laser. High HNSCC sensitivity and specificity was demonstrated, as well as high speed intraoperative diagnosis of microscopic residual disease.¹²⁷

Furthermore, quadrapeutics treatment suppressed tumor growth after the first week. Also it accelerated and improved the effect of chemo- and radiotherapy by 17-fold in a week after a single administration.¹²⁷

Quadrapeutics nanotechnology is a novel intracellular combinatorial micro-treatment, which can be implemented as a primary, second line or adjuvant, intra- or postoperative therapy method and has the potential to achieve impressive results, in the fight against head and neck cancer.¹²⁷

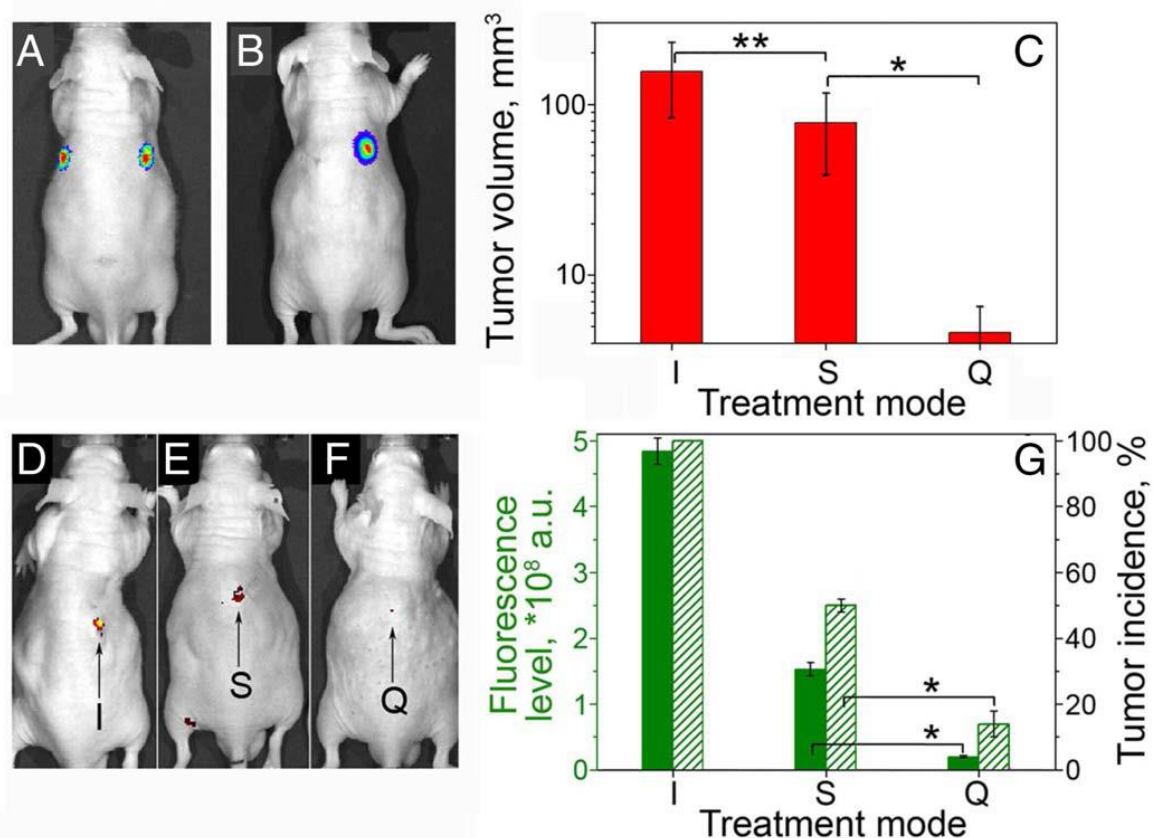


Figure 45: Quadrapeutics in vivo in HNSCC mouse model. (A–C) Primary xenograft tumor. Bioluminescent images before (A) and 7 days after (B) single-time implementation of quadrapeutics (left side, Doxil-C225, AuNPs C225, both IV, laser pulse local, radiation) and chemoradiation (right side, same doses of Doxil and radiation). (C) Tumor volumes 7 days after treatment (I: untreated animals, S: chemoradiation, Q: quadrapeutics - drug, AuNP, laser, radiation). (D–G) Intraoperative treatment of microscopic residual disease: fluorescent images, obtained 28 days after (D) surgery alone (I), (E) surgery and adjuvant chemoradiation (S), (F) surgery and adjuvant quadrapeutics (Q). (G) Metrics of recurrent tumors obtained in 28 days after the intraoperative treatment of MRD49: green - level of the tumor fluorescence, gray - incidence rate of a recurrence tumor.¹²⁷

4.6.3 Single NP-agent for radio- and radio-photothermal therapy in anaplastic thyroid cancer

Another interesting study, with the use of radiometal beta-emitting NPs, was performed by Zhou et al., in 2015, concerning the NP-enhanced radiotherapy combined with photothermal therapy. The advantage, which results from the use of β^- particle emitter radionuclides as RT enhancers, is that the radioactivity produces significant damage to cancer cells, yet it doesn't harm healthy tissue, as the mean range in tissue is less than a few millimeters. Copper 64 (^{64}Cu) has an intermediate half-life ($T_{1/2}=12.7$ h) and decays through β^+ emission (19%), β^- emission (40%) and electron capture (41%).¹²⁸

In this study, chelator-free polyethylene glycol (PEG)-coated [^{64}Cu]CuS NPs were used, which also have a strong NIR absorbance. These NPs were used with PET (positron emission tomography) for imaging, and also combined with radiotherapy (RT), photothermal therapy (PTT) and combination of both, for the treatment of an orthotopic xenograft model of anaplastic thyroid carcinoma (ATC). While noble metal NPs are the most widely used, as agents for PTT, semiconductor copper sulfide (CuS) NPs are also useful, because NP size can be controlled at around 10 nm and absorption peak readily tuned to 930-1100 nm, which makes them suitable for PTT and photoacoustic imaging with the use of a 980-nm or 1064-nm laser.¹²⁸

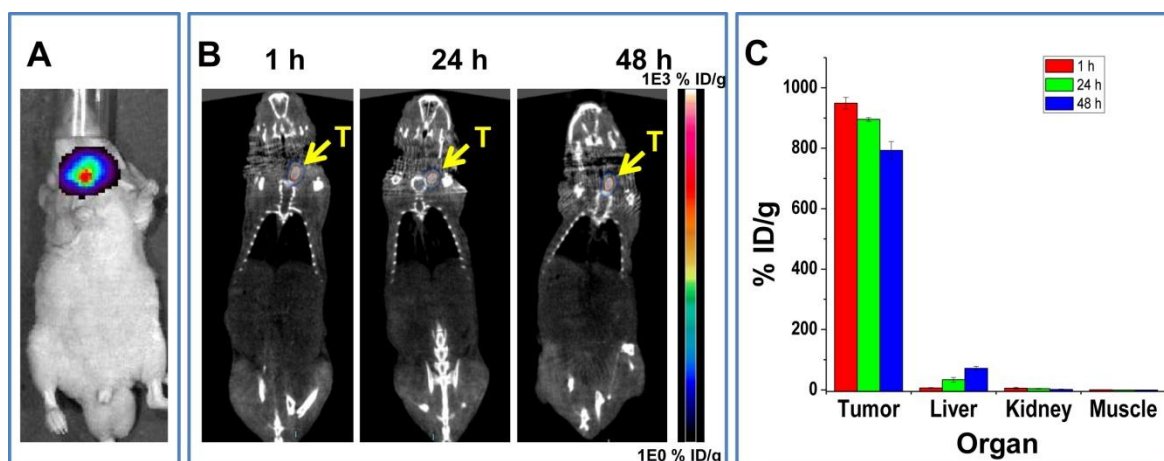


Figure 46: (A) Bioluminescence image of Hth83 ATC tumor-bearing mouse. (B) micro-PET/CT images and (C) graph of NP distribution in major organs, at 1, 24, and 48 h after intratumoral injection of NPs.¹²⁸

The mice were injected orthotopically into the right thyroid gland, with ATC cell line (Hth83-lucif cells, 5×10^5 cells/mouse). The tumors were allowed to grow until their size reached 30-50 mm³.¹²⁸ Micro-PET/CT imaging was performed, showing the tissue

retention of the NPs and tumor presence was confirmed by bioluminescence imaging (figure 46).¹²⁸

Compared with no treatment, treatment with PEG-CuS NPs + NIR laser (combined RT/PTT) inhibited ATC tumor growth by 83.14%. RT/PTT therapy produced a significantly better result, in delaying tumor growth than PTT. However, no significant difference in tumor growth inhibition was observed, between RT/PTT and RT. Thus, tumor growth inhibition in mice treated with RT/PTT resulted in an improved survival advantage.^{XH131} In addition, there were no obvious signs of toxicity in the NPs-injected mice, within 30 days after injection. Furthermore, no significant reduction in body weight was observed in any group.¹²⁸

In conclusion, this study showed that combined RT/PTT, enhanced by PEG-[⁶⁴Cu]CuS NPs, treated ATC tumors, much more effectively than RT or PTT alone. Furthermore, RT/PTT

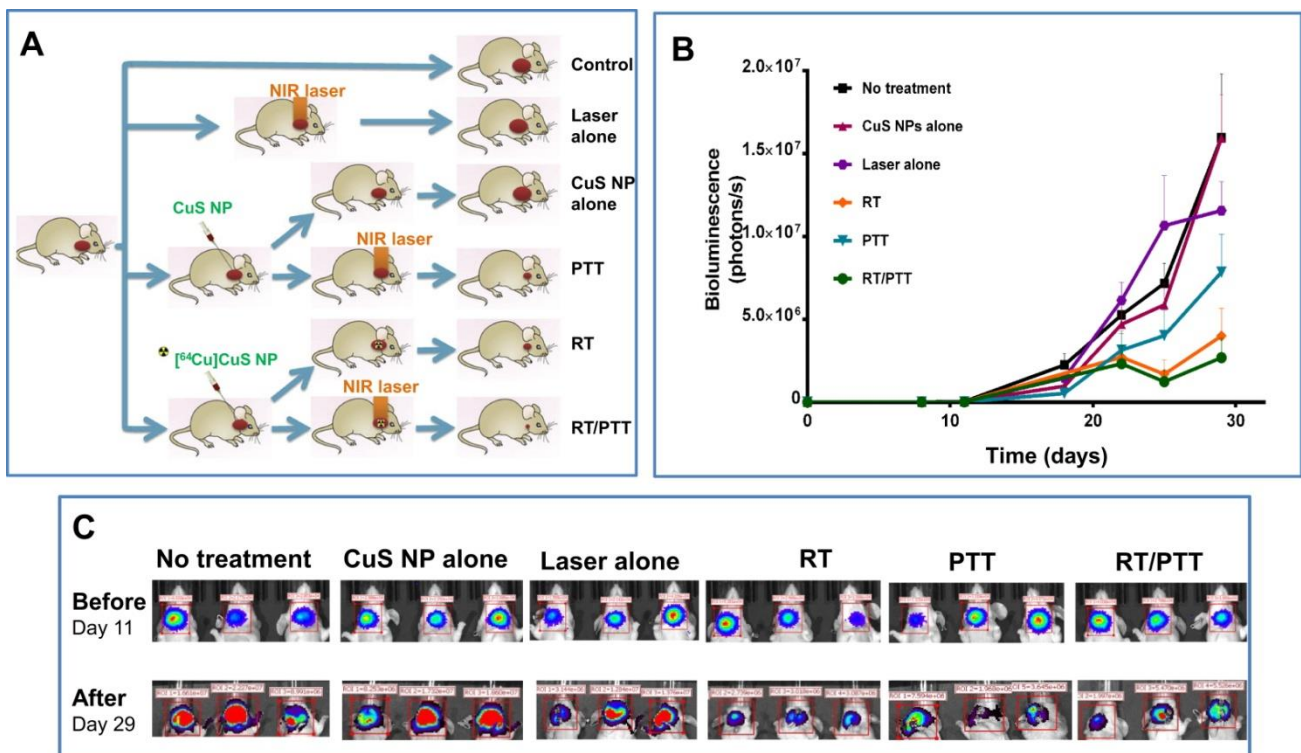
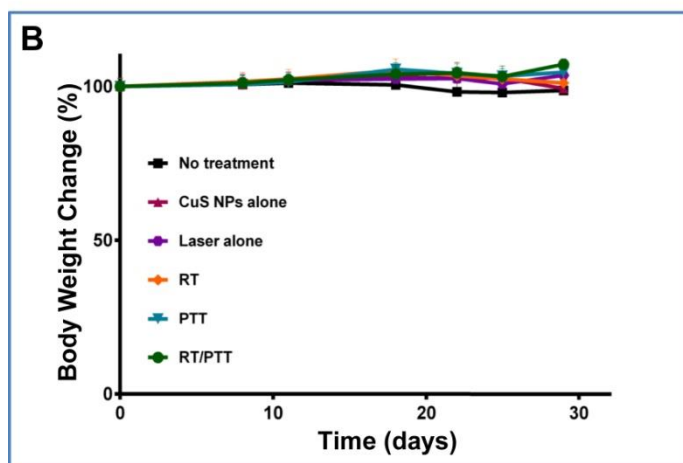
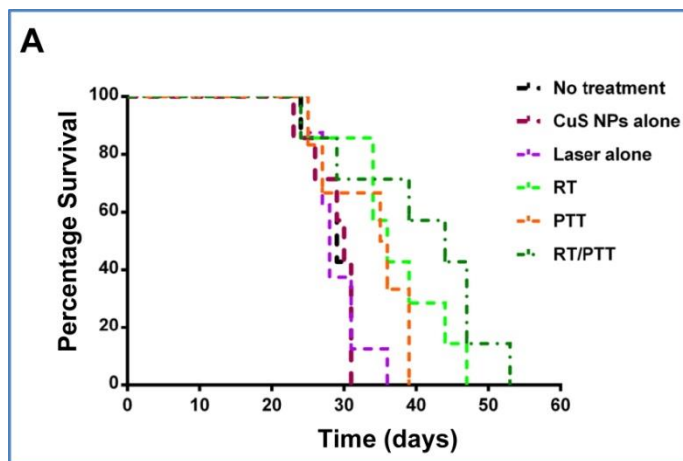


Figure 47: (A) Antitumor activity design, in mice bearing-ATC tumors. (B, C) Tumor growth curves and corresponding bioluminescence images after treatment with CuS NPs alone, laser alone, RT, PTT and combined radio-photothermal therapy (RT/PTT). A no treatment group was control group.¹²⁸

combinatorial treatment, significantly prolonged the survival of orthotopic ATC tumor-bearing mice. Therefore, single compartment multifunctional NP system was successful as a beta-emitter enhancing RT, as well as an efficient agent for PTT.¹²⁸

Figure 48: (A) Kaplan-Meier survival curves of Hth83 ATC tumor-bearing mice after treatment with CuS NPs alone, laser alone, RT, PTT, or RT/PTT. Mice without treatment were the control group. (B) Body weight changes after treatment with CuS NPs alone, laser alone, RT, PTT, or RT/PTT. Mice group without treatment was the control group.¹²⁸



5. Discussion

Radiation therapy is one of the main treatment modalities for head and neck cancer. However, the lack of selectivity (between cancer and healthy tissue), despite the advanced techniques in radiation delivery, can cause severe adverse effects, because of the radiation induced-normal tissue damage. Nano-radio-sensitizers have the ability to effectively enhance the RT efficacy, reducing the total dose absorbed by healthy tissue and thus, the side effects. The most common NPs, used for RT enhancement are AuNPs, owing their potential for effective radio-enhancement, to their unique properties, such as high-Z number, high density and large energy absorption coefficient. However, a number of various elements for NP synthesis have been tested, in order to achieve efficient radiosensitization, with interesting results, regarding their success in tumor control and low toxicity.

A successful cellular uptake of NPs in cancer cells is required for an efficient radiosensitization. Thus, nanoparticles' properties, namely their size, shape, charge and surface modification, are of great importance, in order to achieve an effective

accumulation in tumor site. Moreover, passive and active targeting have an important role, regarding an effective cellular uptake.

In the following table, a summary of the methods (briefly) and results of the application of radiotherapy combined with nanoparticles – from the in-vitro and in-vivo studies – are listed.

Study	Cancer Type	Nanoparticles	Results
Popovtzer et al., 2015 (in-vivo)	HNSCC (A431 cells)	Cetuximab-coated AuNPs	Significant reduction of tumor volume, high apoptosis rate.
Teraoka et al., 2018 (in-vitro)	HNSCC (HSC-3 cells, tongue carcinoma)	AuNPs	Significant reduction of cell number, high apoptosis rate.
Mirrahimi et al., 2018 (in-vitro)	KB cancer cells (mouth epidermal carcinoma)	FA-Au@Fe ₂ O ₃ NPs	High apoptosis rate, considerable dose enhancement and ROS production.
Yehui ping et al., 2009 (in-vivo)	HNSCC (SCCVII cells)	PLGA NPs-EGFR ASOs	Increased radiosensitivity caused by EGFR inhibition.
Hazkani et al., 2017 (in-vivo)	ACC (adenoid cystic carcinoma)	Crizotinib-AuNPs	Significant decrease of tumor volume, near disappearance.
Le Duc et al., 2011 (in vivo)	Gliosarcoma	Polysiloxane shell-Gd ₂ O ₃	Increased contrast in MRI and significant animal survival (theranostic NP).

Table 4: Nanoparticle-enhanced Radiotherapy. HNSCC: human squamous cell carcinoma, ACC: adenoid cystic carcinoma, FA: folic acid, EGFR ASOs: EGFR-antisense oligonucleotides, PLGA NPs: Poly(lactic-co-glycolic acid) nanoparticles.

The ability of gold nanoparticles to absorb NIR laser, renders them suitable agents for thermal effects enhancement. Introduction of AuNPs in photothermal treatment, has restored hyperthermia's significance in cancer therapy, especially as an adjuvant therapy, combined with radiotherapy. Photo-thermal-therapy (PTT) induced cancer cell destruction can be greatly enhanced by the application of AuNPs as photocensitizers. The study of Zhang et al. in 2018 has shown that EGFRmAb-AuNPs demonstrated significant accumulation in FaDu cell (hypopharyngeal carcinoma) nucleus. Furthermore, the combination with NIR laser technique, led to increased apoptosis of FaDu cells. In the study of Rao et al., in 2018, it was indicated that AuNR-loaded PLTs (autologous platelets) enhanced the effects of photothermal therapy, in the treatment of squamous cell carcinoma (personalized medicine).

The implementation of Nano-Magnetic-Hyperthermia treatment combined with iron-oxide nanoparticles (maghemite phase), in the treatment of oral cancer carcinoma, resulted in both apoptosis and fibrosis in tumor site, inducing cancer cell death. Moreover IONPs demonstrated good biocompatibility and biodegradability.

Table 5 shows the results of combined use of NP-enhanced radiotherapy and nano-photothermal therapy, in two in-vitro and one in-vivo studies, concerning the treatment of three different types of head and neck malignant tumors.

Study	Cancer Type	Nanoparticles	Results
NPTT + NP-enhanced RT Movahedi et al., 2018 (in-vitro)	KB nasopharyngeal carcinoma	FA-AuNRs	High level of cell uptake for AuNR-FA nanoconjugates, substantially decrease of cell viability (to 3.5%).
<i>Nano-Quadrapeutics</i> : NPTT + Liposomal drug + NP-enhanced RT Lukianova & Lapotko, 2015 (in-vitro)	HNSCC cell lines	<i>Nanoclusters</i> : functionalized AuNPs + liposomal drug	Suppression of tumor growth after 1 st week, improved effect of chemo- and radiotherapy by 17-fold.
NPTT + NP-enhanced RT Zhou et al., 2015 (in-vivo)	ATC (anaplastic thyroid cancer)	PEG-coated [⁶⁴ Cu] CuS NPs	Improved animal survival, significant tumor growth inhibition, no signs of toxicity,

Table 5: Combined NP-enhanced Radiotherapy and Nano-photothermal therapy in Head and Neck Cancer. NPTT: nano-photothermal therapy, RT radiotherapy, HNSCC: head and neck squamous cell carcinoma, ATC: anaplastic thyroid cancer, FA: folic acid.

5.1 Future Perspectives

In order to proceed to clinical applications of these innovative treatment methods, an in-depth understanding of the related biophysical mechanisms and knowledge of the exact dosimetry of the radiation therapy, are necessary. The irradiation parameters coupling with nanoparticles properties (based on their size, shape, surface chemistry, functionalization and concentration), vary significantly. Optimized protocols in NP-enhanced radiotherapy (RT), nano-photo-thermal therapy (NPTT) and combined RT/NPTT treatment methods, are needed, for a translation to clinical practice.¹²⁴ In addition, immunoactivation and immunosuppression modulation, tissue thermotolerance, knowledge of the mechanisms of NP-induced radiosensitization of cancer cells, remain open challenges in the field of nanobiotechnology.¹²⁴

Based on the results of in-vitro and in-vivo studies, regarding the applications of nanotechnology in cancer radiotherapy, it is reasonable to conclude that various mechanisms, regarding DNA damage and cytoplasmic effects, participate in radiosensitization induced by NPs. It is likely that other unknown mechanisms also involved in the final radiosensitizing effect, emphasizing the need for more systematic future research.⁸⁹ The successful development of nanotechnology-based treatments and

translation to clinical practice, depend on the capacity of the different communities to share their expertise in developing competitive nanoagents and predictive models.⁷⁶

There are various ongoing clinical trials, related to the use of nanoparticles in head and neck cancer therapy, with one of them concerning the application of NBTXR3 Crystalline Nanoparticles, in HNSCC patients. NBTXR3 NPs are administered by a single intratumoral injection, before the first radiotherapy session, in order to enhance radiotherapy outcomes (phase 1/2 trial).¹²⁹ Another phase 1 trial concerns the addition of nanoparticle albumin-bound paclitaxel to the standard treatment regimen of cetuximab and radiation therapy in patients with advanced head and neck squamous cell carcinoma. This study aims to establish a safe dose range of the NP-chemotherapeutic drug given in this combined treatment, as well as determine the benefits and adverse effects, related to the use of the NP-drug.¹³⁰

6. Conclusion

Currently, there have been several studies conducted, regarding the enhancement of radiotherapy outcomes, with the implementation of nanoparticles as radiosensitizers. Many different approaches have been tested, regarding the irradiation conditions and the nanoparticles' properties (type, size, shape, surface functionalization etc.). The results of these studies have shown that NPs successfully enhance the effects of radiation, localizing them in the tumor region, thus preserving functionality of surrounding healthy tissues. Nevertheless, more randomized controlled trials are required, in order to evaluate the therapeutic efficacy and the benefits produced by the application of nanoparticles as enhancing agents in head and neck cancer therapy, as well as the possible toxicity effects. The combination of radiotherapy with hyperthermia can reduce the radiation dose, while improving the effects of radiation in cancer cells. This is achieved through heat-induced death of cancer cells, as well as radiosensitization of tumor. Combined therapy with radiation and hyperthermia, based on dual mode NP enhancement, can produce improved therapeutic results, overcoming the limitations of each treatment method, while reducing adverse effects by normal tissue.¹²⁴

However, there is still need for optimization of protocols in photothermal/radiation synergetic treatment, as well as the NP properties as therapeutic agents, concerning particle size and shape, surface modification and functionalization. Moreover, immunoactivation, solubility, toxicity, biocompatibility and biodegradation of NPs are important parameters that need to be addressed, in order to introduce a nanoparticle-based treatment, in clinical practice.¹²⁴

References

1. S. A. Yeh, *Radiotherapy for Head and Neck Cancer*, 2010, 24, 127-136.
2. G. SR. Mehta, M.V. Suhag, M. Semval and M. N. Sharma, *Radiotherapy: Basic Concepts and Recent Advances*, 2010, 66, 158-162.
3. M.D. Abeloff, in *Abeloff's Clinical Oncology*, ed. E. M. Zeman, E. C. Schreiber, J. E. Tepper, Elsevier, 5th edn, 2013, ch. 27, pp. 393-422.
4. Radiology Key, <https://radiologykey.com/basic-radiation-protection-and-radiobiology-2/>, (accessed August 2019).
5. E. C. Halperin, D. Wazer, C. A. Rerez and L. W. Brandy, *Principles and Practice of Radiation Oncology*, Wolters Kluwer, Alphen aan den Rijn, Netherlands, 2018.
6. RSSC, *Biological effects of ionizing radiation*, 2012.
7. M.E. Lomax, L.K. Folkes and P. O'Neill, *Biological Consequences of Radiation-induced DNA Damage: Relevance to Radiotherapy*, 2013, 25, 578-585.
8. J. E. Tepper, *Clonogenic Potential of Human Tumors A hypothesis*, 2009, 282-288.
9. M. Pruschy, S. Bodis, *Molecular mechanisms of radioresistance: Applications for head and neck cancer*, 1998, 8, 119-123.
10. E. Gargioni, F. Schulz, a. Raabe, S. Burdak-Rothkamm, T. Rieckmann and K. Rothkamm, *Targeted nanoparticles for tumor radiotherapy enhancement - the long dawn of a golden era?*, 2016, 24, DOI: 10.21037/atm.2016.12.46.
11. L. Tang, F. Wei, Y. Wu, et al., *Role of metabolism in cancer cell radioresistance and radiosensitization methods*, 2018, 37, DOI: 10.1186/s13046-018-0758-7.
12. Y. Liu, P. Zhang, F. Li, et al., *Metal-based NanoEnhancers for Future Radiotherapy: Radiosensitizing and Synergistic Effects on Tumor Cells*, 2018, 8, 1824-1849.
13. K. Kabayashi, N. Usami, E. Porcel, et al., *Enhancement of radiation effect by heavy elements*, 2010, 123-131.
14. A. Popovtzer, A. Mizrahi, M. Matiei, et al., *Actively targeted gold nanoparticles as novel radiosensitizer agents: an in vivo head and neck cancer model*, 2016, DOI: 10.1039/c5nr07496g.
15. D. Cooper, D. Bekah and J. Nadeau, *Gold nanoparticles and their alternatives for radiation therapy enhancement*, 2014, 2, DOI: 10.3389/fchem.2014.00086.
16. Z. Kuncic, S. Lacombe, *Nanoparticle radio-enhancement: principles, progress and applications to cancer treatment*, 2017, 63, DOI: 10.1088/1361-6560/aa99ce.
17. V. Stumpf, K. Gokhberg and L. Cederbaum, *The role of metal ions in X-ray induced photochemistry*, 2018.
18. T. Jahnke, H. Sann, T. Havermeier, et al., *Ultrafast energy transfer between water molecules*, 2010, 6, 139-142.
19. M. Mucic, M. Braune, S. Barth, et al. *A Hitherto unrecognized source of low-energy electrons in water*, 2010, 6, 143-146.
20. K. Gokhberg, P. Kolorenc, A. Kuleff and L. Cederbaum, *Site-and energy- selective slow-electron production through intermolecular Coulombic decay*, 2014, 505, 661-666.

21. V. Stumpf, K. Gokhberg and L. Cederbaum, *Efficient pathway to Neutralization of Multiply charges I ons produced in Auger Processes*, 2013, 110, DOI:10.1103/PhysRevLett.110.258302.
22. M. Leung, J. Chow, B. Devinka Chithrani, et al., *Irradiation of gold nanoparticles by X-rays: Monte Crlo simulation of dose enhancements and the spatial properties of the secondary electrons production*, 2011, 38, 624-631.
23. A. Pottier, E. Borghi and L. Levy, *Metal as radio-enhances in oncology: The industry perspective*, 2015, 468, 471-475.
24. J. K. Kim, S.J. Seo, H.T. Kim, et al., *Enhanced proton threatment in mouse tumors through proton irradiated nanoradiator effects on metallic nanoparticles*, 2012, 57, 8309-8323.
25. N. Bertrand, J. Wu, X. Xu, et al., *Cancer nanotechnology: The impact of passive and active tageting in the era of modern cancer biology*, 2014, 66, 2-25.
26. Y. Takakaura, R. Mahato and M. Hashida, *Extravasation of macromolecules*, 1998. 34, 93-108.
27. F. Alexis, E. Pridgen, L. Molnar and O. Farokhzad, *Factors affecting the clearance and Biodistribution of Polymeric Nanoparticles*, 2008, 5, 505-515.
28. N. Bertrand, J. Leroux, *The journey of a drug-carrier in the body: An anatomo-physiological perspective*, 2012, 161, 152-163.
29. M. Dellian, F.Yuan, VS Trubetskoy, et al., *Vascular permeability in a human tumor xenograft: molecular charge dependence*, 2000, 82, 1513-1518.
30. G. Scherprof, J. Kamps, *The role of hepatocytes in the clearance of liposomes from the blood circulation*, 2001, 40, 149-166.
31. K. Nishida, K. Mihara, T. Takino, et al., *Hepatic disposition characteristics of electrically charged Macromolecules in Rat in Vivo and in the Perfused Liver*, 1991, 8, 437-444.
32. C. S. Morales, L. Zhang, R. Langer and O. Farokhzad, *Immunocompatibility properties of lipid-polymer hybrid nanoparticles with heterogeneous surface functional groups*, 2009, 30, 2231-2240.
33. A. Chonn, , P. R. Cullis, and V. Dana, *The role of surface charge in the activation and alternative pathways of complemet of the classical by liposomes*, 1991, 146, 4234-4211.
34. C. He, Y. Hu, L.Yin, et al. , *Effects of particle size and surface charge on cellular uptake and biodistribution of polymeric nanoparticles*, 2010, 31, 3657-3666.
35. K. Xiao, Y. Li, J. Luo, et al., *The effect of surface charge on in vivo biodistribution of PEG-oligochohic acid based micellar nanoparticles*, 2011, 32, 3435-3446.
36. T. S. Levchenko, R. Rammohan, A. N. Lukyanov, et al., *Liposome clearance in mice: the effect of a separate and combined presence of surface charge and polymer coating*, 2002, 240, 95-102.
37. R. R. Arvizo, O. R. Miranda, D. F. Moyano, et al., *Modulating Pharmacokinetics, Tumor Uptake and Biodistribution by Engineered Nanoparticles*, 2011, 6.
38. A. Gabizon, D. Papahadjopoulos, *Liposome formulations with prolonged circulation time in blood and enhanced uptake by tumors*, 1988, 85, 6949-6953.
39. E. Roux, M. Lafleur, E. Lataste, et al., *On the Characterization of pH-sensitive Liposome/Polymer Complexes*, 2003, 4, 240-248.

40. D. Peer, R. Margalit, *Tumor-Targeted Hyaluronan Nanoliposomes Increase the Antitumor Activity of Liposomal Doxorubicin in Syngeneic and Human Xenograft Mouse Tumor Models*, 2004, 343-353.
41. Y. Yamamoto, Y. Nagasaki, Y. Kato, et al., *Long-circulating poly(ethylene glycol)-poly(D,L-lactide) block copolymer micelles with modulated surface charge*, 2001, 77, 27-38.
42. R. B. Campbell, D. Fukumura, E. B. Brown, et al., *Cationic Charge Determines the Distribution of Liposomes between the Vascular and Extravascular Compartments of Tumors*, 2002, 62, 6831-6836.
43. S. Klein, A. Sommer, L. Distel, et al., *Superparamagnetic Iron Oxide Nanoparticles as Novel X-ray Enhancer for Low-Dose Radiation Therapy*, 2914, 118, 6159-6166.
44. B. Yu, H. C. Tai, W. Xue, et al., *Receptor-targeted nanocarriers for therapeutic delivery to cancer*, 2010, 27, 286-298.
45. A. Rieux, V. Pourcelle, P. D. Cani et al., *Targeted nanoparticles with novel non-peptidic ligands for oral delivery*, 2013, 65, 833-844.
46. J. Wang, S. Tian, R. A. Petros, et al., *The Complex Role of Multivalency in Nanoparticles Targeting the Transferrin Receptor for Cancer Therapies*, 2010, 132, 11306-11313.
47. T. Lammers, F. Kiessling, W. E. Hennink and G. Storm, *Drug targeting to tumors: Principles, pitfalls and (pre-) clinical progress*, 2012, 161, 175-187.
48. S. Taurin, H. Nehoff, and K. Greish, *Anticancer nanomedicine and tumor vascular permeability; Where is the missing link?*, 2012, 164, 265-275.
49. K. F. Pirolo, E. H. Chang, *Does a targeting ligand influence nanoparticle tumor localization or uptake?*, 2008, DOI: doi:10.1016/j.tibtech.2008.06.007.
50. D. B. Kirpotin, D. C. Drummond, Y. Shao, et al., *Antibody Targeting of Long-Circulating Lipidic Nanoparticles Does Not Increase Tumor Localization but Does Increase Internalization in Animal Models*, 2006, 66, 6732-6740.
51. D. W. Bartlett, H. Su, I. J. Hildebrandt, et al., *Impact of tumor-specific targeting on the biodistribution and efficacy of siRNA nanoparticles measured by multimodality in vivo imaging*, 2007, 104, 15549-15554.
52. M. Babaei, M. Ganjalikhani, *A systematic review of gold nanoparticles as novel cancer therapeutics*, 2014, 4, 2011-219.
53. H. N. McQuaid, M. F. Muir, L. E. Taggart, et al., *Imaging and radiation effects of gold nanoparticles in tumour cells*, 2016, DOI: 10.1038/srep19442.
54. L. Yao, J. Daniels, A. Moshnikova, et al., *pHLIP peptide targets nanogold particles to tumors*, 2013, 110, 465-470.
55. S. Teraoka, Y. Kakei, M. Akashi, E. Iwata, T. Hasegawa, D. Miyawaki, R. Sasaki, T. Komari, *Gold nanoparticles enhance X-ray irradiation – induced apoptosis in head and neck squamous cell carcinoma in vitro*, 2018, 4, 415-420.
56. M. Mirrahimi, V. Hosseini, A. Shakeri-Zadeh, et al., *Modulation of cancer cells' radiation response in the presence of folate conjugated Au@Fe₂O₃ nanocomplex as a targeted radiosensitizer*, 2019, 21, 479-488.
57. Y. Ping, Z. Jian, Z. Yi, et al., *Inhibition of the EGFR with nanoparticles encapsulating antisense oligonucleotides of the EGFR enhances radiosensitivity in SCCVII cells*, 2010, 27, 715-721.
58. I. Hazkani, M. Motiei, O. Betzer, et al., *Can molecular profiling enhance radiotherapy? Impact of personalized targeted gold nanoparticles on radiosensitivity and imaging of adenoid cystic carcinoma*, 2017,

7, 3962-3971.

59. A. Coca-Pelaz, J. P. Rodrigo, P. J. Bradley, et al., *Adenoid cystic carcinoma of the head and neck - An update*, 2015, 652-661.
60. D. D. Von Hoff, J. J. Stephenson Jr, P. Rosen, et al., *Pilot Study Using Molecular Profiling of Patients' Tumors to Find Potential Targets and Select Treatments for Their Refractory Cancers*, 2010, 28, 4877-4883.
61. J. Liu, C. Shao, M. L. Tan, et al., *The Molecular Biology of Adenoid Cystic Carcinoma*, 2012, 34, 1665-1677.
62. D. Bell, E. Y. Hanna, *Head and neck adenoid cystic carcinoma: what is new in biological markers and treatment?*, 2013, 21, 124-129.
63. A. Lagha, N. Chraiet, M. Ayadi, et al., *Systemic therapy in the management of metastatic or advanced salivary gland cancers*, 2012, 4, DOI:10.1186/1758-3284-4-19.
64. G. Stenman, F. Persson and M. K. Andersson, *Diagnostic and therapeutic implications of new molecular biomarkers in salivary gland cancers*, 2014, 50, 683-690.
65. D. Iacono, R. Chiari, G. Metro, et al., *Future options for ALK-positive non-small cell lung cancer*, 2015, 87, 211-219.
66. M. Soda, Y. L. Choi, M. Enomoto, et al., *Identification of the transforming EML4-ALK fusion gene in non-small-cell lung cancer*, 2007, 448, 561-567.
67. C. Gridelli, S. Peters, A. Sgambato, et al., *ALK inhibitors in the treatment of advanced NSCLC*, 2014, 300-306.
68. M. Scaltriti, C. Verma, M. Guzman, et al., *Lapatinib, a HER2 tyrosine kinase inhibitor, induces stabilization and accumulation of HER2 and potentiates trastuzumab-dependent cell cytotoxicity*, 2009, 28, 803-814.
69. S. Klein, A. Sommer, L. V.R. Distel, et al., *Superparamagnetic iron oxide nanoparticles as radiosensitizer via enhanced reactive oxygen species formation*, 2012, 425, 393-397.
70. A. K. Hauser, M. I. Mitov, E. F. Daley, et al., *Targeted iron oxide nanoparticles for the enhancement of radiation therapy*, 2016, 105, 127-135.
71. R. A. Revia, M. Zhang, *Magnetite nanoparticles for cancer diagnosis, treatment, and treatment monitoring: recent advances*, 2016, 19, 157-168.
72. F. Assa, H. J. Malmiri, H. Ajamein, et al., *A biotechnological perspective on the application of iron oxide nanoparticles*, 2016, 9, 2203-2225.
73. C. L. Tourneau, V. Calugaru, J.O. Thariat, *Hafnium oxide nanoparticles as a promising emergent treatment for head and neck cancer*, DOI: 10.1016/j.ijrobp.2017.12.180.
74. D. R. Cooper, D. Bekah and J. L. Nadeau, *Gold nanoparticles and their alternatives for radiation therapy enhancement*, 2014, 2, DOI: 10.3389/fchem.2014.00086.
75. G. L. Duc, I. Miladi, C. Alric, et al., *Toward an Image-Guided Microbeam Radiation Therapy Using Gadolinium- Based Nanoparticles*, 2011, 5, 9566-9574.
76. S. Lacombe, E. Porcel and E. Scifoni, *Particle therapy and nanomedicine: state of the art and research perspectives*, 2017, 8, DOI 10.1186/s12645-017-0029-x.
77. D. Schardt, T. Elsässer and D. S. Ertner, *Heavy-ion tumor therapy: Physical and radiobiological benefits*, 2010, 82, 383-424.
78. M. Shiomi, S. Mori, M. Shinoto, et al., *Comparison of carbon-ion passive and scanning irradiation for pancreatic cancer*, 2016, 119, 326-330.

79. G. Dollinger, *Comment on 'Therapeutic application of metallic nanoparticles combined with particle-induced x-ray emission effect'*, 2011, 22, DOI::10.1088/0957 4484/22/24/248001.
80. J. C. Polf, L. F. Bronk, W. H. P. Driessen, et al., *Enhanced relative biological effectiveness of proton radiotherapy in tumor cells with internalized gold nanoparticles*, 2011,98.
81. T. Schlathölter, P. Eustache, E. Porcel, et al., *Improving proton therapy by metal-containing nanoparticles: nanoscale insights*, 2016, 11, 1549-1556.
82. H. Kaur , G. Pujari, M.K. Semwal, et al., *In vitro studies on radiosensitization effect of glucose capped gold nanoparticles in photon and ion irradiation of HeLa cells*, 2013, 301, 7-11.
83. E. Porcel, O. Tillement, F.Lux, et al., *Gadolinium-based nanoparticles to improve the hadrontherapy performances*, 2014, 10, 1601-1608.
84. L. Sancey, , F. Lux, S. Kotb,, et al., *The use of theranostic gadolinium-based nanoprobess to improve radiotherapy efficacy*, 2014, 87, DOI:10.1259/bjr.20140134.1259/bjr.20140134.
85. L.Štefančíková, E. Porcel, P. Eustache, et al., *Cell localisation of gadolinium-based nanoparticles and related radiosensitising efficacy in glioblastoma cells*, 2014, 5.
86. E. Porcel, S. Liehn, H. Remita, et al., *Platinum nanoparticles: a promising material for future cancer therapy?*, 2010, 21 , DOI:10.1088/0957-4484/21/8/085103.
87. H. Nikjoo, S. Uehara, D. Emfietzoglou and A. Brahme, *Heavy charged particles in radiation biology and biophysics*, 2008, 10 DOI: 10.1088/1367-2630/10/7/075006.
88. M. Hossain, M. Su, *Nanoparticle location and material dependent dose enhancement in X-ray radiation therapy*, 2012, 116, 23047-23052.
89. E. Pagáčová, L. Štefančíková, F. Schmidt-Kaler, *Challenges and Contradictions of Metal Nano-Particle Applications for Radio-Sensitivity Enhancement in Cancer Therapy*, 2019, 20, DOI: 10.3390/ijms20030588.
90. R. Zhanga, M. J. Piao, K. C. Kim, *Endoplasmic reticulum stress signaling is involved in silver nanoparticles-induced apoptosis*, 2012, 44, 224-232.
91. E. Szegezdi, S. E. Logue, A. M. Gorman and A. Samali, *Mediators of endoplasmic reticulum stress-induced apoptosis*, 2006, 7, 880-885.
92. S. Gao, M. Zheng, X. Ren, et al., *Local hyperthermia in head and neck cancer: mechanism, application and advance*, 2015, 7, 57367-57378.
93. G. Baronzio, G. Parmar, M. Ballerini, et al., *A Brief Overview of Hyperthermia in Cancer Treatment,, 2014, 3, DOI : 10.4172/2329-6771.1000115.*
94. L. Zhu, M. B. Altman, A. Laszlo, et al., *Ultrasound hyperthermia technology for radiosensitization*, 2019, 45, 1025-1043.
95. V. Kouloulias, *Hyperthermia and nanoparticles, presented in National University of Athens, Athens, December, 2018.*
96. T. A. Okhai, C. J. Smith in *Hyperthermia*, ed. Nagraj Huilgol, IntechOpen, India, 2013, ch. 6, pp. 171-181.
97. M. Sethi, S.K. Chakarvarti, *Hyperthermia Techniques for cancer treatment: A Review*, 2015,
98. C. L. Brace, *Radiofrequency and microwave ablation of the liver, lung, kidney and bone: What are the differences: "Organ-specific thermal ablation"*, 2009, 38, 135-143.

99. A. L. Carvalho, I. N. Nishimoto, J.A. Califano and L. P. Kowalski, *Trends in incidence and prognosis for head and neck cancer in the United States: A site-specific analysis of the SEER database*, 2005, 114, 806-816.
100. G. Iliakis, T. Krieg, J. Guan, et al., *Evidence for an S-Phase checkpoint regulating DNA replication after heat shock: a review*, 2004, 20, 240-249.
101. T. Karino, S. Koga and M. Maeta, *Experimental Studies of the Effects of Local Hyperthermia on Blood Flow, Oxygen Pressure and pH in Tumors*, 1988, 18, 276-283.
102. K. Ahmed, S. F. Zaidi, *Treating cancer with heat: hyperthermia as promising strategy to enhance apoptosis*, 2013, 63, 504-508.
103. A. Kanwal, H. Takeshi, Y. D. Yung, et al., *Hyperthermia Chemo-sensitization, Chemical Thermo-sensitization and Apoptosis*, 2008, 24, DOI: 10.3191/thermalmed.24.1.
104. H. Liang, H. J. Zhan, B. G. Wang, et al., *Change in expression of apoptosis genes after hyperthermia, chemotherapy and radiotherapy in human colon cancer transplanted into nude mice*, 2007, 13, 4365-4370.
105. C. Roca, L. Primo, D. Valdembri, et al., *Hyperthermia Inhibits Angiogenesis by a Plasminogen Activator Inhibitor 1-dependent Mechanism*, 2003, 63, 1500-1507.
106. E. L. Jones, J. R. Oleson, L.R. Prosnitz, et al., *Randomized Trial of Hyperthermia and Radiation for Superficial Tumors*, 2005, 23, 3079-3085.
107. V. Kouloulis, S. Triantopoulou, E. Efstathopoulos, K. Platoni, et al., *Microwave Hyperthermia in Conjunction with Radiotherapy in Superficial Tumours: Correlation of Thermal Parameters with Tumour Regression*, 2013, 752-757.
108. J. Beik, Z. Abed, F. S. Ghoreishi, et al., *Nanotechnology in hyperthermia cancer therapy: From fundamental principles to advanced applications*, 2016, 235, 205-221.
109. F. Zhou, D. Xing, Z. Ou, et al., *Cancer photothermal therapy in the near-infrared region by using single walled carbon nanotubes*, 2009, 14.
110. C. Zhiyun, M. Lijing, I. Ying Liu and C. Chunying, *Applications of Functionalized Fullerenes in Tumor Theranostics*, 2012, 2, 238-249.
111. Y. Kai, F. Liangzhu, S. Xiaoze and L. Zhuang, *Nano-graphene in biomedicine: theranostic applications*, 2013, 42, 530-547.
112. K. Riehemann, S. W. Schneider, T. A. Luger, et al., *Nanomedicine - Challenge and Perspectives*, 2009, 48, 872-897.
113. Y. Zhang, Linhai C., H. Jiayan, et al., *Photothermal treatment with EGFRmAb–AuNPs induces apoptosis in hypopharyngeal carcinoma cells via PI3K/AKT/mTOR and DNA damage response pathways*, 2018, 50, 567-578.
114. X. Huang, I. H. E Sayed, W. Qian, et al., *Cancer Cell Imaging and Photothermal Therapy in the Near-Infrared Region by Using Gold Nanorods*, 2006, 128, 2115-2120.
115. Z. Shiwen Zhang, L. Yunlong, H. Xiaoguang, et al., *Photothermolysis mediated by gold nanorods modified with EGFR monoclonal antibody induces Hep-2 cells apoptosis in vitro and in vivo*, 2014, 9, 1931-1946.
116. R. Lang, B. L. Lin, M. Liang, *Platelet-Facilitated Photothermal Therapy of Head and Neck Squamous Cell Carcinoma*, 2018, 57, 986-991.
117. Candido, Calmon, Taboga, et al., *High Efficacy in Hyperthermia-associated with Polyphosphate Magnetic*

- Nanoparticles for Oral Cancer Treatment*, 2014, 5, DOI: 10.4172/2157-7439.1000205.
- 118.W. Wei, H. Quanguo, J. Changzhong, *Magnetic Iron Oxide Nanoparticles: Synthesis and Surface Functionalization Strategies*, 2008, 3, 397-415.
- 119.D. E. Kruse, D. N. Stephens, H. A. Lindfors, et al., *A Radio-frequency Coupling Network for Heating of Citrate-coated Gold Nanoparticles for Cancer Therapy: Design and Analysis*, 2011, 58, 2002-2012.
- 120.C. H. Moran, S. M. Wainerdi, T. K. Cherukuri, et al., *Size-Dependent Joule Heating of Gold Nanoparticles Using Capacitively Coupled Radiofrequency Fields*, 2009, 2, 400-405.
- 121.V. H. B. Ho, M. J. Smith, and N. K. H. Slater, *Effect of magnetite nanoparticle agglomerates on the destruction of tumor spheroids using high intensity focused ultrasound*, 2010, 37, 169-175.
- 122.W. Dongsheng, *Nanoparticle-Related Heat Transfer Phenomenon and Its Application in Biomedical Fields*, 2013, 34, 1171-1179.
- 123.G. Canavesea, A. Anconaa, L. Racca, et al., *Nanoparticle-assisted ultrasound: A special focus on sonodynamic therapy against cancer*, 2018, 340, 155-172.
- 124.E. Spyratou, M. Makropoulou, E. P. Efstathopoulos, et al., *Recent Advances in Cancer Therapy Based on Dual Mode Gold Nanoparticles*, 2017, 9, DOI:10.3390/cancers9120173.
- 125.J. F. Hainfeld, L. Lin, D. N. Slatkin, et al., *Gold nanoparticle hyperthermia reduces radiotherapy dose*, 2014, 10, 1609-1617.
- 126.M. M. Movahedi, A. Mehdizadeh, F. Koosha, et al., *Investigating the photo-thermo-radiosensitization effects of folate conjugated gold nanorods on KB nasopharyngeal carcinoma cells*, 2018, 24, 324-331.
- 127.E. Y. Lukianova Hleb, D. O. Lapotko, *Rapid detection and destruction of squamous cell carcinoma of the head and neck by nano-quadrupole*, 2015, 1547-1555.
- 128.M. Zhou, Y. Chen, M. Adachi, et al., *Single agent nanoparticle for radiotherapy and radio-photothermal therapy in anaplastic thyroid cancer*, 2015, 57, 41-49.
- 129.Clinical Trials, <https://clinicaltrials.gov/ct2/show/NCT01946867>, (accessed August 2019).
- 130.ClinicalTrials, <https://clinicaltrials.gov/ct2/show/NCT01946867term=nanoparticle&cond=Head+and+Neck+Cancer&draw=3&rank=4>, (accessed August 2019).